

ARTICLE TYPE

Identification of young nearby runaway stars based on Gaia data and the lithium test[†]

R. Bischoff*¹ | M. Mugrauer¹ | G. Torres² | T. Heyne¹ | O. Lux¹ | V. Munz¹ | R. Neuhäuser¹ | S. Hoffmann¹ | A. Trepanovski¹

¹Astrophysikalisches Institut und
Universitäts-Sternwarte Jena,
Schillergäßchen 2, 07745 Jena, Germany
²Center for Astrophysics | Harvard &
Smithsonian, 60 Garden Street, Cambridge
MA 02138, United States of America

Correspondence

*R. Bischoff, Astrophysikalisches Institut
und Universitäts-Sternwarte Jena,
Schillergäßchen 2, 07745 Jena, Germany
Email: richard.bischoff@uni-jena.de

Funding Information

NE 515/58-1. MU 2695/27-1.

Young nearby runaway stars are suitable to search for their place of origin and possibly associated objects, for example neutron stars. Tetzlaff, Neuhäuser, & Hohle (2011) selected young (≤ 50 Myr) runaway star candidates from Hipparcos, for which they had estimated the ages from the location in the Hertzsprung-Russell diagram and evolutionary models. Here, we redetermine or constrain their young ages more precisely not only by using the new *Gaia* DR2 data, but also by measuring lithium, which is a youth indicator. For 308 stars, we took spectra to search for the strong resonance doublet of the lithium-7 isotope at 6708 Å. The spectra were taken with the Échelle spectrograph FLECHAS at the University Observatory Jena between February 2015 and June 2018 and with TRES between April 2011 and June 2017 at the Fred L. Whipple Observatory. We found 208 stars with significant occurrence of lithium in their spectra, and five possess a possible age younger or about 50 Myr. Three of these targets are even closer than GJ 182, the nearest known runaway star at about 24 pc. These stars are young runaway stars suitable for further investigation of their origin from either a dynamical or supernova ejection.

KEYWORDS:

stars: HRD, fundamental parameters; methods: observational, data analysis; techniques: spectroscopic; astronomical databases: catalogues

1 | INTRODUCTION

Runaway stars have higher velocities than typical field stars. They can be the result of a supernova explosion in a binary system where the secondary component is ejected as a runaway star (Blaauw, 1961) or they are ejected due to gravitational interactions between stars in dense stellar systems or clusters (Poveda, Ruiz, & Allen, 1967).

Tetzlaff et al. (2011) did a combined analysis of spatial, tangential and radial velocities for all 118 218 stars from the

Hipparcos catalogue (Perryman et al., 1997) to find more runaway star candidates. In their study they did not only focus on O- and B-type stars but extended the use of the term *runaway* to every star with an unusual space velocity. Given the motivation to study runaway stars from core-collapse supernovae in binaries and that such runaway stars cannot be traced back easily (because of the Galactic potential) for more than a few Myr, the age of such runaway stars is below about 50 Myr (including up to 30 Myr until the supernova). The age estimation was done by comparing luminosity and effective temperature of the stars to different evolutionary models. The results of their study were published in the catalogue *Young runaway stars within 3 kpc* which is available at the VizieR¹ database.

[†]Based on observations obtained with telescopes of the University Observatory Jena, which is operated by the Astrophysical Institute of the Friedrich-Schiller University, and telescopes of the Fred L. Whipple Observatory, which is operated by the Harvard-Smithsonian Center for Astrophysics Cambridge MA.

¹<http://cdsarc.u-strasbg.fr/viz-bin/cat/J/MNRAS/410/190>

For selected stars of this catalogue, our spectroscopic observing program was started in order to determine or confirm their possible young age based on the second data release of the *Gaia* mission (*Gaia* DR2) of the European Space Agency (Gaia Collaboration et al., 2018). Furthermore, we searched for the absorption line of the lithium-7 doublet at 6708 Å, which is a youth indicator.

In this paper, we describe in detail the sample selection, as well as the spectroscopic observations and the data reduction in section 2. In section 3, a characterisation of physical properties of the targets, based on their *Gaia* DR2 data, is given. The following section 4 yields information about the equivalent width measurements of the Li (6708 Å) line in the spectra of all observed stars and the lithium abundances of the identified dwarfs. In Section 5 we describe the age estimation of the dwarf stars. The results are discussed in the final section of this paper.

2 | SAMPLE SELECTION, OBSERVATIONS AND DATA REDUCTION

For this project, we chose stars from the catalogue by Tetzlaff et al. (2011) that are observable at air masses $X < 2.4$ from Jena (Dec $> -14^\circ$) and are bright enough ($V \leq 8.5$ mag) to obtain spectra with sufficiently high signal-to-noise-ratio (SNR) > 50 at short integration times of only a few minutes. In total, 460 stars were selected as targets for spectroscopy. While 308 of them are already observed, analysed and discussed in this article, the remaining 152 will be part of a future observing campaign.

The spectra for this study were taken with the fibre-linked Échelle spectrograph FLECHAS (Mugrauer, Avila, & Guirao, 2014), mounted at the Nasmyth telescope ($D = 90$ cm, $f/D = 15$) of the University Observatory Jena. The observatory is located 10 km west of the city of Jena (Pfau, 1984). During two observing epochs between 20th February 2015 and 3rd February 2016, as well as 21st January 2018 and 4th June 2018, 924 spectra with a total integration time of 123 h were obtained in the course of our observing campaign at the University Observatory Jena.

The spectra were taken in the 1x1 binning mode of the spectrograph FLECHAS with individual integration times ranging between 10 s and 1200 s, according to target brightness. FLECHAS covers the spectral range from 3900 Å to 8100 Å in 29 orders with a resolving power of $R \approx 9,300$ (Mugrauer et al., 2014) and the Li (6708 Å) line is detected in the middle of the 24th spectral order of the instrument. In order to achieve a sufficiently high SNR and to remove cosmics, three spectra were always taken for each target. The SNR of all fully reduced spectra was measured at $\lambda = 6700$ Å. At this

wavelength, most spectra yield at least a $\text{SNR} \geq 50$ and $\text{SNR} = 152$ is reached on average. The only exceptions are HIP 56383 (SNR = 25), HIP 107350 (SNR = 39), HIP 94761 (SNR = 42) and HIP 97198 (SNR = 42). The details of all observations are listed in Table A1.

For calibration purposes, three well exposed flat-field frames of a tungsten lamp as well as three spectra of a thorium-argon (ThAr) lamp are recorded immediately before the observation of each target. Each calibration image possess an individual integration time of 5 s. In the ThAr spectra are about 700 detected emission lines for wavelength calibration. The long-term stability of the wavelength calibration of the instrument was previously shown by Irrgang, Desphande, Moehler, Mugrauer, & Janousch (2016), Bischoff et al. (2017) and Heyne et al. (2020). Furthermore, three dark frames for all used integration times are recorded in every observing night for the dark and bias subtraction.

The FLECHAS software pipeline, which was developed at the Astrophysical Institute Jena, was utilised for dark and bias subtraction, flat-fielding, the extraction and wavelength calibration of the individual spectral orders. Additionally, the pipeline includes averaging and normalisation of the recorded spectra for each target (Mugrauer et al., 2014).

As part of a separate long-term spectroscopic monitoring program to measure radial velocities and discover binary systems in another sample of runaway stars from Tetzlaff et al. (2011), overlapping in part with the one in this work, 30 of our objects were also observed between 6th April 2011 and 12th June 2017 with the Tillinghast Reflector Echelle Spectrograph TRES (Szentgyorgyi & Fűrész, 2007), (Fűrész, 2008). The spectrograph is attached to the 1.5 m Tillinghast reflector at the Fred L. Whipple Observatory² on Mount Hopkins (Arizona, USA). This bench-mounted, fiber-fed instrument delivers spectra at a resolving power of $R \approx 44,000$ that cover the wavelength region between 3800 Å and 9100 Å in 51 orders. Exposure times ranged from 45 s to about 10 minutes, depending on brightness and weather conditions, and the SNRs achieved at a mean wavelength of 5200 Å are between about 20 and 130 per resolution element of 6.8 km/s. Exposures of a ThAr lamp were taken before and after each science frame, and the observations were reduced with a dedicated pipeline.

3 | TARGET CHARACTERISATION WITH GAIA DR2 DATA

We typically used data from *Gaia* DR2 for a detailed characterisation of all 308 observed stars. Only entries that have a gold

²<http://linmax.sao.arizona.edu/help/FLW0/whipple.html>

or silver flag (see Andrae et al. (2018) for details) were taken into account for the analysis. In Table A3 in the appendix, we list the *Gaia* DR2 distances d from the catalogue by Bailer-Jones, Rybizki, Fouesneau, Mantelet, & Andrae (2018), the apparent brightness G and extinction A_G in the G -band, effective temperature T_{eff} , stellar radius R and luminosity L of our targets. From these values, the resulting absolute brightness in G -band was calculated. The distance distribution of the whole sample is illustrated in Figure 1 with a median distance of about 370 pc. The individual distances range between $5.91_{-0.01}^{+0.01}$ pc in the case of HIP 94761 and 3536_{-813}^{+1274} pc for HIP 113561.

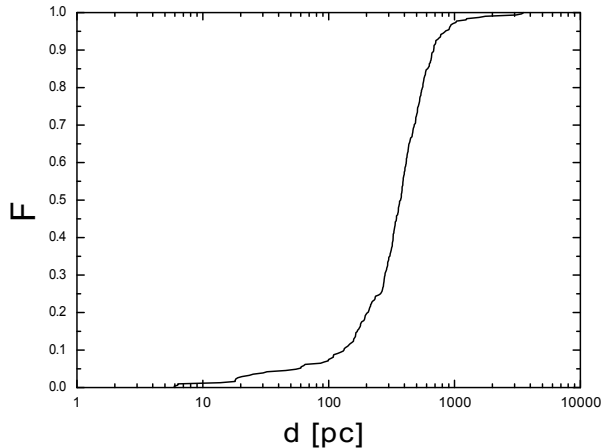


FIGURE 1 The cumulative distribution function of the distances of our sample according to Bailer-Jones et al. (2018).

However, not all of these parameters are available for every target (marked with different flags) in *Gaia* DR2. For six targets without given parallax, for the distance determination, the Hipparcos parallax (van Leeuwen, 2007) was taken instead. In the cases of HIP 18488, HIP 27989, HIP 110991 and HIP 113881 the apparent brightnesses in V - and I -band from the Hipparcos catalogue (Perryman et al., 1997) were converted into G -band using the relations by Jordi et al. (2010).

142 of our targets have no estimation of the interstellar extinction in the G -band. For this reason, measurements of their V -band extinction from the literature, as listed in VizieR (Ochsenbein, Bauer, & Marcout, 2000), were collected instead to calculate the median and standard deviation of the V -band extinction for these targets. This average V -band extinction was then converted into G -band by using the relations from Jordi et al. (2010) as explained in Mugrauer (2019).

For ten objects no sufficient T_{eff} was provided by *Gaia* DR2. These ten stars were identified as giants according to their bright absolute G -band magnitudes. Their temperatures were derived from the spectral type (SpT) listed in the Hipparcos

catalogue with the corresponding T_{eff} -SpT relation by Damiani et al. (2016).

We plot all targets in a Hertzsprung-Russell-Diagram (HRD) which is shown in Figure 2. Most of the investigated stars are clearly on the giant branch and therefore, they can be excluded from the list of possible young runaway stars. In contrast to this, the targets numbered from 1 to 13 in the right panel of Figure 2 can be seen as dwarf stars, because they are located close to the isochrones for 50 Myr and 5 Gyr.

The remaining objects that are marked with Roman numerals in Figure 2 cannot be assigned so easily, from their position in the HRD. At comparable temperatures, the radii of those targets, as listed in Table 1, are too large compared to those of known dwarfs as given by E. Mamajek³ or G. Torres, Andersen, & Giménez (2010). Therefore, they are also giants.

TABLE 1 Targets that were identified as giants due to comparison of effective temperature T_{eff} and radius R from *Gaia* DR2 with those of known dwarfs. These objects are marked with Roman numerals in Figure 2.

Roman numeral	Target	T_{eff} [K]	R [R_{\odot}]
I	HIP 118077	6322_{-460}^{+118}	$3.70_{-0.13}^{+0.61}$
II	HIP 96966	6113_{-80}^{+67}	$4.34_{-0.09}^{+0.12}$
III	HIP 21408	5470_{-52}^{+141}	$7.60_{-0.38}^{+0.14}$
IV	HIP 64543	5383_{-87}^{+99}	$5.26_{-0.19}^{+0.18}$
V	HIP 46977	5305_{-84}^{+365}	$4.72_{-0.59}^{+0.15}$
VI	HIP 63368	4950_{-75}^{+83}	$5.43_{-0.18}^{+0.17}$
VII	HIP 68904	4788_{-87}^{+69}	$4.57_{-0.13}^{+0.17}$

However, further analysis is needed to identify young stars among the dwarfs.

4 | LI (6708 Å) EQUIVALENT WIDTH MEASUREMENTS AND ABUNDANCES

The first step to identify the Li (6708 Å) line was to correct the wavelength shift in every spectrum due to the relative motion between the target and the observing site. Therefore, the position of the Ca (6718 Å) line was measured, by using Gaussian fitting of the IRAF script `splot`, and then was shifted to its characteristic wavelength ($\lambda_0 = 6717.685$ Å), as given in the ILLSS catalogue (Coluzzi, 1993). The Ca (6718 Å) line was chosen because it is the most prominent spectral line next to Li (6708 Å), and is detected in the same spectral order as

³http://www.pas.rochester.edu/~emamajek/EEM_dwarf_UBVIJHK_colors_Teff.dat

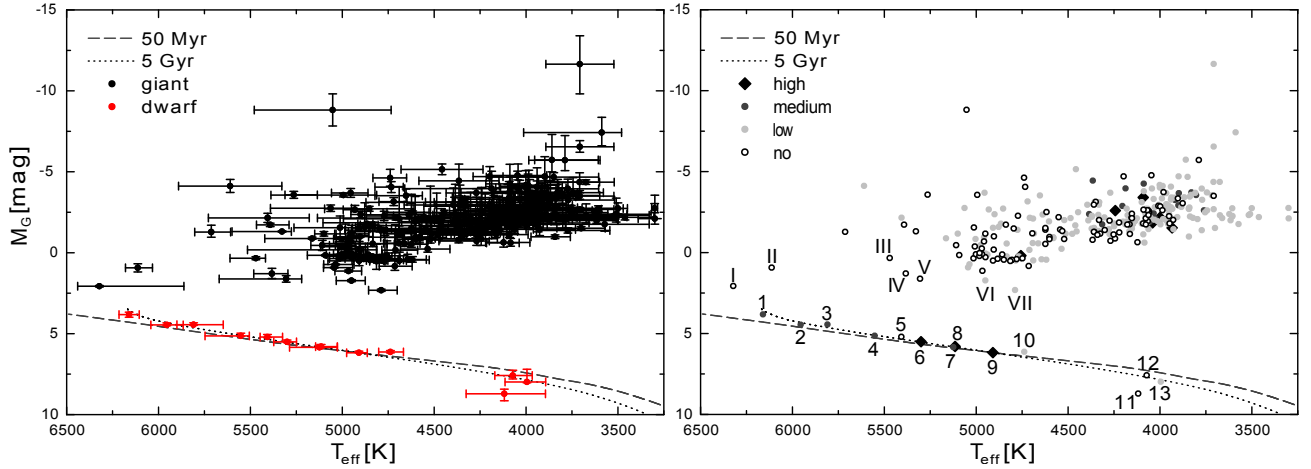


FIGURE 2 Hertzsprung-Russell diagram of all observed targets. On the **left**, we show giant stars marked with a full black dots and dwarf stars with full red dots. On the **right**, the targets are characterised by the measured equivalent width of the Li (6708 Å) line: Targets with $EW_{\text{Li}} < 3 \cdot \sigma EW_{\text{Li}}$ have *no* significant lithium detection, while objects with $EW_{\text{Li}} \geq 3 \cdot \sigma EW_{\text{Li}}$ and $EW_{\text{Li}} < 100 \text{ mÅ}$ are ranked as *low*, $100 \text{ mÅ} \leq EW_{\text{Li}} < 200 \text{ mÅ}$ as *medium* and $EW_{\text{Li}} \geq 200 \text{ mÅ}$ as *high*. Further information about the stars marked with Roman numerals can be found in Table 1 and for the ones marked numbers with from 1 to 13 in Table 5, respectively. We have also plotted the PARSEC isochrones (Bressan et al., 2012) for 50 Myr and 5 Gyr with solar metallicity $Z = 0.0152$ in both distributions.

the lithium line. As an example, we show in Figure 3 the FLECHAS spectrum of the lithium rich dwarf HIP 46843.

The equivalent width

$$EW = \sum_{x=1}^N \left(-\frac{I(x) - C(x)}{C(x)} \right) dx \quad (1)$$

was determined in the reduced spectra by using the IRAF task `splot` with a direct integration of the line profiles, where x is the pixel center coordinate, $I(x)$ the pixel value, $C(x)$ the pixel value of the continuum and dx is the pixel width in Å. `splot` also includes an error estimation based on a Poisson statistics model, where a constant Gaussian error based on the detected flux in the spectral line is calculated individually for every pixel. This takes into account the typical read-noise (11 e- at a readout frequency of 700 kHz) and gain (1.3 e-/ADU) of the instrument (Mugrauer et al., 2014). The final uncertainty is calculated based on Gaussian propagation of the individual pixel uncertainties.

The targets with the largest measured equivalent widths of the Li (6708 Å) lines are listed in Table 2. The equivalent widths of the Li (6708 Å) line of the complete sample can be found in Table A2. We also present in *Target spectra - dwarfs* and *Target spectra - giants*, all spectra of stars which exhibit a significant measurement, that means $EW_{\text{Li}} \geq 3 \cdot \sigma EW_{\text{Li}}$. These spectra are sorted by their spectral type derived from the T_{eff} -SpT-relation given by Damiani et al. (2016). Thereby we

TABLE 2 Targets with the largest measured equivalent widths of the Li (6708 Å) line EW_{Li} detected with FLECHAS and their derived spectral types (SpT) using the T_{eff} -SpT-correlations from Damiani et al. (2016).

Target	EW_{Li} [mÅ]	SpT
HIP 41221	331 ± 10	K5 III
HIP 43030	310 ± 9	K5 III
HIP 27778	266 ± 7	K5 III
HIP 46816	254 ± 11	K2 V
HIP 80941	242 ± 12	K0 III
HIP 115147	239 ± 13	K0 V
HIP 40628	235 ± 9	K5 III
HIP 102377	235 ± 10	K4 III
HIP 46843	200 ± 12	G8 V

distinguish between dwarf and giant stars and the uncertainty of the spectral classification is about two sub-classes.

Furthermore, we compare our equivalent widths from FLECHAS spectra to measurements from TRES. In these additional spectra, we searched for lithium as described above and the results are summarised in Table 3. Due to a mostly lower SNR in the TRES spectra, we list only targets where in every individual measurement the equivalent width is at least three times larger than its uncertainty. The median of each individual measurement per star was then calculated and

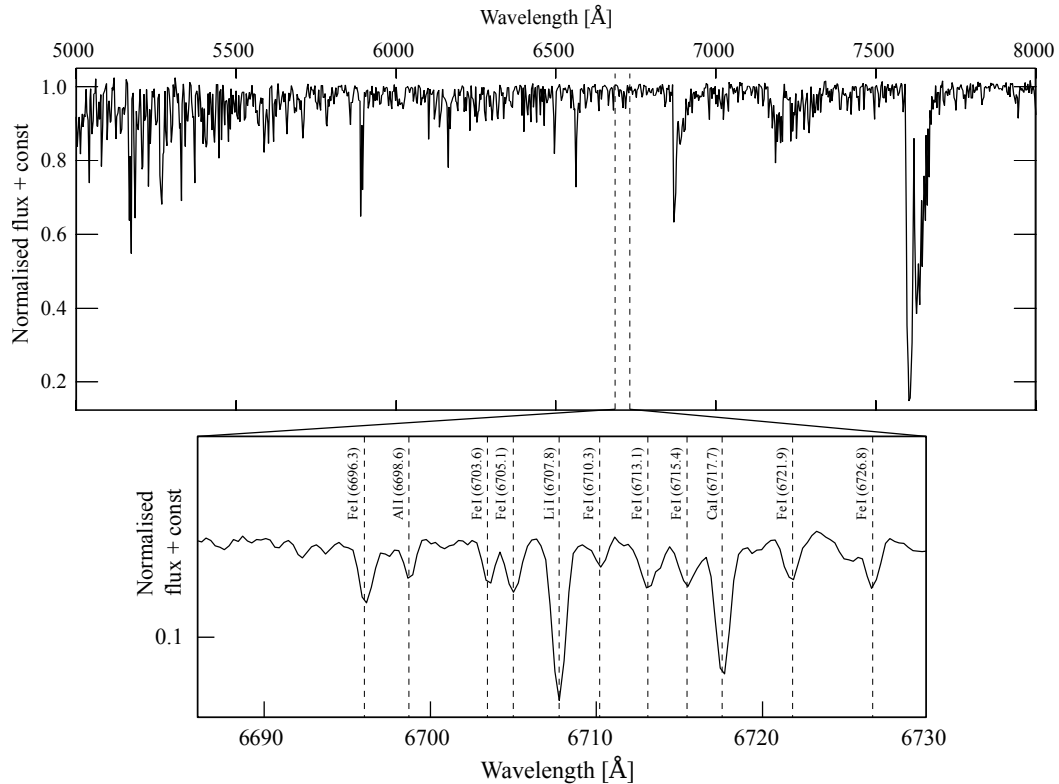


FIGURE 3 Normalised FLECHAS spectrum of the lithium rich dwarf HIP 46843. Besides the prominent Ca (6718 Å) line, the Al (6699 Å) and many iron lines are identified around the Li (6708 Å) line.

the standard deviation represents its accuracy. The values are consistent within 1 to 3σ .

Additionally, the equivalent widths of the 13 dwarf stars were converted into abundances. We used the curves of growth for the Li (6708 Å) line from Soderblom et al. (1993), with an abundance scale based on $\log_{10}(N)_{\text{H}} = 12$. Therefore, the measured equivalent widths from our observing campaign together with the effective temperatures from *Gaia* DR2 were assigned to the corresponding best matching values of $\log_{10}(EW)$ and T_{eff} in the corresponding Table 2 in Soderblom et al. (1993). The results of this conversion are listed in Table 4.

5 | AGE ESTIMATION

The ages of our dwarf stars can be estimated from their location in the HRD with additional isochrones as illustrated in Figure 4. For this we have used again the models of Bressan et al. (2012) with metallicity $Z = 0.0152$, because all of these targets have metallicities listed in the *StarHorse* catalogue (Anders et al., 2019) which are consistent within 2σ with solar metallicity. For young targets we would not expect

a metallicity $[M/H] < 0$. Furthermore, we searched for additional information about the metallicity of our dwarf targets in the *VizieR* database (Ochsenbein et al., 2000). The metallicities for this sample were found in the catalogues of Brewer, Fischer, Valenti, & Piskunov (2016), Casagrande et al. (2011), Franchini, Morossi, di Marcantonio, Malagnini, & Chavez (2014), Gazzano et al. (2010), Gray, Graham, & Hoyt (2001), Gray, Corbally, Garrison, McFadden, & Robinson (2003), Gray et al. (2006), Houdebine, Mullan, Paletou, & Gebran (2016), Houdebine, Mullan, Bercu, Paletou, & Gebran (2017), Karataş, Bilir, & Schuster (2005), Kunder et al. (2017), Marsden et al. (2014), Petigura & Marcy (2011), Rajpurohit et al. (2018), Rojas-Ayala, Covey, Muirhead, & Lloyd (2012), Stassun et al. (2019), Valenti & Fischer (2005) and Worley et al. (2012), with a median of $[M/H] = 0.0$ and standard deviation of 0.2 dex. Taking this scatter of $[M/H]$ into account, we analysed how it influences the position of the isochrones in the HRD. The differences between different metallicities are smaller or at least comparable with the uncertainties of effective temperature or absolute brightness and do not effect the age estimation significantly, as illustrated in the example in Figure 5.

TABLE 3 Comparison of the equivalent widths of the Li (6708 Å) line, measured in the TRES and FLECHAS spectra. We list the median equivalent width EW_{med} and the number of used TRES measurements N as well as the derived values from the FLECHAS spectra EW_{FL} .

Target	EW_{med} [mÅ]	N	EW_{FL} [mÅ]
HIP 1479	21 ± 7	3	46 ± 6
HIP 5912	126 ± 4	4	137 ± 6
HIP 16019	57 ± 7	4	69 ± 7
HIP 17064	93 ± 2	3	94 ± 7
HIP 25386	29 ± 8	6	39 ± 10
HIP 26743	17 ± 3	4	61 ± 12
HIP 41221	357 ± 12	3	331 ± 10
HIP 44580	33 ± 11	3	67 ± 9
HIP 50999	30 ± 3	3	55 ± 9
HIP 74425	19 ± 2	4	34 ± 7
HIP 77178	22 ± 4	5	30 ± 9
HIP 84038	12 ± 6	35	19 ± 9
HIP 100180	26 ± 8	8	43 ± 7
HIP 100534	31 ± 6	9	35 ± 7
HIP 101219	80 ± 11	21	108 ± 8
HIP 107325	38 ± 6	4	39 ± 7

TABLE 4 The identified dwarf stars with their numbers as shown in Figure 2, listed with their effective temperatures T_{eff} from *Gaia* DR2 and the measured equivalent widths of the Li (6708 Å) line EW_{Li} . We list only measurements with $EW_{\text{Li}} \geq 3 \cdot \sigma EW_{\text{Li}}$. Based on these values we give the derived abundances $\log_{10}(N_{\text{Li}})$ according to Soderblom et al. (1993).

id. nr.	Target	T_{eff} [K]	EW_{Li} [mÅ]	$\log(N_{\text{Li}})$
1	HIP 60831	6160^{+55}_{-55}	116 ± 11	$3.170^{+0.090}_{-0.294}$
2	HIP 107350	5955^{+87}_{-89}	138 ± 25	$3.140^{+0.106}_{-0.414}$
3	HIP 44458	5809^{+91}_{-161}	178 ± 13	$3.130^{+0.387}_{-0.125}$
4	HIP 544	5552^{+195}_{-46}	100 ± 11	$2.393^{+0.333}_{-0.070}$
5	HIP 59280	5407^{+40}_{-82}	-	-
6	HIP 46843	5300^{+73}_{-51}	200 ± 12	$2.715^{+0.158}_{-0.135}$
7	HIP 63742	5124^{+163}_{-97}	140 ± 16	$2.071^{+0.401}_{-0.091}$
8	HIP 115147	5115^{+30}_{-88}	239 ± 13	$2.745^{+0.320}_{-0.186}$
9	HIP 46816	4909^{+67}_{-45}	254 ± 11	$2.745^{+0.320}_{-0.341}$
10	HIP 45963	4738^{+64}_{-71}	29 ± 8	$0.853^{+0.103}_{-0.159}$
11	HIP 94761	4118^{+208}_{-224}	-	-
12	HIP 45343	4072^{+98}_{-106}	-	-
13	HIP 120005	3995^{+119}_{-102}	59 ± 12	$0.235^{+0.125}_{-0.112}$

However, nearly all dwarf stars of the sample are also consistent with the main sequence within their uncertainties, as shown in Figure 4, and therefore, isochrone fitting can only be used to estimate a lower limit of their age. The results of this

are listed in Table 5.

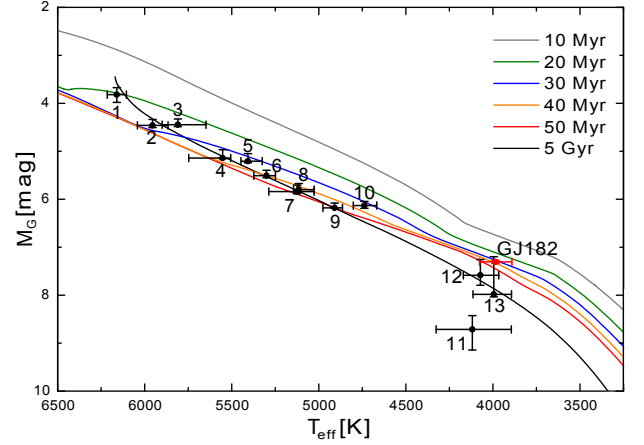


FIGURE 4 The dwarf stars of our sample and GJ 182 (in red) are plotted in the Hertzsprung-Russell diagram with different isochrones using the stellar evolutionary models of Bressan et al. (2012) for solar metallicity $Z = 0.0152$.

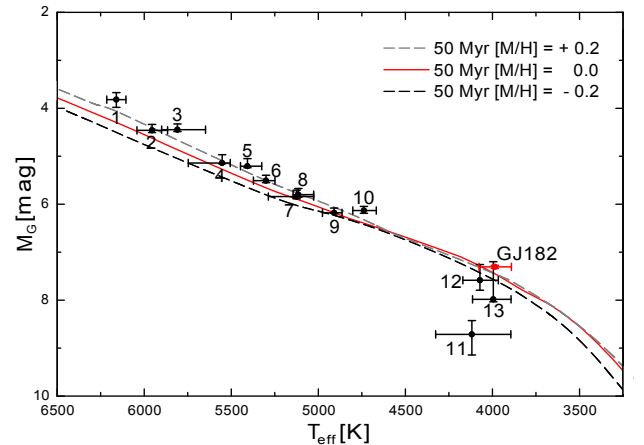


FIGURE 5 The dwarf stars of our sample and GJ 182 (in red) are plotted in the Hertzsprung-Russell diagram with 50 Myr isochrones for different metallicities [M/H] using the stellar evolutionary models of Bressan et al. (2012).

Spectroscopic investigations are necessary to get more precise age estimates. Therefore, the equivalent widths and T_{eff} of all identified dwarfs with a significantly detected Li (6708 Å) line in their spectra were compared to equivalent width distributions of clusters with known ages as seen in Figure 6 (cluster data from E. Mamajek, priv. communication). The curves are polynomial fits to observed T_{eff} vs. $\log_{10}(EW_{\text{Li}})$

data of each cluster, for example α Per (90 Myr) and Hyades (625 Myr). E. Mamajek's plot can be found online⁴ and is based on Neuhäuser (1997).

In Figure 6, HIP 44458 (#3 in Table 5), HIP 115147 (#8) and HIP 46816 (#9) are only consistent with the 50 Myr curve and therefore their age is estimated to ~ 50 Myr. For the same reason we specify HIP 46843 (#6) as ~ 90 Myr old and HIP 63742 (#7) as ~ 175 Myr, respectively. As stated by Soderblom, Hillenbrand, Jeffries, Mamajek, & Naylor (2014) the age errors for this method appear to be 10% – 20% and the detection of lithium in a low-mass star with known effective temperature gives an upper limit to its age. HIP 60831 (#1) and HIP 107350 (#2) cross within their uncertainties, more than one curve and because of that their ages are specified by the range from 50 Myr to 120 Myr. In an analogous way, HIP 544 (#4) is about 175 ... 250 Myr old and HIP 120005 (#13) about 120 ... 250 Myr. In the case of HIP 45963 (#10) within its uncertainties it crosses no curve and therefore the next nearby two were set as limits of its age estimation, namely 220 Myr and 500 Myr.

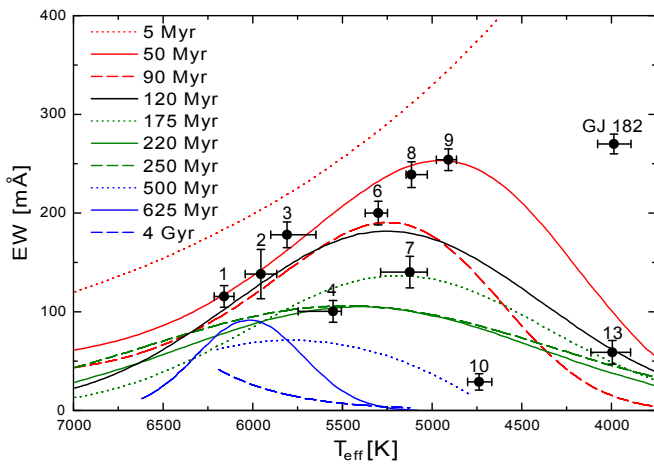


FIGURE 6 Lithium as age indicator for our ten youngest FGKM stars and GJ 182. We show the equivalent widths of the Li (6708 Å) line over the effective temperature for different age curves, that are based on fits done by Eric Mamajek. The derived ages are given in Table 5.

6 | DISCUSSION

We searched for young runaway star candidates within a sample of 308 selected stars from the catalogue *Young runaway*

stars within 3 kpc by Tetzlaff et al. (2011) and estimated the age of the dwarf stars by measuring the equivalent width of the Li (6708 Å) line in their spectra as well as by comparing their location in the HRD with isochrones of stellar evolutionary models. This comparison relies on data from the *Gaia* DR2 catalogue. In total, the sample consists of 4 F-type, 43 G-type, 208 K-type and 53 M-type stars, as derived from their effective temperatures according to the relations by Damiani et al. (2016).

According to their position in the HRD, 295 targets turned out to be giant stars. If objects were located close to the edge of the giant branch, their effective temperatures and radii were compared to those of known dwarfs for an explicit assignment. For example the classification of HIP 118077 as an evolved star is consistent with the work of Fekel, Tomkin, & Williamson (2010) where both components of this binary were classified inter alia as F5 subgiant stars. The separated spectral lines of both components of this binary system are also detected in our FLECHAS spectrum in Figure 7 and the derived radial velocities agree well with its orbital solution from Imbert (1977).

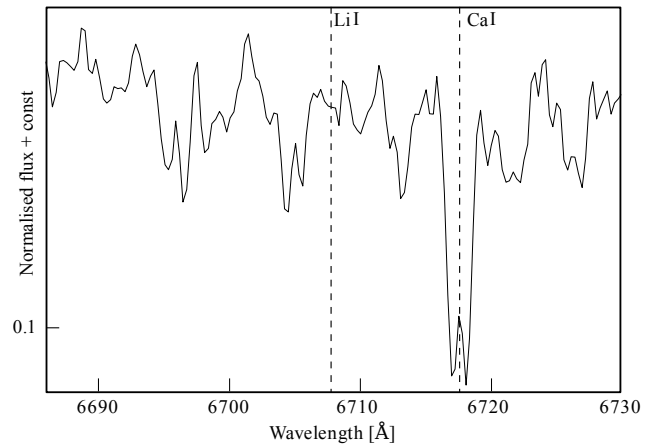


FIGURE 7 The Spectrum of the double-lined binary system HIP 118077 was taken at the Barycentric Julian Date BJD = 2458164.21992. The barycentric corrected radial velocities, that were derived from the Ca (6718 Å) line, are $v_1 = (-12.6 \pm 5.2)$ km/s and $v_2 = (34.2 \pm 4.5)$ km/s, respectively.

The identification of the 13 dwarfs as such is consistent with the results of Anders et al. (2019) given in the *StarHorse* catalogue, where all these objects are listed with a surface gravity $\log(g[\text{cm/s}^2]) > 3.8$. In reverse, the remaining targets from our sample that are actually included in *StarHorse* catalogue are confirmed as giants due to their $\log(g[\text{cm/s}^2]) < 3.8$.

In order to identify possible young runaway star candidates in our sample, we searched for objects that are younger than

⁴<http://www.pas.rochester.edu/~emamajek/images/li.jpg>

TABLE 5 Our dwarf stars with their numbers as shown in Figure 2 and Figure 6 listed with their SpT derived from their T_{eff} using the SpT- T_{eff} -relation from Damiani et al. (2016), their distances d according to Bailer-Jones et al. (2018), the measured equivalent width of the Hydrogen Balmer line $EW_{H\alpha}$ (all in absorption) and the measured equivalent width of Li (6708 Å) EW_{Li} . Furthermore, we list the estimated age derived from the position in the HRD (**lower limit**), as well as the age according to the lithium test (**upper limit**) from this work and the age from Tetzlaff et al. (2011).

id. nr.	Target	SpT *	d [pc] Bailer-Jones	$EW_{H\alpha}$ [mÅ] *	EW_{Li} [mÅ] *	age (HRD) [Myr] *	age (EW_{Li}) [Myr] *	age [Myr] Tetzlaff
1	HIP 60831	F6 V	45.5 ± 0.1	1898 ± 23	116 ± 11	> 10	50 ... 120	20.0 ± 6.7
2	HIP 107350	F8 V	18.1 ± 0.1	907 ± 31	138 ± 25	> 20	50 ... 120	29.1 ± 7.9
3	HIP 44458	G0 V	30.2 ± 0.1	1428 ± 27	178 ± 13	> 10	~ 50	27.0 ± 4.7
4	HIP 544	G5 V	13.8 ± 0.1	1339 ± 16	100 ± 11	> 20	175 ... 250	20.1 ± 6.4
5	HIP 59280	G8 V	25.1 ± 0.1	1442 ± 17	-	> 20	-	20.1 ± 6.4
6	HIP 46843	G8 V	18.1 ± 0.1	1135 ± 20	200 ± 12	> 30	~ 90	51.9 ± 23.1
7	HIP 63742	K0 V	20.5 ± 0.4	879 ± 24	140 ± 16	> 30	~ 175	40.9 ± 9.9
8	HIP 115147	K0 V	19.0 ± 0.1	261 ± 13	239 ± 13	> 30	~ 50	30.3 ± 14.5
9	HIP 46816	K2 V	18.3 ± 0.1	75 ± 11	254 ± 11	> 30	~ 50	51.9 ± 17.5
10	HIP 45963	K2 V	23.4 ± 0.1	$159 \pm 11; 141 \pm 11^\dagger$	29 ± 8	> 20	220 ... 500	15.0 ± 4.8
11	HIP 94761	K5 V	5.91 ± 0.01	571 ± 25	-	> 50	-	≤ 0.1
12	HIP 45343	K7 V	6.33 ± 0.01	549 ± 10	-	> 20	-	28.2 ± 3.0
13	HIP 120005	K7 V	6.33 ± 0.01	555 ± 11	59 ± 12	> 10	120 ... 250	51.1 ± 32.0

* this work

† both $H\alpha$ -lines of this spectroscopic binary could be measured

50 Myr via isochrone fitting. We compared their location in the HRD to isochrones based on models of Bressan et al. (2012) assuming solar metallicity. This assumption is justified, because all 13 dwarfs are nearby stars with distances $d < 50$ pc and their metallicities in the VizieR databases scatter around solar one. Possible metallicity effects on the isochrones due to the scatter of $\sigma[\text{M}/\text{H}] = \pm 0.2$ have no significant impact, as explained in section 5. Due to their location in the HRD, illustrated in Figure 2 and Figure 4, they are all clearly older than 10 Myr.

Hereby, we also consider the multiplicity of HIP 45963 (#10) as spectroscopic binary consisting of two stars with equal mass, as described by Halbwegs, Mayor, & Udry (2018). The individual components are about 0.75 mag fainter than given by *Gaia* DR2, because of its equal mass binary nature. Its spectrum was taken at the BJD = 2458175.48525 and the barycentric corrected radial velocities, that were again derived from the Ca (6718 Å) line, are $v_1 = (-60.1 \pm 1.2)$ km/s and $v_2 = (51.7 \pm 1.5)$ km/s, respectively. These velocities agree well with the orbital solution from Halbwegs et al. (2018).

However, isochrone fitting can only give a lower limit on the age, because all dwarfs in our sample are consistent with the main sequence within their uncertainties of 2σ .

Another main part of this article was to search for lithium in the spectra of our targets in order to have an additional age indicator besides isochrone fitting. Therefore, we measured the equivalent width of the Li (6708 Å) lines. The strongest

Li (6708 Å) line was measured in the spectrum of HIP 41221 with an equivalent width of (331 ± 10) mÅ. HIP 27778, HIP 40628, HIP 43030, HIP 80941 and HIP 102377 are further examples of lithium rich giants that possess an $EW_{\text{Li}} \geq 200$ mÅ. In contrast to this, HIP 21408, HIP 46977, HIP 64543, and HIP 96966 are examples for giants without any significant detection of the Li (6708 Å) line.

The measured equivalent widths of the lithium lines in the TRES spectra are in good agreement with the data from FLECHAS and are all consistent within 3σ as seen in Table 3. The additional TRES spectra of the remaining 14 stars were not taken into account because of too low SNR around the Li (6708 Å) line.

HIP 59280 (#5), HIP 94761 (#11) and HIP 45343 (#12) are dwarfs without significant detection of the Li (6708 Å) line. The other dwarf stars showed significant lithium at 6708 Å in their spectra. Their equivalent widths were converted into abundances by using the curves of growth from Soderblom et al. (1993). Ramírez, Fish, Lambert, & Allende Prieto (2012) also present lithium abundances for HIP 544 and HIP 107350 in their catalogue, namely $\log(N_{\text{Li}}) = 2.38 \pm 0.04$ and $\log(N_{\text{Li}}) = 2.93 \pm 0.11$, respectively. These abundances agree well with the corresponding values in Table 4 from this study.

The equivalent width measurements of the Li (6708 Å) lines and the corresponding effective temperatures of the dwarf stars were then compared to those of clusters with known age

as seen in Figure 6. These lithium based ages for HIP 44458 (#3), HIP 46816 (#9), HIP 60831 (#1), HIP 115147 (#8) and HIP 107350 (#2) in Figure 6 are in good agreement with the derived ages from their location in the HRD in Figure 4 as well as with the values from the Tetzlaff catalogue. These five stars can be classified as young according to Tetzlaff et al. (2011) and also from the methods presented in this paper. HIP 46843 (#6) is located between the 50- and 90 Myr-curve in Figure 6 and the classification of its age with ~ 90 Myr is also consistent with (51.9 ± 23.1) Myr from Tetzlaff et al. (2011).

In the cases of HIP 544 (#4) and HIP 63742 (#7) the estimated values from the lithium method and the HRD, suggest that these stars are significantly older than determined by Tetzlaff et al. (2011). Both targets were ranked as gold flag by *Gaia* photometry and the differences between the parallaxes of *Hipparcos* and *Gaia* are negligible. Our lithium derived age for HIP 544 agrees well with the range of (200 ± 100) Myr from Ramírez et al. (2012).

HIP 120005 (#13) was considered as 120 to 250 Myr old from the estimation of the Li (6708 \AA) equivalent width. However, for cooler temperatures as seen in Figure 6, five different curves are close together and therefore HIP 120005 could, within its error bars, still be in agreement with the derived age of (51.1 ± 32.0) Myr by Tetzlaff et al. (2011). This is also supported by its position in Figure 4 that suggests an age > 10 Myr.

As mentioned above, HIP 45963 (#10) is a spectroscopic binary consisting of two stars with equal mass. This can be confirmed by our equivalent width measurements of the $H\alpha$ -line in Table 5. The spectral lines of both components are visible and comparable to each other. This can be also found in its spectrum for the Ca (6718 \AA) line as illustrated in the appendix. However, the Li (6708 \AA) line shows no splitting. In that case the derived measurement of $(29 \pm 8) \text{ m\AA}$ is more likely an upper limit due its equal mass components. Its age range of 220 Myr to 500 Myr should be taken with care, because the lithium method does not give very reliable age estimations below 20 Myr and above 200 Myr (Soderblom et al., 2014). However, our derived ages for HIP 45963 disagree with the estimate of (15.0 ± 4.8) Myr, from Tetzlaff et al. (2011).

Another example where we found a significant difference compared to the age from Tetzlaff et al. (2011) is HIP 94761 (#11). From its position in Figure 4 it is expected to be at least older than 50 Myr, which significantly differs from the age estimate of about 0.1 Myr by Tetzlaff et al. (2011). An age of 5 Gyr for HIP 94761 was also given by Passegger et al. (2019).

Further dwarfs without showing lithium in their spectra are HIP 45343 (#12) and HIP 59280 (#5). These two objects were estimated to be older than 20 Myr due to their position in

the HRD in Figure 4 and are compatible with the ages from Tetzlaff et al. (2011).

Furthermore, we compare our targets with the young runaway star GJ 182 (HIP 23200) as seen in Figure 4 and Figure 6. For this star, we also used the *Gaia* DR2 data as described above, and adopted the equivalent width of $(270 \pm 10) \text{ m\AA}$ for the Li (6708 \AA) line from C. A. O. Torres et al. (2006). This object is slightly younger than our targets, as shown in Table 6, and given its distance of $(24.38 \pm 0.02) \text{ pc}$, there is no other star known, that is younger and nearer than GJ 182. Our age estimations for GJ 182 are in good agreement with common values as seen in Table 6.

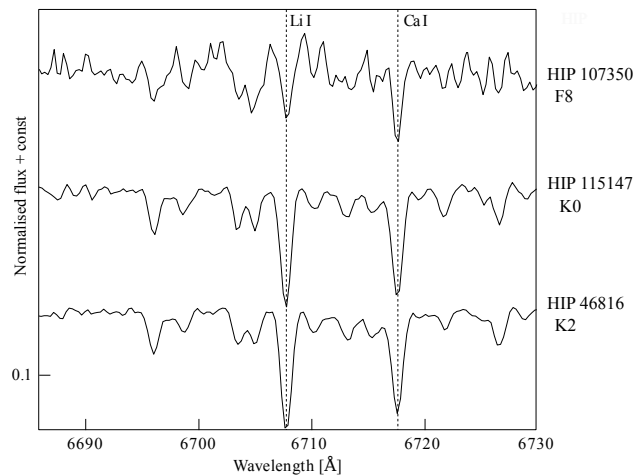


FIGURE 8 Spectra of the three young and very nearby runaway stars.

TABLE 6 Ages and used determination methods for GJ 182 as well as their references.

age [Myr]	method	ref.
8 ... 20	HRD isochrone fitting	Z 01
0.1 ... 14.3	HRD isochrone fitting	T 11
17 ... 26	kinematic & activity/rotation indicators	B 14
17 ... 25	lithium test for moving group members	BJ 14
21 ... 27	HRD isochrone fitting	B 15
20 ... 50	HRD isochrone fitting & lithium test	this work

References: Z 01 (Zuckerman, Song, Bessell, & Webb, 2001); T 11 (Tetzlaff et al., 2011); B 14 (Brandt et al., 2017); BJ 14 (Binks & Jeffries, 2014); B 15 (Bell, Mamajek, & Naylor, 2015)

This study provides a large database of spectra which will be made available in the *VizieR* database together with the measured equivalent widths of the Li (6708 Å) line, after publication. Furthermore, we identified HIP 107350 (#2), HIP 115147 (#8) and HIP 46816 (#9) as runaway stars with comparable ages to GJ 182, while they are even closer to Earth. That would mean that these three objects are now the nearest known young runaway stars so far. Their spectra are shown in Figure 8.

HIP 60831 (#1) and HIP 44458 (#3) are further examples of classified young runaway stars in this study. These five young targets are suitable for follow-up investigation of their origin from either dynamical or supernova ejection. Further five objects were identified to range between 50 Myr and 500 Myr, while three other are main sequence stars. The remaining 295 targets are giants according to their position in the HRD as well as their radii, effective temperatures and $\log(g)$.

ACKNOWLEDGMENTS

We thank all observers who have been involved in some of the observations of this project, obtained at the University Observatory Jena, in particular H. Gilbert, A. Pannicke, D. Wagner, J. Greif, S. Masda and F. Schiefeneder. We also thank P. Berlind, M. Calkins, and G. Esquerdo for their expert assistance in obtaining the TRES observations, and J. Mink for maintaining the Center for Astrophysics echelle database.

This publication makes use of data products of the *VizieR* databases, operated at CDS, Strasbourg, France. We also thank the *Gaia* Data Processing and Analysis Consortium of the European Space Agency (ESA) for processing and providing the data of the *Gaia* mission.

We thank Eric Mamajek for providing the curves of lithium as age indicator for FGKM stars.

This work was supported by the Deutsche Forschungsgemeinschaft with financing the projects *NE 515/58-1* and *MU 2695/27-1*.

How cite this article: R. Bischoff, M. Mugrauer, G. Torres, et al. (2020), Identification of young nearby runaway stars based on *Gaia* data and the lithium test, *Astron. Nachr.*, 2020.

APPENDIX A: ADDITIONAL TARGET INFORMATION

TABLE A1 Observation log. For each target we list the date and mid-time of the observation, as well as the individual exposure time (T_{exp}) of each FLECHAS spectrum and the signal-to-noise ratios (SNR) of the three combined spectra, as measured at $\lambda = 6700$ Å.

Target	Date [UT]	T_{exp} [s]	SNR
HIP 410	2018 Feb 23, 18:24	300	112
HIP 544	2018 Feb 23, 18:43	300	133
HIP 695	2018 Feb 05, 20:26	300	123
HIP 926	2018 Mar 02, 18:15	600	50
HIP 1008	2018 Feb 23, 19:05	450	114
HIP 1118	2018 Feb 23, 19:29	300	108
HIP 1352	2018 Feb 23, 19:48	300	146
HIP 1479	2018 Apr 08, 20:36	1200	149
HIP 1486	2018 Feb 24, 20:34	300	130
HIP 2537	2018 Feb 24, 20:53	300	125
HIP 2583	2018 Mar 01, 18:10	300	112
HIP 2838	2018 Apr 08, 21:38	1200	143
HIP 3083	2015 Dec 03, 21:48	300	217
HIP 3360	2018 Mar 01, 18:33	450	78
HIP 3649	2018 Feb 24, 21:12	300	206
HIP 3693	2018 Feb 01, 20:19	150	382
HIP 3779	2018 Mar 01, 19:03	600	107
HIP 4477	2018 Feb 25, 21:23	450	115
HIP 4961	2018 Feb 24, 21:31	300	140
HIP 5013	2018 Feb 25, 21:50	450	98
HIP 5251	2018 Mar 05, 18:42	300	94
HIP 5372	2018 Feb 01, 20:31	150	320
HIP 5912	2015 Mar 19, 19:18	600	155
HIP 6492	2015 Dec 03, 22:10	300	116
HIP 6811	2018 Feb 25, 22:16	300	118
HIP 7650	2018 Feb 01, 20:41	150	172
HIP 8321	2018 Feb 25, 22:38	300	91
HIP 8979	2015 Apr 20, 21:23	600	154
HIP 9077	2018 Mar 05, 19:05	450	86
HIP 9357	2015 Apr 20, 22:37	600	80
HIP 10855	2018 Apr 06, 19:47	450	104
HIP 11460	2018 Apr 06, 21:10	900	102
HIP 12686	2018 Feb 01, 22:37	150	140
HIP 13098	2018 Feb 28, 19:24	600	102
HIP 13160	2018 Feb 22, 18:19	300	110
HIP 13462	2018 Feb 28, 19:00	300	138
HIP 13645	2018 Feb 28, 18:41	300	122
HIP 13700	2018 Feb 24, 02:33	300	196
HIP 13962	2018 Feb 27, 21:19	300	131
HIP 14350	2015 Mar 19, 20:29	600	190

Continued			
Target	Date [UT]	T_{exp} [s]	SNR
HIP 14382	2018 Feb 01, 22:47	150	229
HIP 15219	2018 Feb 08, 23:15	150	153
HIP 15795	2018 Feb 28, 19:54	300	122
HIP 15890	2018 Feb 02, 00:49	150	250
HIP 16019	2018 Feb 27, 21:43	600	133
HIP 16165	2018 Mar 05, 21:28	300	70
HIP 16489	2018 Feb 01, 20:52	150	148
HIP 17064	2015 Feb 28, 21:06	600	127
HIP 17342	2018 Feb 12, 23:53	150	145
HIP 18088	2018 Feb 13, 00:05	300	105
HIP 18488	2018 Feb 08, 23:31	150	144
HIP 19057	2018 Feb 27, 22:46	600	86
HIP 19679	2018 Feb 27, 17:42	300	135
HIP 20426	2018 Feb 28, 21:37	450	84
HIP 20513	2018 Feb 28, 20:26	300	111
HIP 20776	2015 Apr 12, 22:43	600	275
HIP 20958	2018 Feb 28, 17:53	300	120
HIP 20974	2015 Feb 26, 01:37	600	235
HIP 21408	2018 Feb 21, 22:07	300	115
HIP 21476	2018 Feb 05, 21:32	150	281
HIP 21601	2015 Feb 26, 02:14	600	205
HIP 22154	2015 Apr 19, 20:56	600	134
HIP 22261	2018 Apr 07, 20:50	900	163
HIP 22453	2018 Feb 05, 21:42	150	219
HIP 22928	2018 Feb 24, 22:32	600	158
HIP 23268	2018 Feb 05, 21:56	300	160
HIP 23359	2018 Apr 18, 20:20	900	136
HIP 23360	2018 Feb 24, 23:07	600	120
HIP 23582	2015 Mar 17, 23:55	300	160
HIP 23766	2018 Jan 27, 20:05	150	89
HIP 24303	2015 Mar 19, 22:11	600	114
HIP 24716	2018 Mar 01, 20:47	600	104
HIP 24914	2018 Jan 27, 20:24	150	121
HIP 25184	2015 Feb 28, 20:27	600	238
HIP 25226	2018 Feb 05, 22:15	300	114
HIP 25386	2018 Apr 06, 21:59	900	101
HIP 25668	2018 Feb 23, 21:57	450	106
HIP 25877	2015 Apr 12, 21:32	600	72
HIP 26070	2016 Feb 03, 20:27	300	77
HIP 26386	2018 Jan 27, 20:44	150	59
HIP 26743	2018 Mar 01, 20:01	450	97
HIP 27227	2015 Mar 17, 23:31	300	121
HIP 27750	2018 Jan 27, 21:14	150	69
HIP 27778	2018 Feb 05, 22:34	300	149
HIP 27989	2018 Jan 27, 21:01	10	117
HIP 28185	2018 Feb 23, 23:26	600	113

Continued			
Target	Date [UT]	T_{exp} [s]	SNR
HIP 28366	2015 Feb 26, 03:33	600	98
HIP 30341	2015 Feb 20, 20:49	300	118
HIP 32094	2018 Feb 18, 20:46	300	139
HIP 32276	2015 Feb 20, 21:09	300	81
HIP 32631	2018 Feb 21, 22:34	450	109
HIP 33515	2018 Apr 08, 19:11	300	96
HIP 33789	2015 Feb 20, 21:27	300	155
HIP 33927	2015 Feb 20, 21:46	300	303
HIP 33937	2015 Feb 20, 22:04	300	263
HIP 34026	2015 Feb 20, 22:23	300	110
HIP 34055	2015 Feb 20, 22:42	300	233
HIP 34909	2015 Feb 20, 23:02	300	402
HIP 35537	2015 Mar 16, 22:56	900	125
HIP 35551	2018 Jan 30, 21:56	300	91
HIP 35796	2015 Feb 20, 23:22	300	133
HIP 36041	2015 Feb 20, 23:41	300	287
HIP 36629	2018 Mar 19, 19:26	300	68
HIP 37104	2018 Mar 19, 19:49	450	103
HIP 39398	2015 Apr 22, 20:59	600	102
HIP 39958	2018 Feb 08, 23:47	300	109
HIP 40628	2015 Apr 22, 20:20	600	112
HIP 41221	2018 Mar 19, 20:18	450	110
HIP 41283	2018 Apr 10, 23:08	1200	99
HIP 41704	2018 Jan 30, 23:00	150	361
HIP 41896	2015 Feb 21, 00:01	300	109
HIP 42211	2018 Apr 08, 22:44	1200	126
HIP 42331	2018 Feb 26, 23:45	600	80
HIP 42580	2018 Mar 24, 20:44	900	122
HIP 42876	2018 Feb 21, 00:32	450	136
HIP 43030	2018 Feb 21, 01:00	450	125
HIP 44231	2018 Jan 30, 23:16	300	125
HIP 44458	2018 Feb 21, 02:55	450	85
HIP 44580	2018 Apr 07, 19:20	600	120
HIP 44784	2018 Apr 04, 23:24	900	111
HIP 44831	2018 Feb 21, 01:57	450	99
HIP 45104	2018 Feb 25, 00:43	600	133
HIP 45105	2018 Apr 05, 23:33	900	77
HIP 45343	2018 Feb 25, 01:17	600	137
HIP 45963	2018 Feb 25, 23:32	600	111
HIP 46207	2018 Mar 19, 21:18	900	126
HIP 46693	2018 Feb 14, 03:51	450	133
HIP 46816	2018 Apr 07, 19:59	900	114
HIP 46843	2018 Feb 09, 00:44	450	105
HIP 46977	2018 Jan 30, 23:35	150	113
HIP 47193	2018 Feb 01, 23:02	150	331
HIP 48851	2018 Feb 21, 03:23	450	110

Continued			
Target	Date [UT]	T_{exp} [s]	SNR
HIP 48921	2018 Feb 21, 02:26	450	100
HIP 49688	2018 Feb 06, 00:17	300	182
HIP 49729	2018 Feb 05, 23:51	300	109
HIP 50310	2018 Mar 24, 22:32	900	119
HIP 50999	2018 Apr 17, 20:29	1200	118
HIP 51973	2018 Feb 09, 01:37	450	117
HIP 52032	2018 Feb 06, 00:37	300	153
HIP 52098	2018 Feb 02, 01:02	150	253
HIP 52373	2018 Feb 15, 01:14	450	169
HIP 52556	2018 Feb 22, 00:26	600	117
HIP 52831	2018 Mar 19, 22:21	900	130
HIP 53831	2018 Feb 26, 00:01	600	129
HIP 54024	2018 Feb 09, 01:10	450	119
HIP 55193	2018 Feb 05, 01:58	300	91
HIP 55682	2018 Feb 05, 02:19	300	139
HIP 55945	2018 Feb 02, 01:17	150	210
HIP 56383	2018 Feb 06, 00:55	300	25
HIP 57240	2018 Feb 06, 01:14	300	209
HIP 57261	2018 Apr 06, 22:51	900	111
HIP 58217	2018 Feb 09, 02:05	450	112
HIP 58313	2018 Apr 08, 23:48	1200	143
HIP 58661	2018 Feb 06, 01:34	300	120
HIP 59280	2018 Feb 22, 01:41	600	121
HIP 59501	2018 Feb 02, 01:28	150	153
HIP 59760	2018 Feb 09, 02:31	450	111
HIP 60731	2018 Feb 14, 02:02	450	141
HIP 60831	2018 Feb 14, 04:16	450	104
HIP 61290	2018 Feb 09, 03:01	450	117
HIP 61617	2018 Apr 07, 22:41	1200	132
HIP 61799	2018 Apr 09, 23:43	1200	122
HIP 62455	2018 Feb 15, 01:42	450	123
HIP 62595	2018 Apr 07, 23:48	1200	109
HIP 63356	2018 Feb 06, 01:53	300	117
HIP 63368	2018 Mar 29, 23:18	900	94
HIP 63742	2018 Feb 27, 00:21	600	61
HIP 63803	2018 Feb 14, 02:29	450	139
HIP 64149	2018 Mar 30, 00:07	900	155
HIP 64523	2018 Apr 06, 00:24	900	107
HIP 64543	2018 Feb 06, 02:13	300	120
HIP 65192	2018 Mar 19, 23:45	900	136
HIP 65435	2018 Feb 27, 01:01	600	96
HIP 65915	2018 Apr 11, 00:19	1200	108
HIP 66467	2018 Feb 09, 04:23	450	133
HIP 66690	2018 Feb 02, 03:58	300	174
HIP 67300	2018 Feb 02, 04:23	300	127
HIP 67385	2018 Feb 09, 04:01	300	113

Continued			
Target	Date [UT]	T_{exp} [s]	SNR
HIP 68879	2018 Feb 27, 01:38	600	113
HIP 68904	2018 Feb 27, 23:27	600	107
HIP 69624	2018 Apr 09, 00:53	1200	160
HIP 70000	2018 Apr 08, 00:51	1200	110
HIP 70108	2018 Feb 02, 04:45	300	127
HIP 70145	2018 Feb 02, 05:05	300	145
HIP 70349	2018 Feb 09, 04:50	450	148
HIP 71436	2018 Feb 28, 00:36	600	129
HIP 72499	2018 Feb 06, 03:23	300	127
HIP 72578	2018 Feb 06, 02:32	300	119
HIP 73977	2018 Feb 14, 04:40	300	164
HIP 74070	2018 Apr 06, 01:14	900	96
HIP 74425	2018 Feb 14, 04:59	450	144
HIP 74938	2018 Apr 12, 00:53	1200	155
HIP 75257	2018 Feb 02, 01:41	150	181
HIP 76733	2018 Feb 06, 03:55	300	146
HIP 76947	2018 Apr 06, 23:43	900	143
HIP 77092	2018 Mar 01, 01:43	600	120
HIP 77178	2018 Feb 28, 22:34	600	111
HIP 78802	2018 Apr 18, 22:41	1200	142
HIP 79187	2018 Feb 21, 03:52	300	105
HIP 79357	2018 Feb 02, 01:53	150	132
HIP 80021	2018 Feb 06, 04:15	300	173
HIP 80941	2018 Apr 19, 22:03	1200	116
HIP 81104	2018 Feb 14, 02:56	450	157
HIP 81289	2018 Feb 02, 03:09	150	145
HIP 81922	2018 Apr 19, 23:58	1200	136
HIP 82324	2018 Feb 06, 04:36	300	141
HIP 82385	2018 Feb 14, 03:22	450	118
HIP 82504	2018 Feb 02, 03:20	150	213
HIP 82604	2018 Feb 17, 02:33	300	62
HIP 83254	2018 Feb 02, 03:30	150	147
HIP 84038	2018 Feb 28, 23:28	600	116
HIP 84239	2018 Apr 20, 22:30	1200	122
HIP 84380	2018 Feb 06, 03:43	30	238
HIP 84671	2018 Feb 02, 05:42	150	237
HIP 85200	2018 Apr 20, 23:50	1200	143
HIP 85560	2018 Feb 28, 01:13	600	120
HIP 86153	2018 Feb 06, 04:55	300	173
HIP 86476	2018 Mar 20, 03:42	300	185
HIP 86483	2018 Apr 21, 23:30	450	89
HIP 86625	2018 Mar 25, 02:19	600	127
HIP 86709	2018 Feb 22, 02:43	450	119
HIP 87107	2018 Apr 22, 00:01	600	92
HIP 87244	2018 Apr 22, 02:44	600	141
HIP 87251	2018 Mar 20, 01:31	600	134

Continued			
Target	Date [UT]	T_{exp} [s]	SNR
HIP 88411	2018 May 01, 22:20	1200	97
HIP 88518	2018 Feb 15, 02:36	450	88
HIP 88984	2018 May 26, 00:55	450	105
HIP 91200	2018 Feb 21, 04:12	300	110
HIP 92249	2018 May 04, 21:42	1200	117
HIP 92404	2018 Mar 01, 02:19	600	89
HIP 92651	2018 Mar 25, 01:16	600	112
HIP 92713	2018 Feb 21, 04:33	300	134
HIP 93801	2018 May 26, 01:22	300	90
HIP 93913	2018 Mar 20, 00:54	600	73
HIP 94220	2018 May 05, 01:25	450	82
HIP 94229	2018 Apr 06, 02:51	600	116
HIP 94518	2018 Apr 23, 22:39	1200	104
HIP 94761	2015 Sep 24, 18:58	600	43
HIP 95297	2018 Apr 29, 21:57	1200	97
HIP 95744	2018 Feb 22, 03:31	450	100
HIP 96203	2018 May 06, 21:58	1200	129
HIP 96966	2018 May 07, 01:29	1200	105
HIP 97135	2015 Apr 23, 01:39	600	186
HIP 97198	2015 Sep 24, 19:32	600	42
HIP 97359	2018 Mar 02, 04:06	450	107
HIP 97402	2015 Sep 24, 20:00	300	161
HIP 98073	2018 Feb 02, 03:42	150	243
HIP 98443	2015 Sep 24, 20:57	300	82
HIP 98610	2015 Apr 23, 23:26	600	161
HIP 98762	2015 Apr 23, 22:07	600	126
HIP 99853	2018 Feb 23, 05:18	150	139
HIP 100172	2018 Mar 02, 04:36	600	75
HIP 100180	2018 May 05, 21:53	1200	130
HIP 100390	2018 Mar 25, 03:45	300	136
HIP 100534	2018 May 07, 22:15	900	127
HIP 100684	2018 Mar 01, 04:14	600	86
HIP 101219	2018 May 05, 02:19	600	116
HIP 101412	2018 Feb 23, 01:36	300	124
HIP 101692	2018 May 29, 01:41	150	182
HIP 101841	2018 May 06, 00:15	600	141
HIP 101953	2018 Apr 30, 01:31	450	82
HIP 102377	2018 Feb 01, 18:43	300	115
HIP 102440	2018 May 26, 01:43	300	167
HIP 102912	2018 Feb 23, 03:05	300	104
HIP 103035	2018 Feb 23, 01:59	450	88
HIP 103242	2018 Apr 30, 01:52	300	124
HIP 103263	2018 Feb 01, 19:01	300	80
HIP 103637	2018 Feb 24, 03:51	300	101
HIP 103868	2018 Jun 04, 01:28	300	121
HIP 104172	2018 Mar 30, 02:37	300	119

Continued			
Target	Date [UT]	T_{exp} [s]	SNR
HIP 105182	2018 Feb 23, 03:29	450	99
HIP 105205	2018 May 29, 00:18	300	117
HIP 105669	2018 Feb 27, 03:46	600	98
HIP 105949	2018 Feb 01, 19:19	300	249
HIP 106306	2018 May 29, 00:37	300	123
HIP 106848	2018 Feb 24, 04:43	450	94
HIP 106973	2018 Feb 24, 05:06	300	105
HIP 106974	2018 Jun 04, 00:24	450	126
HIP 107205	2018 Feb 27, 04:21	600	109
HIP 107259	2018 Feb 07, 17:08	150	464
HIP 107315	2018 May 31, 00:55	30	113
HIP 107325	2018 May 08, 21:41	1200	117
HIP 107350	2018 May 31, 01:03	150	39
HIP 107723	2018 Feb 05, 18:15	300	152
HIP 107923	2018 May 06, 01:25	300	163
HIP 108030	2018 Mar 25, 00:18	450	72
HIP 108202	2018 May 08, 01:27	900	123
HIP 108233	2018 May 08, 00:59	300	125
HIP 108296	2018 May 29, 00:55	300	159
HIP 108378	2018 Feb 05, 19:54	300	124
HIP 109247	2018 May 06, 02:10	450	128
HIP 109492	2018 Feb 07, 17:19	150	454
HIP 109602	2018 May 29, 01:11	150	119
HIP 110504	2018 Mar 25, 03:08	300	174
HIP 110991	2018 Feb 13, 17:17	150	380
HIP 110992	2018 Jun 03, 01:14	150	170
HIP 111810	2018 Jun 04, 00:45	150	92
HIP 112098	2018 Feb 24, 18:38	300	205
HIP 112248	2018 Feb 24, 19:05	600	160
HIP 112987	2018 Jun 04, 00:58	300	120
HIP 113561	2018 Feb 05, 20:11	150	120
HIP 113881	2018 Jun 03, 01:02	30	253
HIP 114155	2018 Feb 13, 17:29	150	235
HIP 115147	2018 Feb 27, 20:48	600	93
HIP 117299	2018 Feb 13, 17:39	150	208
HIP 117956	2018 Feb 14, 17:29	150	139
HIP 118077	2018 Feb 14, 17:19	150	147
HIP 120005	2018 Feb 25, 01:51	600	125

TABLE A2 Measured equivalent widths (EW_{Li}) of the Li(6708 Å) line. Targets without significant detection ($EW_{\text{Li}} < 3 \cdot \sigma EW_{\text{Li}}$) are listed with "-"

Target	EW_{Li} [mÅ]	Target	EW_{Li} [mÅ]
HIP 410	–	HIP 59280	–
HIP 544	100 ± 11	HIP 59501	26 ± 7
HIP 695	–	HIP 59760	53 ± 11
HIP 926	–	HIP 60731	21 ± 7
HIP 1008	45 ± 10	HIP 60831	116 ± 11
HIP 1118	–	HIP 61290	38 ± 8
HIP 1352	83 ± 8	HIP 61617	–
HIP 1479	46 ± 6	HIP 61799	–
HIP 1486	–	HIP 62455	61 ± 10
HIP 2537	–	HIP 62595	–
HIP 2583	–	HIP 63356	–
HIP 2838	29 ± 7	HIP 63368	98 ± 11
HIP 3083	47 ± 5	HIP 63742	140 ± 16
HIP 3360	–	HIP 63803	27 ± 8
HIP 3649	–	HIP 64149	38 ± 7
HIP 3693	71 ± 3	HIP 64523	42 ± 10
HIP 3779	38 ± 12	HIP 64543	–
HIP 4477	151 ± 11	HIP 65192	27 ± 7
HIP 4961	–	HIP 65435	–
HIP 5013	57 ± 13	HIP 65915	–
HIP 5251	157 ± 12	HIP 66467	27 ± 8
HIP 5372	46 ± 4	HIP 66690	25 ± 7
HIP 5912	137 ± 6	HIP 67300	43 ± 9
HIP 6492	50 ± 10	HIP 67385	–
HIP 6811	161 ± 11	HIP 68879	–
HIP 7650	43 ± 7	HIP 68904	79 ± 9
HIP 8321	–	HIP 69624	–
HIP 8979	39 ± 6	HIP 70000	–
HIP 9077	64 ± 12	HIP 70108	–
HIP 9357	65 ± 12	HIP 70145	21 ± 7
HIP 10855	–	HIP 70349	48 ± 8
HIP 11460	–	HIP 71436	–
HIP 12686	56 ± 7	HIP 72499	59 ± 9
HIP 13098	27 ± 9	HIP 72578	30 ± 8
HIP 13160	–	HIP 73977	22 ± 6
HIP 13462	33 ± 9	HIP 74070	35 ± 11
HIP 13645	42 ± 8	HIP 74425	21 ± 7
HIP 13700	45 ± 6	HIP 74938	48 ± 7
HIP 13962	–	HIP 75257	43 ± 6
HIP 14350	32 ± 5	HIP 76733	23 ± 7
HIP 14382	25 ± 5	HIP 76947	54 ± 7

Continued

Target	EW_{Li} [mÅ]	Target	EW_{Li} [mÅ]
HIP 15219	27 ± 7	HIP 77092	–
HIP 15795	55 ± 8	HIP 77178	30 ± 9
HIP 15890	87 ± 4	HIP 78802	–
HIP 16019	69 ± 7	HIP 79187	39 ± 10
HIP 16165	–	HIP 79357	24 ± 8
HIP 16489	–	HIP 80021	20 ± 6
HIP 17064	94 ± 7	HIP 80941	242 ± 12
HIP 17342	33 ± 8	HIP 81104	26 ± 7
HIP 18088	–	HIP 81289	31 ± 7
HIP 18488	184 ± 9	HIP 81922	32 ± 8
HIP 19057	–	HIP 82324	–
HIP 19679	–	HIP 82385	–
HIP 20426	44 ± 12	HIP 82504	45 ± 6
HIP 20513	109 ± 10	HIP 82604	63 ± 16
HIP 20776	48 ± 4	HIP 83254	60 ± 8
HIP 20958	45 ± 9	HIP 84038	–
HIP 20974	19 ± 5	HIP 84239	–
HIP 21408	–	HIP 84380	34 ± 5
HIP 21476	44 ± 4	HIP 84671	26 ± 4
HIP 21601	42 ± 6	HIP 85200	30 ± 7
HIP 22154	31 ± 8	HIP 85560	–
HIP 22261	46 ± 6	HIP 86153	35 ± 6
HIP 22453	108 ± 5	HIP 86476	45 ± 6
HIP 22928	39 ± 7	HIP 86483	60 ± 10
HIP 23268	159 ± 7	HIP 86625	29 ± 7
HIP 23359	24 ± 7	HIP 86709	53 ± 9
HIP 23360	–	HIP 87107	39 ± 11
HIP 23582	87 ± 7	HIP 87244	54 ± 7
HIP 23766	–	HIP 87251	–
HIP 24303	76 ± 10	HIP 88411	–
HIP 24716	44 ± 11	HIP 88518	30 ± 10
HIP 24914	37 ± 10	HIP 88984	49 ± 9
HIP 25184	135 ± 5	HIP 91200	–
HIP 25226	40 ± 9	HIP 92249	31 ± 9
HIP 25386	39 ± 10	HIP 92404	44 ± 13
HIP 25668	–	HIP 92651	68 ± 9
HIP 25877	–	HIP 92713	29 ± 8
HIP 26070	–	HIP 93801	–
HIP 26386	–	HIP 93913	–
HIP 26743	61 ± 12	HIP 94220	68 ± 11
HIP 27227	–	HIP 94229	–
HIP 27750	58 ± 14	HIP 94518	–
HIP 27778	266 ± 7	HIP 94761	–
HIP 27989	32 ± 9	HIP 95297	–
HIP 28185	42 ± 10	HIP 95744	31 ± 10
HIP 28366	–	HIP 96203	85 ± 8

Continued			
Target	EW_{Li} [mÅ]	Target	EW_{Li} [mÅ]
HIP 30341	57 ± 11	HIP 96966	–
HIP 32094	91 ± 7	HIP 97135	69 ± 6
HIP 32276	179 ± 14	HIP 97198	–
HIP 32631	32 ± 9	HIP 97359	27 ± 9
HIP 33515	46 ± 11	HIP 97402	–
HIP 33789	38 ± 7	HIP 98073	42 ± 4
HIP 33927	16 ± 4	HIP 98443	–
HIP 33937	82 ± 4	HIP 98610	40 ± 6
HIP 34026	–	HIP 98762	35 ± 8
HIP 34055	23 ± 5	HIP 99853	46 ± 9
HIP 34909	34 ± 3	HIP 100172	–
HIP 35537	–	HIP 100180	43 ± 7
HIP 35551	–	HIP 100390	111 ± 8
HIP 35796	36 ± 9	HIP 100534	35 ± 7
HIP 36041	24 ± 4	HIP 100684	–
HIP 36629	–	HIP 101219	108 ± 8
HIP 37104	–	HIP 101412	50 ± 8
HIP 39398	152 ± 10	HIP 101692	33 ± 6
HIP 39958	–	HIP 101841	76 ± 7
HIP 40628	235 ± 9	HIP 101953	34 ± 11
HIP 41221	331 ± 10	HIP 102377	235 ± 10
HIP 41283	36 ± 10	HIP 102440	74 ± 7
HIP 41704	15 ± 3	HIP 102912	30 ± 9
HIP 41896	–	HIP 103035	–
HIP 42211	–	HIP 103242	40 ± 8
HIP 42331	–	HIP 103263	–
HIP 42580	45 ± 10	HIP 103637	–
HIP 42876	42 ± 8	HIP 103868	150 ± 8
HIP 43030	310 ± 9	HIP 104172	–
HIP 44231	140 ± 8	HIP 105182	67 ± 12
HIP 44458	178 ± 13	HIP 105205	–
HIP 44580	67 ± 9	HIP 105669	–
HIP 44784	–	HIP 105949	83 ± 4
HIP 44831	–	HIP 106306	34 ± 8
HIP 45104	176 ± 9	HIP 106848	–
HIP 45105	–	HIP 106973	60 ± 10
HIP 45343	–	HIP 106974	62 ± 9
HIP 45963	29 ± 8	HIP 107205	27 ± 9
HIP 46207	45 ± 8	HIP 107259	25 ± 2
HIP 46693	116 ± 9	HIP 107315	37 ± 10
HIP 46816	254 ± 11	HIP 107325	39 ± 7
HIP 46843	200 ± 12	HIP 107350	138 ± 25
HIP 46977	–	HIP 107723	114 ± 7
HIP 47193	46 ± 3	HIP 107923	114 ± 7
HIP 48851	32 ± 9	HIP 108030	43 ± 14
HIP 48921	–	HIP 108202	93 ± 8

Continued			
Target	EW_{Li} [mÅ]	Target	EW_{Li} [mÅ]
HIP 49688	65 ± 6	HIP 108233	78 ± 9
HIP 49729	–	HIP 108296	161 ± 7
HIP 50310	148 ± 9	HIP 108378	36 ± 9
HIP 50999	55 ± 9	HIP 109247	47 ± 8
HIP 51973	–	HIP 109492	61 ± 3
HIP 52032	25 ± 7	HIP 109602	171 ± 8
HIP 52098	13 ± 4	HIP 110504	57 ± 7
HIP 52373	90 ± 6	HIP 110991	–
HIP 52556	–	HIP 110992	41 ± 6
HIP 52831	60 ± 9	HIP 111810	–
HIP 53831	25 ± 8	HIP 112098	27 ± 5
HIP 54024	–	HIP 112248	58 ± 8
HIP 55193	45 ± 12	HIP 112987	37 ± 9
HIP 55682	89 ± 8	HIP 113561	–
HIP 55945	25 ± 5	HIP 113881	53 ± 4
HIP 56383	101 ± 35	HIP 114155	30 ± 5
HIP 57240	32 ± 5	HIP 115147	239 ± 13
HIP 57261	29 ± 8	HIP 117299	44 ± 6
HIP 58217	50 ± 10	HIP 117956	62 ± 8
HIP 58313	27 ± 7	HIP 118077	–
HIP 58661	–	HIP 120005	59 ± 12

TABLE A3 Physical properties of the targets, as provided by *Gaia* DR2. We list the apparent brightness G , the extinction in the G -band A_G , the effective temperature T_{eff} , stellar radius R , and luminosity L of the target stars (if available). From these parameters together with the distances d by Bailer-Jones et al. (2018), the absolute G -band brightness M_G of the targets was calculated. The last column yields further remarks, with details listed in the footnote of this table.

Target	d [pc]	G [mag]	A_G [mag]	M_G [mag]	T_{eff} [K]	R [R_{\odot}]	L [L_{\odot}]	rem.
HIP 410	157 ⁺³ ₋₃	6.199 ± 0.001	0.116 ^{+0.048} _{-0.048}	0.101 ^{+0.086} _{-0.086}	4968 ⁺⁵⁵ ₋₄₀	11.2 ^{+0.2} _{-0.3}	68.4 ^{+1.4} _{-1.4}	c
HIP 544	13.8 ^{+0.1} _{-0.1}	5.861 ± 0.001	0.025 ^{+0.172} _{-0.014}	5.141 ^{+0.016} _{-0.030}	5552 ⁺¹⁹⁵ ₋₄₆	0.87 ^{+0.02} _{-0.06}	0.651 ^{+0.001} _{-0.001}	
HIP 695	373 ⁺¹⁷ ₋₁₆	6.087 ± 0.001	0.501 ^{+0.196} _{-0.196}	-2.271 ^{+0.290} _{-0.292}	4772 ⁺⁹⁷ ₋₅₁	31.1 ^{+0.7} _{-1.2}	451 ⁺²³ ₋₂₃	c
HIP 926	530 ⁺¹² ₋₁₂	6.834 ± 0.001	0.823 ^{+0.767} _{-0.435}	-2.610 ^{+0.485} _{-0.485}	4068 ⁺⁶⁷ ₋₁₁₄	50.8 ^{+3.0} _{-1.6}	636 ⁺²¹ ₋₂₁	
HIP 1008	515 ⁺¹⁶ ₋₁₅	6.869 ± 0.001	0.616 ^{+1.176} _{-0.255}	-2.307 ^{+0.320} _{-0.321}	4175 ⁺¹⁴⁹ ₋₂₀₀	44.7 ^{+4.6} _{-3.0}	546 ⁺²² ₋₂₂	
HIP 1118	317 ⁺⁸ ₋₇	6.565 ± 0.001	0.467 ^{+1.599} _{-0.403}	-1.405 ^{+0.455} _{-0.455}	4623 ⁺¹⁶⁷ ₋₆₅	23.1 ^{+0.7} _{-1.6}	220 ⁺⁷ ₋₇	
HIP 1352	560 ⁺³³ ₋₃₀	5.516 ± 0.002	0.308 ^{+0.124} _{-0.124}	-3.533 ^{+0.244} _{-0.245}	3717 ⁺¹⁷⁴ ₋₁₁₈	132 ⁺⁹ ₋₁₂	3009 ⁺²⁰⁰ ₋₂₀₀	c
HIP 1479	657 ⁺¹³ ₋₁₃	7.410 ± 0.001	0.511 ^{+0.206} _{-0.206}	-2.187 ^{+0.249} _{-0.250}	3905 ⁺¹⁹² ₋₁₈₅	55.4 ^{+5.6} _{-5.1}	644 ⁺²¹ ₋₂₁	c
HIP 1486	320 ⁺³ ₋₃	6.361 ± 0.001	0.566 ^{+0.605} _{-0.425}	-1.733 ^{+0.449} _{-1.175}	4076 ⁺⁵⁸ ₋₆₇	37.7 ^{+1.3} _{-1.1}	353 ⁺⁶ ₋₆	
HIP 2537	448 ⁺⁹ ₋₉	6.355 ± 0.001	0.595 ^{+1.199} _{-0.230}	-2.495 ^{+0.275} _{-0.276}	4059 ⁺¹²⁴ ₋₁₂₇	53.8 ^{+3.5} _{-3.1}	707 ⁺²¹ ₋₂₁	
HIP 2583	170 ⁺¹ ₋₁	6.014 ± 0.001	0.116 ^{+0.019} _{-0.019}	-0.248 ^{+0.036} _{-0.036}	4969 ⁺⁵⁵ ₋₄₄	13.1 ^{+0.2} _{-0.3}	94.4 ^{+1.0} _{-1.0}	c
HIP 2838	326 ⁺³ ₋₃	7.406 ± 0.001	1.278 ^{+0.316} _{-0.358}	-1.437 ^{+0.377} _{-0.377}	3926 ⁺⁷⁴ ₋₁₉₅	26.8 ^{+2.9} _{-1.0}	154 ⁺² ₋₂	
HIP 3083	414 ⁺²⁷ ₋₂₄	4.779 ± 0.003	0.362 ^{+0.054} _{-0.054}	-3.670 ^{+0.185} _{-0.186}	3965 ⁺²⁷⁵ ₋₇₈	110 ⁺⁴ ₋₁₄	2713 ⁺¹⁸⁷ ₋₁₈₇	c
HIP 3360	208 ⁺³ ₋₃	7.069 ± 0.001	0.024 ^{+0.220} _{-0.020}	0.453 ^{+0.050} _{-0.050}	4805 ⁺⁴⁶ ₋₄₆	10.8 ^{+0.2} _{-0.2}	56.2 ^{+1.0} _{-1.0}	
HIP 3649	643 ⁺¹⁰ ₋₁₀	6.077 ± 0.001	1.090 ^{+0.299} _{-0.299}	-4.054 ^{+0.335} _{-0.335}	4733 ⁺⁸⁹ ₋₆₅	55.7 ^{+1.6} _{-2.0}	1401 ⁺³⁹ ₋₃₉	c
HIP 3693	54.9 ^{+1.1} _{-1.1}	3.676 ± 0.005	0.206 ^{+0.689} _{-0.144}	-0.227 ^{+0.192} _{-0.192}	4535 ⁺¹⁴⁸ ₋₁₂₁	15.9 ^{+0.9} _{-1.0}	96.3 ^{+2.2} _{-2.2}	
HIP 3779	659 ⁺¹⁹ ₋₁₈	6.952 ± 0.001	0.656 ^{+1.142} _{-0.439}	-2.798 ^{+0.498} _{-0.500}	4028 ⁺¹⁹⁶ ₋₉₈	62.0 ^{+3.1} _{-5.6}	912 ⁺³⁷ ₋₃₇	
HIP 4477	1028 ⁺⁷¹ ₋₆₂	6.461 ± 0.001	0.653 ^{+1.069} _{-0.469}	-4.252 ^{+0.606} _{-0.610}	4088 ⁺¹³¹ ₋₉₅	117 ⁺⁶ ₋₇	3423 ⁺²⁹⁰ ₋₂₉₀	
HIP 4961	284 ⁺⁴ ₋₄	5.998 ± 0.001	0.528 ^{+0.675} _{-0.312}	-1.794 ^{+0.343} _{-0.343}	3947 ⁺¹⁵⁷ ₋₁₆₁	43.8 ^{+3.8} _{-3.3}	419 ⁺⁸ ₋₈	
HIP 5013	268 ⁺² ₋₂	6.748 ± 0.001	0.162 ^{+1.322} _{-0.162}	-0.556 ^{+0.182} _{-0.182}	4834 ⁺¹³² ₋₇₈	15.9 ^{+0.5} _{-0.8}	125 ⁺² ₋₂	
HIP 5251	441 ⁺⁹ ₋₈	5.750 ± 0.001	0.400 ^{+0.011} _{-0.011}	-2.875 ^{+0.053} _{-0.053}	4204 ⁺³⁵² ₋₁₈₅	62.5 ^{+5.9} _{-9.3}	1101 ⁺³⁰ ₋₃₀	c
HIP 5372	86.4 ^{+2.2} _{-2.1}	3.799 ± 0.003	0.278 ^{+0.693} _{-0.185}	-1.161 ^{+0.242} _{-0.243}	4513 ⁺⁶² ₋₁₀₅	24.0 ^{+1.2} _{-0.6}	215 ⁺⁶ ₋₆	
HIP 5912	507 ⁺¹⁰ ₋₁₀	6.758 ± 0.001	0.393 ^{+0.159} _{-0.159}	-2.161 ^{+0.201} _{-0.202}	4033 ⁺⁴³⁵ ₋₈₀	51.8 ^{+2.1} _{-9.6}	639 ⁺¹⁹ ₋₁₉	c
HIP 6492	330 ⁺¹⁷ ₋₁₆	5.163 ± 0.003	0.308 ^{+0.031} _{-0.031}	-2.736 ^{+0.140} _{-0.140}	3954 ⁺²⁴⁶ ₋₂₀₃	74.3 ^{+8.3} _{-8.4}	1214 ⁺⁶⁹ ₋₆₉	c
HIP 6811	567 ⁺¹⁰ ₋₁₀	6.178 ± 0.001	1.127 ^{+0.774} _{-0.425}	-3.715 ^{+0.465} _{-0.465}	3828 ⁺²⁶⁶ ₋₁₀₈	89.8 ^{+3.3} _{-11.3}	1560 ⁺⁴⁵ ₋₄₅	
HIP 7650	145 ⁺² ₋₂	4.980 ± 0.002	0.112 ^{+0.061} _{-0.061}	-0.937 ^{+0.093} _{-0.093}	4957 ⁺⁷⁶ ₋₃₄	18.1 ^{+0.3} _{-0.5}	179 ⁺³ ₋₃	c
HIP 8321	325 ⁺⁴ ₋₄	6.452 ± 0.001	0.377 ^{+0.174} _{-0.174}	-1.483 ^{+0.201} _{-0.201}	4795 ⁺⁵⁴ ₋₆₃	22.6 ^{+0.6} _{-0.5}	244 ⁺⁴ ₋₄	c
HIP 8979	357 ⁺⁵ ₋₅	6.110 ± 0.001	0.574 ^{+0.594} _{-0.463}	-2.227 ^{+0.492} _{-0.492}	3836 ⁺¹⁶⁵ ₋₈₁	57.7 ^{+2.5} _{-4.7}	648 ⁺¹³ ₋₁₃	
HIP 9077	644 ⁺¹⁶ ₋₁₅	6.578 ± 0.001	0.658 ^{+0.212} _{-0.212}	-3.124 ^{+0.264} _{-0.265}	4355 ⁺¹⁹² ₋₁₅₇	56.2 ^{+4.3} _{-4.6}	1023 ⁺³⁷ ₋₃₇	c
HIP 9357	568 ⁺¹² ₋₁₁	7.377 ± 0.001	0.384 ^{+0.155} _{-0.155}	-1.780 ^{+0.200} _{-0.201}	4098 ⁺¹²⁷ ₋₁₇₅	41.5 ^{+3.8} _{-2.4}	437 ⁺¹⁴ ₋₁₄	c
HIP 10855	213 ⁺² ₋₂	6.896 ± 0.001	0.439 ^{+0.111} _{-0.111}	-0.180 ^{+0.131} _{-0.131}	4904 ⁺⁶¹² ₋₉₂	11.4 ^{+0.4} _{-2.4}	67.0 ^{+0.9} _{-0.9}	c
HIP 11460	300 ⁺³ ₋₃	7.326 ± 0.001	0.576 ^{+0.550} _{-0.269}	-0.635 ^{+0.290} _{-0.571}	4122 ⁺⁹⁸ ₋₁₄₃	21.8 ^{+1.6} _{-1.0}	124 ⁺² ₋₂	
HIP 12686	99.4 ^{+0.9} _{-0.9}	5.520 ± 0.001	0.042 ^{+0.501} _{-0.032}	0.491 ^{+0.054} _{-0.523}	4689 ⁺⁷⁹ ₋₃₈	11.2 ^{+0.2} _{-0.4}	54.9 ^{+0.6} _{-0.6}	
HIP 13098	298 ⁺⁴ ₋₄	7.203 ± 0.001	0.416 ^{+0.053} _{-0.053}	-0.583 ^{+0.084} _{-0.084}	4692 ⁺⁸³ ₋₅₀	15.6 ^{+0.3} _{-0.5}	106 ⁺² ₋₂	c
HIP 13160	366 ⁺⁶ ₋₅	6.460 ± 0.001	0.063 ^{+0.608} _{-0.047}	-1.420 ^{+0.080} _{-0.642}	4543 ⁺¹⁴⁷ ₋₁₁₉	29.6 ^{+1.6} _{-1.8}	335 ⁺⁷ ₋₇	
HIP 13462	498 ⁺⁹ ₋₉	5.881 ± 0.001	0.916 ^{+0.370} _{-0.370}	-3.521 ^{+0.411} _{-0.412}	4653 ⁺¹⁶⁹ ₋₈₉	49.2 ^{+1.9} _{-3.4}	1023 ⁺²⁹ ₋₂₉	c
HIP 13645	336 ⁺¹⁷ ₋₁₆	5.616 ± 0.002	0.354 ^{+0.044} _{-0.044}	-2.373 ^{+0.151} _{-0.156}	3622 ⁺⁴⁰⁹ ₋₁₇₁	82.2 ^{+8.4} _{-15.8}	1047 ⁺⁵⁹ ₋₅₉	c
HIP 13700	631 ⁺⁴² ₋₃₇	5.214 ± 0.002	0.886 ^{+0.131} _{-0.131}	-4.673 ^{+0.264} _{-0.272}	3849 ⁺³⁶⁷ ₋₂₄₄	153 ⁺²¹ ₋₂₅	4611 ⁺³⁴⁴ ₋₃₄₄	c
HIP 13962	1565 ⁺¹³⁷ ₋₁₁₇	5.937 ± 0.001	0.676 ^{+1.339} _{-0.472}	-5.712 ^{+0.642} _{-1.523}	3788 ⁺¹⁹⁷ ₋₁₉₁	295 ⁺³² ₋₂₈	16132 ⁺¹⁸²⁸ ₋₁₈₂₈	
HIP 14350	651 ⁺¹² ₋₁₂	6.287 ± 0.001	0.780 ^{+0.625} _{-0.316}	-3.561 ^{+0.357} _{-0.666}	3830 ⁺¹⁶¹ ₋₁₂₂	98.2 ^{+6.6} _{-7.8}	1870 ⁺⁵⁸ ₋₅₈	

Continued

Target	d [pc]	G [mag]	A_G [mag]	M_G [mag]	T_{eff} [K]	R [R_{\odot}]	L [L_{\odot}]	rem.
HIP 14382	$65.1^{+1.0}_{-0.9}$	4.419 ± 0.003	$0.114^{+1.287}_{-0.106}$	$0.238^{+0.140}_{-1.322}$	4768^{+118}_{-38}	$11.7^{+0.2}_{-0.6}$	$63.2^{+1.0}_{-1.0}$	
HIP 15219	224^{+9}_{-9}	4.631 ± 0.003	$0.366^{+0.049}_{-0.049}$	$-2.486^{+0.136}_{-0.140}$	4445^{+54}_{-61}	$44.4^{+1.3}_{-1.1}$	694^{+31}_{-31}	c
HIP 15795	314^{+5}_{-5}	6.157 ± 0.001	$0.149^{+0.418}_{-0.141}$	$-1.478^{+0.173}_{-0.451}$	4371^{+113}_{-108}	$32.6^{+1.7}_{-1.6}$	350^{+7}_{-7}	
HIP 15890	659^{+120}_{-88}	4.102 ± 0.003	$0.742^{+1.204}_{-0.422}$	$-5.733^{+0.737}_{-1.571}$	3859^{+94}_{-252}	257^{+37}_{-12}	13236^{+2117}_{-2117}	
HIP 16019	383^{+5}_{-5}	6.606 ± 0.001	$0.992^{+0.686}_{-0.431}$	$-2.303^{+0.462}_{-0.718}$	3673^{+160}_{-178}	$56.9^{+5.9}_{-4.6}$	530^{+11}_{-11}	
HIP 16165	289^{+4}_{-4}	5.790 ± 0.001	$0.502^{+0.521}_{-0.396}$	$-2.016^{+0.426}_{-0.552}$	3928^{+283}_{-145}	$49.9^{+3.9}_{-6.5}$	534^{+10}_{-10}	
HIP 16489	109^{+2}_{-2}	5.364 ± 0.001	$0.015^{+0.009}_{-0.009}$	$0.161^{+0.040}_{-0.041}$	5092^{+98}_{-86}	$10.7^{+0.4}_{-0.4}$	$69.0^{+1.1}_{-1.1}$	c
HIP 17064	570^{+9}_{-9}	7.171 ± 0.001	$0.443^{+0.179}_{-0.179}$	$-2.052^{+0.212}_{-0.213}$	3965^{+157}_{-167}	$50.9^{+4.6}_{-3.8}$	578^{+15}_{-15}	c
HIP 17342	503^{+30}_{-27}	4.956 ± 0.002	$0.622^{+0.772}_{-0.475}$	$-4.174^{+0.596}_{-0.900}$	4001^{+82}_{-179}	120^{+12}_{-5}	3342^{+221}_{-221}	
HIP 18088	276^{+2}_{-2}	6.406 ± 0.001	$0.291^{+0.293}_{-0.221}$	$-1.088^{+0.240}_{-0.312}$	4340^{+133}_{-153}	$26.1^{+1.9}_{-1.5}$	217^{+3}_{-3}	
HIP 18488	448^{+130}_{-82}	4.48 ± 0.03	$0.655^{+0.459}_{-0.459}$	$-4.438^{+0.928}_{-1.040}$	4365^{+218}_{-218}	-	-	abcd
HIP 19057	1236^{+65}_{-59}	7.175 ± 0.009	$1.417^{+0.498}_{-0.498}$	$-4.701^{+0.614}_{-0.619}$	4197^{+91}_{-72}	$93.2^{+3.3}_{-3.9}$	2431^{+182}_{-182}	c
HIP 19679	335^{+6}_{-6}	5.914 ± 0.001	$0.905^{+0.517}_{-0.517}$	$-2.613^{+0.558}_{-0.559}$	3986^{+138}_{-186}	$52.0^{+5.2}_{-3.4}$	615^{+15}_{-15}	c
HIP 20426	518^{+11}_{-11}	6.689 ± 0.000	$0.814^{+1.932}_{-0.373}$	$-2.697^{+0.420}_{-1.979}$	4076^{+119}_{-137}	$52.7^{+3.7}_{-3.0}$	691^{+22}_{-22}	
HIP 20513	389^{+11}_{-11}	5.936 ± 0.002	$0.593^{+0.240}_{-0.240}$	$-2.604^{+0.301}_{-0.303}$	3760^{+150}_{-120}	$72.6^{+4.9}_{-5.5}$	950^{+34}_{-34}	c
HIP 20776	277^{+7}_{-7}	5.055 ± 0.002	$0.185^{+0.214}_{-0.185}$	$-2.344^{+0.238}_{-0.269}$	4638^{+253}_{-83}	$40.2^{+1.5}_{-4.1}$	673^{+20}_{-20}	c
HIP 20958	331^{+13}_{-12}	5.708 ± 0.002	$0.323^{+0.054}_{-0.054}$	$-2.212^{+0.134}_{-0.137}$	3607^{+384}_{-156}	$78.6^{+7.3}_{-14.4}$	941^{+41}_{-41}	c
HIP 20974	330^{+4}_{-4}	5.896 ± 0.001	$0.685^{+0.674}_{-0.458}$	$-2.381^{+0.484}_{-0.700}$	3950^{+300}_{-168}	$53.3^{+4.8}_{-7.3}$	623^{+11}_{-11}	
HIP 21408	131^{+3}_{-3}	6.124 ± 0.001	$0.204^{+0.038}_{-0.038}$	$0.339^{+0.092}_{-0.093}$	5470^{+141}_{-52}	$7.60^{+0.14}_{-0.38}$	$46.6^{+1.3}_{-1.3}$	c
HIP 21476	195^{+26}_{-21}	3.719 ± 0.004	$0.377^{+0.098}_{-0.098}$	$-3.112^{+0.345}_{-0.375}$	4330^{+170}_{-207}	$62.5^{+6.4}_{-4.6}$	1237^{+151}_{-151}	c
HIP 21601	365^{+5}_{-4}	6.064 ± 0.001	$0.639^{+0.258}_{-0.258}$	$-2.388^{+0.285}_{-0.286}$	4156^{+158}_{-121}	$46.3^{+2.8}_{-3.3}$	577^{+11}_{-11}	c
HIP 22154	469^{+8}_{-8}	7.199 ± 0.001	$0.614^{+1.197}_{-0.314}$	$-1.771^{+0.353}_{-1.237}$	4249^{+142}_{-88}	$33.0^{+1.4}_{-2.1}$	320^{+9}_{-9}	
HIP 22261	198^{+2}_{-2}	6.575 ± 0.001	$1.851^{+0.472}_{-0.403}$	$-1.756^{+0.425}_{-0.494}$	3572^{+335}_{-242}	$32.5^{+4.9}_{-5.3}$	155^{+2}_{-2}	
HIP 22453	164^{+19}_{-15}	4.249 ± 0.003	$0.246^{+0.041}_{-0.041}$	$-2.077^{+0.259}_{-0.282}$	4030^{+100}_{-50}	$52.0^{+1.3}_{-2.5}$	642^{+70}_{-70}	c
HIP 22928	427^{+12}_{-11}	6.247 ± 0.002	$0.408^{+0.012}_{-0.012}$	$-2.314^{+0.070}_{-0.071}$	3516^{+414}_{-186}	$86.6^{+9.9}_{-17.3}$	1032^{+36}_{-36}	c
HIP 23268	358^{+10}_{-10}	5.722 ± 0.002	$0.867^{+0.425}_{-0.348}$	$-2.917^{+0.409}_{-0.487}$	3899^{+292}_{-151}	$65.5^{+5.4}_{-8.8}$	893^{+31}_{-31}	
HIP 23359	750^{+35}_{-35}	7.369 ± 0.001	$0.315^{+0.941}_{-0.191}$	$-2.323^{+0.287}_{-1.041}$	4335^{+172}_{-182}	$46.2^{+4.1}_{-3.5}$	678^{+40}_{-40}	
HIP 23360	1757^{+180}_{-150}	7.338 ± 0.008	$0.735^{+0.310}_{-0.310}$	$-4.621^{+0.512}_{-0.530}$	4739^{+94}_{-89}	$87.3^{+3.4}_{-3.4}$	3463^{+446}_{-446}	c
HIP 23582	323^{+7}_{-6}	5.522 ± 0.002	$0.894^{+0.838}_{-0.426}$	$-2.915^{+0.471}_{-0.884}$	3955^{+187}_{-91}	$61.7^{+2.9}_{-5.4}$	837^{+22}_{-22}	
HIP 23766	179^{+4}_{-3}	5.493 ± 0.002	$0.394^{+0.706}_{-0.324}$	$-1.166^{+0.368}_{-0.750}$	4325^{+148}_{-137}	$25.9^{+1.7}_{-1.7}$	212^{+5}_{-5}	
HIP 24303	974^{+53}_{-48}	7.469 ± 0.001	$0.476^{+0.930}_{-0.413}$	$-2.950^{+0.524}_{-1.047}$	4395^{+268}_{-132}	$55.3^{+3.5}_{-6.2}$	1027^{+73}_{-73}	
HIP 24716	344^{+15}_{-14}	5.961 ± 0.005	$0.388^{+1.350}_{-0.249}$	$-2.107^{+0.342}_{-1.446}$	3299^{+91}_{-14}	-	-	
HIP 24914	475^{+28}_{-25}	4.867 ± 0.003	$0.595^{+0.857}_{-0.378}$	$-4.113^{+0.499}_{-0.985}$	3985^{+160}_{-100}	120^{+6}_{-9}	3263^{+213}_{-213}	
HIP 25184	353^{+6}_{-6}	6.038 ± 0.001	$1.029^{+0.526}_{-0.357}$	$-2.732^{+0.394}_{-0.564}$	3957^{+227}_{-203}	$53.2^{+5.9}_{-5.6}$	625^{+15}_{-15}	
HIP 25226	193^{+1}_{-1}	6.504 ± 0.001	$0.231^{+1.548}_{-0.151}$	$-0.160^{+0.169}_{-1.565}$	4710^{+75}_{-120}	$13.8^{+0.7}_{-0.4}$	$84.0^{+0.9}_{-0.9}$	
HIP 25386	689^{+23}_{-22}	7.029 ± 0.001	$0.528^{+0.213}_{-0.213}$	$-2.688^{+0.284}_{-0.286}$	3842^{+134}_{-252}	$73.1^{+10.6}_{-4.9}$	1048^{+48}_{-48}	c
HIP 25668	273^{+7}_{-7}	6.779 ± 0.001	$0.461^{+1.037}_{-0.353}$	$-0.864^{+0.410}_{-1.095}$	4244^{+228}_{-88}	$23.3^{+1.0}_{-2.3}$	158^{+5}_{-5}	
HIP 25877	576^{+21}_{-19}	6.025 ± 0.007	$0.951^{+0.712}_{-0.455}$	$-3.727^{+0.535}_{-0.794}$	3980^{+374}_{-165}	$86.0^{+7.6}_{-14.2}$	1671^{+77}_{-77}	
HIP 26070	405^{+5}_{-5}	6.210 ± 0.001	$0.331^{+0.134}_{-0.134}$	$-2.160^{+0.163}_{-0.163}$	4154^{+229}_{-68}	$48.2^{+1.6}_{-4.9}$	624^{+13}_{-13}	c
HIP 26386	287^{+10}_{-9}	5.273 ± 0.003	$0.231^{+0.099}_{-0.099}$	$-2.245^{+0.172}_{-0.174}$	3950^{+195}_{-86}	$61.5^{+2.8}_{-5.7}$	831^{+32}_{-32}	c
HIP 26743	392^{+7}_{-7}	6.786 ± 0.001	$0.563^{+1.090}_{-0.246}$	$-1.741^{+0.283}_{-1.128}$	4188^{+271}_{-124}	$34.8^{+2.2}_{-4.1}$	336^{+8}_{-8}	
HIP 27227	359^{+4}_{-3}	6.042 ± 0.001	$0.665^{+1.071}_{-0.476}$	$-2.395^{+0.497}_{-1.092}$	4152^{+231}_{-138}	$46.1^{+3.2}_{-4.7}$	569^{+9}_{-9}	
HIP 27750	346^{+24}_{-21}	4.253 ± 0.004	$0.246^{+0.111}_{-0.111}$	$-3.689^{+0.254}_{-0.263}$	4270^{+165}_{-96}	$92.2^{+4.3}_{-6.7}$	2547^{+187}_{-187}	c
HIP 27778	190^{+7}_{-6}	5.184 ± 0.007	$0.316^{+0.153}_{-0.153}$	$-1.527^{+0.235}_{-0.238}$	3934^{+170}_{-151}	$43.0^{+3.5}_{-3.5}$	399^{+16}_{-16}	c
HIP 27989	153^{+22}_{-17}	-0.55 ± 0.02	$0.077^{+0.062}_{-0.062}$	$-6.547^{+0.341}_{-0.376}$	3707^{+185}_{-185}	-	-	abcd
HIP 28185	528^{+13}_{-12}	7.189 ± 0.001	$0.344^{+0.778}_{-0.336}$	$-1.767^{+0.387}_{-0.830}$	4146^{+163}_{-96}	$40.4^{+1.9}_{-3.0}$	434^{+15}_{-15}	

Continued

Target	d [pc]	G [mag]	A_G [mag]	M_G [mag]	T_{eff} [K]	R [R_{\odot}]	L [L_{\odot}]	rem.
HIP 28366	358 ⁺⁴ ₋₄	7.472 ± 0.001	0.422 ^{+0.336} _{-0.241}	-0.719 ^{+0.265} _{-0.361}	4269 ⁺²⁰⁵ ₋₆₉	21.8 ^{+0.7} _{-2.0}	143 ⁺³ ₋₃	
HIP 30341	421 ⁺¹⁰ ₋₁₀	6.665 ± 0.001	0.544 ^{+2.066} _{-0.485}	-1.999 ^{+0.536} _{-2.118}	4520 ⁺⁶³ ₋₅₁	31.4 ^{+0.7} _{-0.9}	370 ⁺¹² ₋₁₂	
HIP 32094	524 ⁺¹¹ ₋₁₀	6.101 ± 0.001	0.759 ^{+0.430} _{-0.430}	-3.255 ^{+0.473} _{-0.474}	3770 ⁺²⁸⁹ ₋₂₅₂	90.4 ^{+13.4} _{-12.4}	1488 ⁺⁴⁴ ₋₄₄	c
HIP 32276	778 ⁺³⁸ ₋₃₅	7.517 ± 0.001	0.437 ^{+1.748} _{-0.421}	-2.376 ^{+0.521} _{-1.853}	4385 ⁺⁶⁷ ₋₅₈	43.3 ^{+1.2} _{-1.3}	623 ⁺³⁹ ₋₃₉	
HIP 32631	383 ⁺⁶ ₋₆	6.891 ± 0.001	0.370 ^{+0.134} _{-0.134}	-1.396 ^{+0.170} _{-0.170}	4775 ⁺²¹¹ ₋₁₅₂	22.1 ^{+1.5} _{-1.8}	229 ⁺⁵ ₋₅	c
HIP 33515	462 ⁺¹² ₋₁₁	6.360 ± 0.001	0.185 ^{+0.075} _{-0.075}	-2.146 ^{+0.129} _{-0.130}	4708 ⁺⁴²⁷ ₋₇₃	35.4 ^{+1.1} _{-5.6}	554 ⁺¹⁹ ₋₁₉	c
HIP 33789	337 ⁺⁵ ₋₅	6.132 ± 0.001	0.517 ^{+0.409} _{-0.398}	-2.024 ^{+0.431} _{-0.443}	4030 ⁺²¹⁰ ₋₁₅₅	45.8 ^{+3.7} _{-4.4}	499 ⁺¹¹ ₋₁₁	
HIP 33927	301 ⁺¹⁴ ₋₁₃	4.888 ± 0.003	0.245 ^{+0.099} _{-0.099}	-2.747 ^{+0.200} _{-0.204}	5063 ⁺³²⁸ ₋₁₁₃	37.3 ^{+1.7} _{-4.4}	822 ⁺⁴⁴ ₋₄₄	c
HIP 33937	572 ⁺⁵⁷ ₋₄₈	4.991 ± 0.003	0.216 ^{+0.035} _{-0.035}	-4.013 ^{+0.227} _{-0.245}	4000 ⁺¹⁶⁵ ₋₂₁₈	134 ⁺¹⁶ ₋₁₀	4171 ⁺⁴²⁴ ₋₄₂₄	c
HIP 34026	1035 ⁺⁵³ ₋₄₈	6.762 ± 0.001	0.262 ^{+0.106} _{-0.106}	-3.575 ^{+0.211} _{-0.216}	5264 ⁺⁴⁸ ₋₁₂₈	50.4 ^{+2.5} _{-0.9}	1754 ⁺¹²¹ ₋₁₂₁	c
HIP 34055	384 ⁺²⁷ ₋₂₄	5.347 ± 0.003	0.696 ^{+1.011} _{-0.394}	-3.270 ^{+0.537} _{-1.163}	3940 ⁺²⁰² ₋₃₅	80.2 ^{+1.4} _{-7.6}	1397 ⁺¹⁰⁴ ₋₁₀₄	
HIP 34909	179 ⁺⁸ ₋₈	3.689 ± 0.006	0.154 ^{+0.062} _{-0.062}	-2.731 ^{+0.162} _{-0.167}	3606 ⁺⁵¹⁶ ₋₁₃₅	107 ⁺⁹ ₋₂₅	1754 ⁺⁸⁸ ₋₈₈	c
HIP 35537	289 ⁺⁴ ₋₄	6.823 ± 0.001	0.351 ^{+1.348} _{-0.208}	-0.834 ^{+0.238} _{-1.378}	4521 ⁺¹⁸¹ ₋₅₂	20.0 ^{+0.5} _{-1.5}	150 ⁺³ ₋₃	
HIP 35551	424 ⁺⁸ ₋₈	6.604 ± 0.001	0.185 ^{+0.075} _{-0.075}	-1.720 ^{+0.116} _{-0.116}	4838 ⁺⁶⁴ ₋₃₃	27.0 ^{+0.4} _{-0.7}	360 ⁺¹⁰ ₋₁₀	c
HIP 35796	295 ⁺⁴ ₋₄	6.420 ± 0.001	0.239 ^{+0.109} _{-0.109}	-1.166 ^{+0.141} _{-0.142}	5100 ⁺⁵⁰ ₋₅₉	17.8 ^{+0.4} _{-0.3}	192 ⁺⁴ ₋₄	c
HIP 36041	234 ⁺¹⁴ ₋₁₂	4.676 ± 0.004	0.193 ^{+0.078} _{-0.078}	-2.364 ^{+0.198} _{-0.204}	4900 ⁺⁵³ ₋₂₂	34.7 ^{+0.3} _{-0.7}	624 ⁺³⁸ ₋₃₈	c
HIP 36629	710 ⁺¹⁹ ₋₁₈	6.411 ± 0.001	0.285 ^{+0.115} _{-0.115}	-3.130 ^{+0.173} _{-0.174}	4349 ⁺⁸⁷ ₋₈₀	67.3 ^{+2.6} _{-2.6}	1459 ⁺⁵⁹ ₋₅₉	c
HIP 37104	589 ⁺¹⁷ ₋₁₆	6.547 ± 0.001	0.545 ^{+0.220} _{-0.220}	-2.849 ^{+0.280} _{-0.281}	3998 ⁺⁶⁸ ₋₁₂₇	68.2 ^{+4.6} _{-2.3}	1070 ⁺⁴² ₋₄₂	c
HIP 39398	702 ⁺²⁵ ₋₂₃	6.762 ± 0.001	1.080 ^{+0.709} _{-0.414}	-3.550 ^{+0.488} _{-0.784}	3803 ⁺¹⁹⁸ ₋₃₆	87.2 ^{+1.7} _{-8.4}	1434 ⁺⁶⁹ ₋₆₉	
HIP 39958	346 ⁺⁵ ₋₅	6.265 ± 0.001	0.289 ^{+0.071} _{-0.071}	-1.720 ^{+0.104} _{-0.105}	5392 ⁺⁷⁵ ₋₁₀₂	19.6 ^{+0.8} _{-0.5}	294 ⁺⁶ ₋₆	c
HIP 40628	546 ⁺¹⁶ ₋₁₅	6.625 ± 0.001	0.100 ^{+0.040} _{-0.040}	-2.161 ^{+0.101} _{-0.103}	4000 ⁺¹¹³ ₋₁₃₇	61.0 ^{+4.4} _{-3.3}	857 ⁺³³ ₋₃₃	c
HIP 41221	596 ⁺¹³ ₋₁₂	6.390 ± 0.001	0.919 ^{+0.951} _{-0.253}	-3.403 ^{+0.297} _{-0.996}	4091 ⁺³¹⁰ ₋₉₁	68.9 ^{+3.2} _{-9.4}	1198 ⁺³⁸ ₋₃₈	
HIP 41283	711 ⁺²⁴ ₋₂₂	7.584 ± 0.001	0.587 ^{+0.853} _{-0.387}	-2.262 ^{+0.457} _{-0.925}	4076 ⁺¹²² ₋₉₆	48.2 ^{+2.4} _{-2.8}	577 ⁺²⁷ ₋₂₇	
HIP 41704	60.4 ^{+1.4} _{-1.3}	3.027 ± 0.001	0.000 ^{+0.036} _{-0.000}	-0.880 ^{+0.048} _{-0.085}	5164 ⁺²⁵⁸ ₋₂₅₈	-	-	c d e
HIP 41896	338 ⁺⁵ ₋₅	6.613 ± 0.001	0.131 ^{+0.054} _{-0.054}	-1.164 ^{+0.085} _{-0.086}	4950 ⁺⁸⁴ ₋₉₄	20.1 ^{+0.8} _{-0.7}	219 ⁺⁴ ₋₄	c
HIP 42211	326 ⁺⁵ ₋₅	7.809 ± 0.001	0.135 ^{+0.071} _{-0.071}	0.108 ^{+0.106} _{-0.107}	5001 ⁺⁸⁶ ₋₁₃₆	10.9 ^{+0.6} _{-0.4}	66.9 ^{+1.5} _{-1.5}	c
HIP 42331	378 ⁺⁷ ₋₇	7.066 ± 0.001	0.322 ^{+0.285} _{-0.173}	-1.145 ^{+0.212} _{-0.324}	4163 ⁺¹⁰¹ ₋₈₂	30.1 ^{+1.2} _{-1.4}	245 ⁺⁶ ₋₆	
HIP 42580	461 ⁺¹¹ ₋₁₁	7.365 ± 0.001	0.347 ^{+1.081} _{-0.304}	-1.300 ^{+0.355} _{-1.133}	4453 ⁺⁵¹⁴ ₋₁₈₂	26.1 ^{+2.3} _{-5.1}	241 ⁺⁸ ₋₈	
HIP 42876	383 ⁺⁷ ₋₇	6.547 ± 0.001	0.548 ^{+1.008} _{-0.192}	-1.916 ^{+0.232} _{-1.049}	4180 ⁺¹⁴⁶ ₋₈₀	38.2 ^{+1.5} _{-2.5}	401 ⁺¹⁰ ₋₁₀	
HIP 43030	366 ⁺⁶ ₋₅	6.496 ± 0.001	0.517 ^{+0.297} _{-0.236}	-1.837 ^{+0.269} _{-0.331}	4040 ⁺³¹⁸ ₋₃₈₃	41.7 ^{+9.2} _{-5.9}	418 ⁺⁹ ₋₉	
HIP 44231	391 ⁺¹⁷ ₋₁₅	5.519 ± 0.001	0.796 ^{+0.928} _{-0.393}	-3.240 ^{+0.482} _{-1.021}	3917 ⁺²²⁸ ₋₅₃	77.4 ^{+2.1} _{-8.3}	1271 ⁺⁶³ ₋₆₃	
HIP 44458	30.2 ^{+0.1} _{-0.1}	6.910 ± 0.001	0.066 ^{+0.114} _{-0.036}	4.446 ^{+0.040} _{-0.119}	5809 ⁺⁹¹ ₋₁₆₁	1.07 ^{+0.06} _{-0.04}	1.167 ^{+0.003} _{-0.002}	
HIP 44580	630 ⁺²⁴ ₋₂₂	7.036 ± 0.001	0.737 ^{+1.421} _{-0.406}	-2.698 ^{+0.483} _{-1.501}	4066 ⁺²⁰⁸ ₋₁₁₈	55.3 ^{+3.4} _{-5.3}	752 ⁺³⁷ ₋₃₇	
HIP 44784	278 ⁺⁶ ₋₆	7.705 ± 0.001	0.011 ^{+0.027} _{-0.011}	0.477 ^{+0.061} _{-0.077}	4809 ⁺⁶⁰ ₋₅₇	10.8 ^{+0.3} _{-0.3}	55.8 ^{+1.6} _{-1.6}	
HIP 44831	561 ⁺¹⁴ ₋₁₃	6.581 ± 0.001	0.878 ^{+1.131} _{-0.285}	-3.043 ^{+0.338} _{-1.186}	3876 ⁺¹²² ₋₇₆	71.0 ^{+2.9} _{-4.3}	1023 ⁺³⁶ ₋₃₆	
HIP 45104	521 ⁺²² ₋₂₀	7.049 ± 0.001	0.342 ^{+0.855} _{-0.189}	-1.877 ^{+0.275} _{-0.945}	4057 ⁺¹³⁰ ₋₁₁₉	45.6 ^{+2.8} _{-2.8}	508 ⁺²⁶ ₋₂₆	
HIP 45105	281 ⁺⁵ ₋₅	7.710 ± 0.001	0.024 ^{+0.293} _{-0.016}	0.443 ^{+0.053} _{-0.331}	4849 ⁺⁹⁸ ₋₇₂	10.6 ^{+0.3} _{-0.4}	56.3 ^{+1.2} _{-1.2}	
HIP 45343	6.33 ^{+0.01} _{-0.01}	6.969 ± 0.001	0.376 ^{+0.326} _{-0.208}	7.585 ^{+0.209} _{-0.327}	4072 ⁺⁹⁸ ₋₁₀₆	0.56 ^{+0.03} _{-0.03}	0.078 ^{+0.001} _{-0.001}	
HIP 45963	23.4 ^{+0.1} _{-0.1}	8.033 ± 0.001	0.054 ^{+0.083} _{-0.054}	6.129 ^{+0.058} _{-0.087}	4738 ⁺⁶⁴ ₋₇₁	1.14 ^{+0.04} _{-0.03}	0.591 ^{+0.001} _{-0.001}	c f
HIP 46207	420 ⁺¹¹ ₋₁₀	7.478 ± 0.001	0.307 ^{+1.259} _{-0.156}	-0.943 ^{+0.210} _{-1.314}	4580 ⁺²¹¹ ₋₁₁₂	20.7 ^{+1.1} _{-1.8}	170 ⁺⁶ ₋₆	
HIP 46693	415 ⁺⁶ ₋₅	6.911 ± 0.001	0.563 ^{+1.231} _{-0.251}	-1.740 ^{+0.280} _{-1.260}	4314 ⁺¹⁰⁹ ₋₁₃₇	31.7 ^{+2.1} _{-1.5}	314 ⁺⁷ ₋₇	
HIP 46816	18.3 ^{+0.1} _{-0.1}	7.497 ± 0.002	0.008 ^{+0.095} _{-0.005}	6.179 ^{+0.010} _{-0.100}	4909 ⁺⁶⁷ ₋₄₅	0.73 ^{+0.02} _{-0.02}	0.282 ^{+0.001} _{-0.001}	
HIP 46843	18.1 ^{+0.1} _{-0.1}	6.831 ± 0.002	0.039 ^{+0.108} _{-0.039}	5.508 ^{+0.043} _{-0.112}	5300 ⁺⁷³ ₋₅₁	0.81 ^{+0.02} _{-0.02}	0.472 ^{+0.001} _{-0.001}	
HIP 46977	32.3 ^{+0.2} _{-0.2}	4.276 ± 0.003	0.114 ^{+0.185} _{-0.185}	1.616 ^{+0.200} _{-0.200}	5305 ⁺³⁶⁵ ₋₈₄	4.72 ^{+0.15} _{-0.59}	15.9 ^{+0.1} _{-0.1}	c
HIP 47193	269 ⁺²³ ₋₂₀	3.705 ± 0.005	0.510 ^{+1.341} _{-0.363}	-3.955 ^{+0.535} _{-1.525}	4043 ⁺⁵⁶ ₋₂₀	109 ⁺¹ ₋₃	2885 ⁺²⁵² ₋₂₅₂	
HIP 48851	433 ⁺¹⁵ ₋₁₄	6.460 ± 0.001	0.986 ^{+0.560} _{-0.316}	-2.707 ^{+0.388} _{-0.635}	3980 ⁺¹⁴³ ₋₁₃₄	52.7 ^{+3.7} _{-3.6}	628 ⁺²⁷ ₋₂₇	

Continued

Target	d [pc]	G [mag]	A_G [mag]	M_G [mag]	T_{eff} [K]	R [R_{\odot}]	L [L_{\odot}]	rem.
HIP 48921	388 ⁺¹³¹ ₋₇₈	6.621 ± 0.001	0.223 ^{+0.090} _{-0.090}	-1.545 ^{+0.579} _{-0.721}	5011 ⁺²⁵¹ ₋₂₅₁	-	-	a c d
HIP 49688	320 ⁺⁸ ₋₈	5.601 ± 0.002	0.008 ^{+0.003} _{-0.003}	-1.933 ^{+0.057} _{-0.058}	4012 ⁺²⁰⁴ ₋₁₄₈	56.3 ^{+4.4} _{-5.3}	740 ⁺²³ ₋₂₃	c
HIP 49729	173 ⁺³ ₋₃	6.624 ± 0.001	0.073 ^{+0.310} _{-0.065}	0.359 ^{+0.098} _{-0.343}	4748 ⁺¹⁰³ ₋₆₃	11.4 ^{+0.3} _{-0.5}	59.5 ^{+1.1} _{-1.1}	c
HIP 50310	776 ⁺³³ ₋₃₁	7.328 ± 0.001	0.000 ^{+0.311} _{-0.000}	-2.120 ^{+0.089} _{-0.403}	4027 ⁺²¹³ ₋₈₂	61.7 ^{+2.6} _{-6.0}	902 ⁺⁵¹ ₋₅₁	c
HIP 50999	510 ⁺¹⁸ ₋₁₇	7.375 ± 0.001	0.216 ^{+0.087} _{-0.087}	-1.378 ^{+0.161} _{-0.163}	3772 ⁺¹⁷¹ ₋₂₂₈	48.8 ^{+6.5} _{-4.1}	434 ⁺¹⁹ ₋₁₉	c
HIP 51973	195 ⁺² ₋₂	6.890 ± 0.001	0.036 ^{+0.281} _{-0.028}	0.408 ^{+0.050} _{-0.303}	4780 ⁺⁵⁰ ₋₈₈	11.1 ^{+0.4} _{-0.2}	58.3 ^{+0.8} _{-0.8}	c
HIP 52032	438 ⁺²³ ₋₂₁	5.980 ± 0.001	0.039 ^{+0.016} _{-0.016}	-2.268 ^{+0.122} _{-0.127}	4370 ⁺¹⁸⁷ ₋₄₄	49.5 ^{+1.0} _{-4.0}	805 ⁺⁴⁷ ₋₄₇	c
HIP 52098	192 ⁺¹⁷ ₋₁₄	4.415 ± 0.005	0.141 ^{+0.103} _{-0.103}	-2.148 ^{+0.278} _{-0.292}	5406 ⁺³²³ ₋₂₂₆	25.1 ^{+2.2} _{-2.8}	485 ⁺⁴³ ₋₄₃	c
HIP 52373	429 ⁺¹⁰ ₋₁₀	6.440 ± 0.001	0.015 ^{+0.006} _{-0.006}	-1.739 ^{+0.056} _{-0.057}	3997 ⁺¹⁰³ ₋₁₁₂	52.0 ^{+3.1} _{-2.6}	623 ⁺¹⁹ ₋₁₉	c
HIP 52556	464 ⁺²⁰ ₋₁₈	6.892 ± 0.001	0.490 ^{+0.726} _{-0.303}	-1.932 ^{+0.392} _{-0.818}	4066 ⁺¹⁷⁴ ₋₇₄	43.3 ^{+1.6} _{-3.5}	461 ⁺²³ ₋₂₃	c
HIP 52831	234 ⁺² ₋₂	7.424 ± 0.001	0.088 ^{+0.057} _{-0.072}	0.494 ^{+0.095} _{-0.080}	4784 ⁺¹²³ ₋₉₆	10.4 ^{+0.4} _{-0.5}	51.4 ^{+0.7} _{-0.7}	c
HIP 53831	910 ⁺¹⁴⁷ ₋₁₁₃	7.018 ± 0.001	0.567 ^{+1.187} _{-0.266}	-3.344 ^{+0.553} _{-1.514}	3989 ⁺¹⁴⁰ ₋₁₃₃	87.2 ^{+6.1} _{-5.8}	1736 ⁺²⁸⁴ ₋₂₈₄	c
HIP 54024	382 ⁺⁷ ₋₆	6.764 ± 0.001	0.039 ^{+0.019} _{-0.019}	-1.184 ^{+0.056} _{-0.057}	4694 ⁺⁷⁹ ₋₂₈	24.5 ^{+0.3} _{-0.8}	262 ⁺⁶ ₋₆	c
HIP 55193	133 ⁺¹ ₋₁	6.588 ± 0.001	0.050 ^{+0.016} _{-0.016}	0.918 ^{+0.032} _{-0.032}	5044 ⁺⁵⁸ ₋₁₀₀	7.60 ^{+0.31} _{-0.18}	33.6 ^{+0.3} _{-0.3}	c
HIP 55682	478 ⁺⁸ ₋₈	6.100 ± 0.001	1.104 ^{+1.231} _{-0.339}	-3.399 ^{+0.376} _{-1.268}	3937 ⁺⁸⁷ ₋₁₀₀	71.4 ^{+3.8} _{-3.1}	1102 ⁺²⁹ ₋₂₉	c
HIP 55945	158 ⁺⁸ ₋₇	4.627 ± 0.005	0.162 ^{+0.104} _{-0.104}	-1.525 ^{+0.206} _{-0.210}	4908 ⁺³⁷ ₋₅₃	23.8 ^{+0.5} _{-0.4}	296 ⁺¹⁵ ₋₁₅	c
HIP 56383	280 ⁺⁸ ₋₈	6.630 ± 0.001	0.353 ^{+0.924} _{-0.144}	-0.960 ^{+0.204} _{-0.985}	4601 ⁺²⁵⁶ ₋₁₀₆	20.1 ^{+1.0} _{-2.1}	163 ⁺⁵ ₋₅	c
HIP 57240	374 ⁺²⁰ ₋₁₈	5.405 ± 0.002	0.487 ^{+1.222} _{-0.363}	-2.947 ^{+0.475} _{-1.339}	4006 ⁺²³⁴ ₋₄₃	72.4 ^{+1.6} _{-7.8}	1215 ⁺⁷² ₋₇₂	c
HIP 57261	399 ⁺⁵ ₋₅	7.577 ± 0.001	0.023 ^{+0.107} _{-0.023}	-0.450 ^{+0.050} _{-0.134}	4976 ⁺⁹⁴ ₋₄₆	15.1 ^{+0.3} _{-0.6}	125 ⁺² ₋₂	c
HIP 58217	206 ⁺³ ₋₃	6.782 ± 0.001	0.062 ^{+0.047} _{-0.047}	0.148 ^{+0.080} _{-0.080}	4969 ⁺⁵⁵ ₋₄₃	11.2 ^{+0.2} _{-0.3}	69.0 ^{+1.3} _{-1.3}	c
HIP 58313	325 ⁺⁵ ₋₅	7.992 ± 0.001	0.078 ^{+0.905} _{-0.072}	0.354 ^{+0.104} _{-0.936}	4874 ⁺⁴⁴ ₋₃₈	10.7 ^{+0.2} _{-0.2}	58.0 ^{+1.2} _{-1.2}	c
HIP 58661	169 ⁺² ₋₂	6.406 ± 0.001	1.545 ^{+0.403} _{-0.293}	-1.277 ^{+0.317} _{-0.427}	5713 ⁺⁹⁰ ₋₁₀₅	7.84 ^{+0.29} _{-0.24}	58.9 ^{+0.8} _{-0.8}	c
HIP 59280	25.1 ^{+0.1} _{-0.1}	7.240 ± 0.001	0.036 ^{+0.154} _{-0.029}	5.207 ^{+0.033} _{-0.158}	5407 ⁺⁴⁰ ₋₈₂	0.89 ^{+0.03} _{-0.01}	0.616 ^{+0.001} _{-0.001}	c
HIP 59501	110 ⁺¹ ₋₁	5.313 ± 0.001	0.046 ^{+0.024} _{-0.024}	0.065 ^{+0.045} _{-0.045}	4948 ⁺²⁸ ₋₄₃	11.8 ^{+0.2} _{-0.1}	75.6 ^{+0.9} _{-0.9}	c
HIP 59760	852 ⁺³⁸ ₋₃₅	7.023 ± 0.001	0.031 ^{+0.169} _{-0.031}	-2.659 ^{+0.123} _{-0.264}	4931 ⁺⁶⁴ ₋₈₅	43.1 ^{+1.5} _{-1.1}	989 ⁺⁵⁹ ₋₅₉	c
HIP 60731	324 ⁺⁷ ₋₇	6.884 ± 0.001	0.569 ^{+0.595} _{-0.345}	-1.240 ^{+0.393} _{-0.645}	4221 ⁺²¹³ ₋₈₁	26.8 ^{+1.1} _{-2.5}	206 ⁺⁶ ₋₆	c
HIP 60831	45.5 ^{+0.1} _{-0.1}	7.284 ± 0.001	0.175 ^{+0.140} _{-0.158}	3.819 ^{+0.163} _{-0.145}	6160 ⁺⁵⁵ ₋₅₅	1.20 ^{+0.02} _{-0.02}	1.86 ^{+0.01} _{-0.01}	c
HIP 61290	541 ⁺²² ₋₂₀	6.272 ± 0.002	1.315 ^{+0.846} _{-0.272}	-3.711 ^{+0.355} _{-0.932}	3744 ⁺¹⁵⁶ ₋₁₆₅	88.3 ^{+8.3} _{-6.9}	1381 ⁺⁶⁸ ₋₆₈	c
HIP 61617	915 ⁺⁴² ₋₃₈	7.663 ± 0.001	0.039 ^{+0.016} _{-0.016}	-2.182 ^{+0.110} _{-0.114}	4551 ⁺²²³ ₋₁₄₀	42.9 ^{+2.8} _{-3.9}	712 ⁺⁴⁴ ₋₄₄	c
HIP 61799	708 ⁺¹³ ₋₁₂	7.555 ± 0.001	0.031 ^{+0.012} _{-0.012}	-1.726 ^{+0.051} _{-0.051}	4177 ⁺⁸⁶ ₋₁₇₁	45.0 ^{+3.9} _{-1.8}	554 ⁺¹⁷ ₋₁₇	c
HIP 62455	163 ⁺¹ ₋₁	6.874 ± 0.001	0.363 ^{+0.198} _{-0.128}	0.446 ^{+0.139} _{-0.209}	4618 ⁺⁴⁹ ₋₉₁	10.3 ^{+0.4} _{-0.2}	43.8 ^{+0.3} _{-0.3}	c
HIP 62595	434 ⁺¹⁵ ₋₁₄	7.818 ± 0.001	0.160 ^{+0.784} _{-0.120}	-0.531 ^{+0.190} _{-0.857}	4623 ⁺⁹⁴ ₋₈₂	17.9 ^{+0.7} _{-0.7}	132 ⁺⁵ ₋₅	c
HIP 63356	276 ⁺³ ₋₃	6.591 ± 0.001	0.077 ^{+0.042} _{-0.042}	-0.687 ^{+0.064} _{-0.064}	4957 ⁺⁷⁴ ₋₅₅	16.5 ^{+0.4} _{-0.5}	148 ⁺² ₋₂	c
HIP 63368	178 ⁺¹ ₋₁	8.052 ± 0.002	0.077 ^{+0.047} _{-0.047}	1.727 ^{+0.062} _{-0.062}	4950 ⁺⁸³ ₋₇₅	5.43 ^{+0.17} _{-0.18}	16.0 ^{+0.2} _{-0.2}	c
HIP 63742	20.5 ^{+0.4} _{-0.4}	7.411 ± 0.001	0.016 ^{+0.094} _{-0.008}	5.841 ^{+0.048} _{-0.135}	5124 ⁺¹⁶³ ₋₉₇	0.77 ^{+0.03} _{-0.05}	0.364 ^{+0.008} _{-0.007}	c
HIP 63803	444 ⁺⁹ ₋₉	6.761 ± 0.001	0.200 ^{+1.006} _{-0.147}	-1.674 ^{+0.192} _{-1.052}	4460 ⁺³⁶⁵ ₋₁₆₅	33.0 ^{+2.6} _{-4.8}	387 ⁺¹¹ ₋₁₁	c
HIP 64149	588 ⁺⁸ ₋₈	7.110 ± 0.001	1.003 ^{+0.506} _{-0.470}	-2.740 ^{+0.499} _{-0.536}	3842 ⁺¹⁶³ ₋₉₇	60.1 ^{+3.1} _{-4.8}	708 ⁺¹⁷ ₋₁₇	c
HIP 64523	391 ⁺⁴ ₋₄	7.638 ± 0.001	0.244 ^{+0.666} _{-0.158}	-0.566 ^{+0.181} _{-0.690}	4662 ⁺⁴⁴¹ ₋₈₅	17.1 ^{+0.6} _{-2.8}	124 ⁺² ₋₂	c
HIP 64543	105 ⁺¹⁵ ₋₁₁	6.471 ± 0.001	0.077 ^{+0.046} _{-0.046}	1.295 ^{+0.298} _{-0.330}	5383 ⁺⁹⁹ ₋₈₇	5.26 ^{+0.18} _{-0.19}	21.0 ^{+2.6} _{-2.6}	c
HIP 65192	394 ⁺⁹ ₋₈	7.107 ± 0.001	0.116 ^{+0.065} _{-0.065}	-0.985 ^{+0.113} _{-0.114}	3842 ⁺¹³¹ ₋₈₃	40.0 ^{+1.8} _{-2.6}	314 ⁺⁹ ₋₉	c
HIP 65435	684 ⁺¹² ₋₁₂	7.161 ± 0.001	0.627 ^{+0.515} _{-0.400}	-2.642 ^{+0.438} _{-0.554}	4089 ⁺¹¹¹ ₋₉₇	55.7 ^{+2.8} _{-2.9}	783 ⁺²³ ₋₂₃	c
HIP 65915	216 ⁺² ₋₂	7.908 ± 0.002	0.108 ^{+0.039} _{-0.039}	1.132 ^{+0.061} _{-0.062}	4966 ⁺⁷⁴ ₋₇₁	6.99 ^{+0.20} _{-0.21}	26.8 ^{+0.4} _{-0.4}	c
HIP 66467	381 ⁺⁵ ₋₅	6.775 ± 0.001	0.394 ^{+0.930} _{-0.293}	-1.523 ^{+0.322} _{-0.959}	4358 ⁺¹⁰⁵ ₋₆₇	30.1 ^{+0.9} _{-1.4}	294 ⁺⁶ ₋₆	c
HIP 66690	142 ⁺¹ ₋₁	5.936 ± 0.001	0.077 ^{+0.013} _{-0.013}	0.099 ^{+0.026} _{-0.026}	4965 ⁺⁸³ ₋₅₂	11.4 ^{+0.2} _{-0.4}	71.0 ^{+0.6} _{-0.6}	c
HIP 67300	334 ⁺⁷ ₋₇	6.677 ± 0.001	0.235 ^{+0.169} _{-0.169}	-1.174 ^{+0.219} _{-0.220}	4685 ⁺⁷² ₋₈₇	22.3 ^{+0.9} _{-0.7}	216 ⁺⁶ ₋₆	c
HIP 67385	338 ⁺⁵ ₋₅	6.199 ± 0.001	0.524 ^{+0.704} _{-0.294}	-1.970 ^{+0.324} _{-0.734}	4274 ⁺¹⁰² ₋₁₃₇	36.9 ^{+2.5} _{-1.7}	409 ⁺⁸ ₋₈	c

Continued

Target	d [pc]	G [mag]	A_G [mag]	M_G [mag]	T_{eff} [K]	R [R_{\odot}]	L [L_{\odot}]	rem.
HIP 68879	771 ⁺⁴⁴ ₋₄₀	6.995 ± 0.001	0.023 ^{+0.009} _{-0.009}	-2.465 ^{+0.125} _{-0.131}	4080 ⁺⁶⁹⁸ ₋₁₆₆	68.4 ^{+5.9} _{-18.5}	1167 ⁺⁸⁰ ₋₈₀	c
HIP 68904	92.2 ^{+0.9} _{-0.9}	7.187 ± 0.002	0.046 ^{+0.044} _{-0.044}	2.318 ^{+0.067} _{-0.067}	4788 ⁺⁶⁹ ₋₈₇	4.57 ^{+0.17} _{-0.13}	9.87 ^{+0.12} _{-0.12}	c
HIP 69624	490 ⁺⁶ ₋₆	7.698 ± 0.001	0.514 ^{+1.353} _{-0.319}	-1.267 ^{+0.346} _{-1.380}	4356 ⁺³¹⁸ ₋₉₃	25.4 ^{+1.1} _{-3.3}	209 ⁺⁴ ₋₄	
HIP 70000	490 ⁺¹³ ₋₁₂	7.803 ± 0.001	0.469 ^{+0.373} _{-0.283}	-1.117 ^{+0.338} _{-0.429}	4252 ⁺¹⁰⁹ ₋₁₄₆	26.1 ^{+1.9} _{-1.3}	200 ⁺⁷ ₋₇	
HIP 70108	231 ⁺¹⁰ ₋₉	6.530 ± 0.001	0.089 ^{+0.061} _{-0.061}	-0.375 ^{+0.152} _{-0.156}	5007 ⁺¹¹¹ ₋₁₄₆	13.8 ^{+0.8} _{-0.6}	108 ⁺⁵ ₋₅	c
HIP 70145	580 ⁺¹⁵ ₋₁₄	6.213 ± 0.001	1.183 ^{+0.831} _{-0.481}	-3.786 ^{+0.536} _{-0.887}	4087 ⁺⁹¹ ₋₁₆₅	72.9 ^{+6.3} _{-3.1}	1336 ⁺⁴⁹ ₋₄₉	
HIP 70349	395 ⁺⁵ ₋₅	6.654 ± 0.001	0.413 ^{+0.381} _{-0.212}	-1.740 ^{+0.238} _{-0.407}	4149 ⁺²²⁴ ₋₉₉	38.4 ^{+1.9} _{-3.8}	394 ⁺⁷ ₋₇	
HIP 71436	587 ⁺⁹ ₋₉	6.963 ± 0.001	1.001 ^{+0.742} _{-0.413}	-2.880 ^{+0.448} _{-0.777}	4008 ⁺¹⁶⁶ ₋₁₁₃	55.8 ^{+3.3} _{-4.3}	723 ⁺¹⁹ ₋₁₉	
HIP 72499	137 ⁺¹ ₋₁	6.271 ± 0.001	0.169 ^{+0.304} _{-0.113}	0.418 ^{+0.130} _{-0.321}	4644 ⁺⁵³ ₋₁₀₁	11.3 ^{+0.5} _{-0.3}	53.2 ^{+0.5} _{-0.5}	
HIP 72578	403 ⁺⁵ ₋₅	6.295 ± 0.001	0.046 ^{+0.019} _{-0.019}	-1.780 ^{+0.047} _{-0.048}	3956 ⁺¹⁶¹ ₋₁₅₆	54.1 ^{+4.5} _{-4.2}	646 ⁺¹³ ₋₁₃	c
HIP 73977	307 ⁺⁵ ₋₅	6.020 ± 0.001	0.488 ^{+0.836} _{-0.316}	-1.906 ^{+0.354} _{-0.874}	4200 ⁺²⁹⁸ ₋₂₂₁	38.4 ^{+4.4} _{-4.9}	414 ⁺¹⁰ ₋₁₀	
HIP 74070	311 ⁺⁴ ₋₃	7.633 ± 0.001	0.039 ^{+0.004} _{-0.004}	0.133 ^{+0.029} _{-0.030}	4938 ⁺⁶⁶ ₋₄₂	11.6 ^{+0.2} _{-0.3}	72.5 ^{+1.2} _{-1.2}	c
HIP 74425	403 ⁺⁷ ₋₇	6.487 ± 0.001	0.528 ^{+0.213} _{-0.213}	-2.065 ^{+0.251} _{-0.252}	3936 ⁺⁹² ₋₁₆₉	50.3 ^{+4.6} _{-2.3}	546 ⁺¹⁴ ₋₁₄	c
HIP 74938	903 ⁺²⁴ ₋₂₃	7.235 ± 0.002	1.406 ^{+0.534} _{-0.321}	-3.950 ^{+0.379} _{-0.594}	3772 ⁺¹⁷⁵ ₋₁₆₇	93.4 ^{+8.8} _{-8.1}	1590 ⁺⁶⁹ ₋₆₉	
HIP 75257	629 ⁺⁵³ ₋₄₆	4.864 ± 0.003	0.570 ^{+1.050} _{-0.431}	-4.701 ^{+0.597} _{-1.229}	3898 ⁺¹⁵⁰ ₋₂₈	172 ⁺² ₋₁₂	6132 ⁺⁵⁵⁹ ₋₅₅₉	
HIP 76733	215 ⁺² ₋₂	5.970 ± 0.001	0.135 ^{+0.136} _{-0.135}	-0.831 ^{+0.154} _{-0.155}	5003 ⁺⁴⁴ ₋₃₁	16.7 ^{+0.2} _{-0.3}	158 ⁺² ₋₂	c
HIP 76947	663 ⁺¹⁴ ₋₁₄	6.878 ± 0.002	0.031 ^{+0.012} _{-0.012}	-2.259 ^{+0.060} _{-0.061}	3605 ⁺¹⁵⁸ ₋₉₂	93.1 ^{+4.9} _{-7.7}	1318 ⁺⁴⁵ ₋₄₅	c
HIP 77092	418 ⁺¹¹ ₋₁₀	6.911 ± 0.001	0.549 ^{+0.416} _{-0.315}	-1.746 ^{+0.369} _{-0.472}	4165 ⁺¹⁴⁸ ₋₂₂₂	35.7 ^{+4.1} _{-2.4}	346 ⁺¹¹ ₋₁₁	
HIP 77178	509 ⁺⁶ ₋₆	6.748 ± 0.001	0.994 ^{+0.607} _{-0.393}	-2.779 ^{+0.420} _{-0.634}	3839 ⁺²⁴⁹ ₋₁₁₉	61.4 ^{+4.0} _{-7.3}	737 ⁺¹⁶ ₋₁₆	
HIP 78802	687 ⁺¹² ₋₁₂	7.826 ± 0.001	0.031 ^{+0.012} _{-0.012}	-1.389 ^{+0.051} _{-0.051}	4300 ⁺¹⁴¹ ₋₉₂	35.1 ^{+1.6} _{-2.2}	380 ⁺¹¹ ₋₁₁	c
HIP 79187	320 ⁺⁴ ₋₄	6.212 ± 0.001	0.379 ^{+1.577} _{-0.320}	-1.691 ^{+0.348} _{-1.605}	4160 ⁺¹⁰⁹ ₋₇₄	37.7 ^{+1.4} _{-1.9}	384 ⁺⁷ ₋₇	
HIP 79357	220 ⁺⁴ ₋₄	5.317 ± 0.002	0.458 ^{+1.736} _{-0.275}	-1.853 ^{+0.312} _{-1.775}	4222 ⁺⁸⁸³ ₋₁₈₄	37.3 ^{+3.5} _{-11.8}	398 ⁺⁸ ₋₈	
HIP 80021	99.7 ^{+0.4} _{-0.4}	5.775 ± 0.001	0.054 ^{+0.022} _{-0.022}	0.727 ^{+0.030} _{-0.030}	5036 ⁺⁶⁵ ₋₁₀₀	8.31 ^{+0.34} _{-0.21}	40.0 ^{+0.2} _{-0.2}	c
HIP 80941	294 ⁺³ ₋₃	7.687 ± 0.001	0.154 ^{+0.903} _{-0.098}	0.191 ^{+0.121} _{-0.926}	4757 ⁺¹⁴⁶ ₋₁₁₀	11.8 ^{+0.6} _{-0.7}	64.7 ^{+1.0} _{-1.0}	
HIP 81104	378 ⁺³ ₋₃	6.653 ± 0.001	0.384 ^{+0.523} _{-0.131}	-1.617 ^{+0.149} _{-0.541}	4249 ⁺³¹⁸ ₋₇₄	34.1 ^{+1.2} _{-4.6}	341 ⁺⁵ ₋₅	
HIP 81289	272 ⁺⁴ ₋₄	5.547 ± 0.001	0.154 ^{+0.056} _{-0.056}	-1.781 ^{+0.085} _{-0.086}	4865 ⁺³⁰ ₋₃₂	27.6 ^{+0.4} _{-0.6}	386 ⁺⁷ ₋₇	c
HIP 81922	530 ⁺⁸ ₋₈	7.548 ± 0.001	0.399 ^{+1.248} _{-0.261}	-1.474 ^{+0.294} _{-1.282}	4152 ⁺⁶⁴⁶ ₋₁₀₅	34.3 ^{+1.8} _{-8.6}	314 ⁺⁸ ₋₈	
HIP 82324	294 ⁺² ₋₂	6.174 ± 0.001	0.154 ^{+0.109} _{-0.109}	-1.325 ^{+0.125} _{-0.125}	4531 ⁺³⁶ ₋₁₀₂	27.3 ^{+1.3} _{-0.4}	282 ⁺³ ₋₃	c
HIP 82385	210 ⁺¹ ₋₁	7.020 ± 0.001	0.054 ^{+0.022} _{-0.022}	0.357 ^{+0.036} _{-0.036}	5014 ⁺⁵⁶ ₋₂₉	9.99 ^{+0.12} _{-0.22}	56.8 ^{+0.5} _{-0.5}	c
HIP 82504	219 ⁺⁸ ₋₇	4.627 ± 0.003	0.139 ^{+0.124} _{-0.124}	-2.209 ^{+0.202} _{-0.204}	4370 ⁺⁷³ ₋₅	45.7 ^{+0.1} _{-1.5}	687 ⁺²⁸ ₋₂₈	c
HIP 82604	432 ⁺⁶ ₋₆	6.367 ± 0.001	0.897 ^{+1.160} _{-0.368}	-2.707 ^{+0.399} _{-1.191}	4181 ⁺¹⁸⁹ ₋₁₅₁	46.9 ^{+3.6} _{-4.0}	605 ⁺¹³ ₋₁₃	
HIP 83254	428 ⁺²⁸ ₋₂₅	5.259 ± 0.002	0.054 ^{+0.022} _{-0.022}	-2.952 ^{+0.155} _{-0.163}	4332 ⁺³⁶ ₋₉₇	68.9 ^{+3.2} _{-1.1}	1506 ⁺¹⁰⁷ ₋₁₀₇	c
HIP 84038	652 ⁺¹³ ₋₁₂	6.769 ± 0.006	1.040 ^{+0.436} _{-0.241}	-3.341 ^{+0.288} _{-0.484}	3902 ⁺¹⁸¹ ₋₁₂₀	74.0 ^{+4.8} _{-6.4}	1145 ⁺³⁷ ₋₃₇	
HIP 84239	300 ⁺² ₋₂	7.838 ± 0.001	0.064 ^{+0.687} _{-0.048}	0.389 ^{+0.065} _{-0.704}	4883 ⁺⁵⁷ ₋₃₂	10.5 ^{+0.2} _{-0.2}	56.6 ^{+0.7} _{-0.7}	
HIP 84380	109 ⁺⁵ ₋₅	2.552 ± 0.001	0.077 ^{+0.053} _{-0.053}	-2.712 ^{+0.152} _{-0.157}	4853 ⁺²⁴³ ₋₂₄₃	-	-	c d
HIP 84671	161 ⁺⁴ ₋₄	4.385 ± 0.003	0.459 ^{+1.051} _{-0.264}	-2.110 ^{+0.323} _{-1.111}	4125 ⁺⁷⁵ ₋₁₃₆	45.1 ^{+3.1} _{-1.6}	530 ⁺¹⁶ ₋₁₆	
HIP 85200	506 ⁺⁸ ₋₈	7.797 ± 0.001	0.426 ^{+0.866} _{-0.290}	-1.152 ^{+0.326} _{-0.903}	4477 ⁺⁸⁸ ₋₈₈	23.1 ^{+0.9} _{-0.9}	194 ⁺⁵ ₋₅	
HIP 85560	534 ⁺⁹ ₋₉	6.878 ± 0.001	0.845 ^{+1.068} _{-0.486}	-2.605 ^{+0.524} _{-1.107}	4064 ⁺⁷⁹ ₋₇₃	50.4 ^{+1.8} _{-1.9}	623 ⁺¹⁷ ₋₁₇	
HIP 86153	275 ⁺⁸ ₋₇	5.271 ± 0.003	0.200 ^{+0.004} _{-0.004}	-2.127 ^{+0.065} _{-0.067}	3661 ⁺¹⁹⁸ ₋₁₆₀	76.1 ^{+7.1} _{-7.6}	936 ⁺³¹ ₋₃₁	c
HIP 86476	164 ⁺⁴ ₋₄	5.078 ± 0.003	0.524 ^{+0.044} _{-0.044}	-1.516 ^{+0.095} _{-0.096}	3700 ⁺¹³² ₋₁₃₁	47.6 ^{+3.6} _{-3.2}	382 ⁺¹⁰ ₋₁₀	c
HIP 86483	321 ⁺⁴ ₋₄	6.593 ± 0.001	0.185 ^{+0.414} _{-0.156}	-1.121 ^{+0.183} _{-0.441}	4090 ⁺²³² ₋₁₀₁	33.5 ^{+1.7} _{-3.5}	283 ⁺⁵ ₋₅	
HIP 86625	430 ⁺²⁴ ₋₂₂	6.823 ± 0.001	0.714 ^{+0.481} _{-0.268}	-2.059 ^{+0.382} _{-0.602}	4074 ⁺¹³⁴ ₋₁₀₉	40.9 ^{+2.3} _{-2.6}	416 ⁺²⁶ ₋₂₆	
HIP 86709	345 ⁺¹¹ ₋₁₀	5.735 ± 0.002	0.239 ^{+0.096} _{-0.096}	-2.190 ^{+0.165} _{-0.167}	3461 ⁺²⁶⁶ ₋₁₅₇	92.9 ^{+9.1} _{-12.8}	1117 ⁺⁴³ ₋₄₃	c
HIP 87107	362 ⁺⁸ ₋₈	6.252 ± 0.002	0.447 ^{+0.120} _{-0.120}	-1.988 ^{+0.168} _{-0.169}	3615 ⁺²⁵⁶ ₋₁₁₆	66.6 ^{+4.5} _{-8.5}	682 ⁺¹⁹ ₋₁₉	c
HIP 87244	377 ⁺¹⁰ ₋₁₀	6.413 ± 0.002	0.903 ^{+0.939} _{-0.423}	-2.374 ^{+0.481} _{-0.999}	3509 ⁺³²⁵ ₋₁₈₉	71.2 ^{+8.4} _{-11.5}	692 ⁺²³ ₋₂₃	
HIP 87251	552 ⁺¹⁰ ₋₉	6.821 ± 0.001	0.223 ^{+0.090} _{-0.090}	-2.111 ^{+0.127} _{-0.128}	4077 ⁺¹¹⁴ ₋₆₉	52.9 ^{+1.8} _{-2.8}	696 ⁺¹⁹ ₋₁₉	c

Continued

Target	d [pc]	G [mag]	A_G [mag]	M_G [mag]	T_{eff} [K]	R [R_{\odot}]	L [L_{\odot}]	rem.
HIP 88411	1247^{+46}_{-42}	7.771 ± 0.003	$0.246^{+1.145}_{-0.211}$	$-2.955^{+0.289}_{-1.225}$	4359^{+136}_{-156}	$63.8^{+4.8}_{-3.8}$	1326^{+79}_{-79}	
HIP 88518	307^{+2}_{-2}	6.895 ± 0.001	$0.244^{+1.408}_{-0.158}$	$-0.783^{+0.172}_{-1.422}$	4366^{+166}_{-102}	$22.7^{+1.1}_{-1.6}$	169^{+2}_{-2}	
HIP 88984	470^{+12}_{-11}	6.578 ± 0.001	$1.028^{+0.778}_{-0.332}$	$-2.812^{+0.386}_{-0.833}$	3883^{+193}_{-101}	$59.0^{+3.2}_{-5.5}$	712^{+24}_{-24}	
HIP 91200	413^{+5}_{-5}	6.244 ± 0.001	$0.173^{+1.333}_{-0.118}$	$-2.007^{+0.143}_{-1.358}$	4331^{+273}_{-73}	$42.5^{+1.5}_{-4.9}$	571^{+11}_{-11}	
HIP 92249	687^{+17}_{-16}	7.416 ± 0.001	$0.085^{+0.034}_{-0.034}$	$-1.852^{+0.086}_{-0.088}$	4069^{+88}_{-78}	$50.5^{+2.0}_{-2.1}$	631^{+23}_{-23}	c
HIP 92404	446^{+4}_{-7}	7.189 ± 0.001	$0.390^{+0.193}_{-0.228}$	$-1.448^{+0.260}_{-0.226}$	4062^{+187}_{-102}	$36.4^{+1.9}_{-3.1}$	325^{+8}_{-8}	
HIP 92651	399^{+4}_{-4}	6.875 ± 0.001	$0.189^{+0.034}_{-0.034}$	$-1.321^{+0.057}_{-0.057}$	4166^{+92}_{-120}	$34.7^{+2.1}_{-1.5}$	326^{+6}_{-6}	c
HIP 92713	398^{+7}_{-7}	5.919 ± 0.001	$1.225^{+1.137}_{-0.481}$	$-3.304^{+0.518}_{-1.175}$	4034^{+300}_{-130}	$59.5^{+4.0}_{-7.9}$	845^{+21}_{-21}	
HIP 93801	346^{+6}_{-6}	6.286 ± 0.001	$0.107^{+2.052}_{-0.091}$	$-1.515^{+0.131}_{-2.093}$	4623^{+70}_{-48}	$28.8^{+0.6}_{-0.9}$	340^{+8}_{-8}	
HIP 93913	655^{+12}_{-12}	7.099 ± 0.001	$0.139^{+0.034}_{-0.034}$	$-2.121^{+0.075}_{-0.075}$	4152^{+116}_{-178}	$52.2^{+4.8}_{-2.8}$	730^{+22}_{-22}	c
HIP 94220	413^{+11}_{-11}	6.575 ± 0.001	$0.282^{+1.480}_{-0.148}$	$-1.786^{+0.205}_{-1.538}$	4250^{+60}_{-110}	$38.6^{+2.1}_{-1.1}$	438^{+15}_{-15}	
HIP 94229	811^{+19}_{-18}	7.209 ± 0.001	$0.162^{+0.034}_{-0.034}$	$-2.498^{+0.083}_{-0.084}$	4617^{+140}_{-89}	$44.9^{+1.8}_{-2.6}$	824^{+31}_{-31}	c
HIP 94518	546^{+8}_{-8}	7.595 ± 0.001	$0.182^{+0.355}_{-0.127}$	$-1.274^{+0.159}_{-0.388}$	4359^{+175}_{-58}	$29.7^{+0.8}_{-2.2}$	286^{+7}_{-7}	
HIP 94761	$5.91^{+0.01}_{-0.01}$	8.098 ± 0.001	$0.527^{+0.284}_{-0.428}$	$8.713^{+0.430}_{-0.286}$	4118^{+208}_{-224}	-	-	
HIP 95297	466^{+5}_{-5}	7.881 ± 0.001	$0.362^{+1.346}_{-0.283}$	$-0.825^{+0.309}_{-1.371}$	4601^{+72}_{-87}	$18.9^{+0.7}_{-0.6}$	145^{+3}_{-3}	
HIP 95744	294^{+3}_{-3}	6.543 ± 0.001	$0.645^{+0.578}_{-0.332}$	$-1.445^{+0.354}_{-0.600}$	4277^{+266}_{-144}	$27.3^{+1.9}_{-3.1}$	225^{+3}_{-3}	
HIP 96203	540^{+7}_{-7}	7.807 ± 0.001	$0.477^{+1.826}_{-0.246}$	$-1.334^{+0.276}_{-1.856}$	4335^{+291}_{-73}	$27.1^{+0.9}_{-3.3}$	233^{+5}_{-5}	
HIP 96966	236^{+2}_{-2}	8.104 ± 0.001	$0.308^{+0.232}_{-0.232}$	$0.933^{+0.253}_{-0.253}$	6113^{+67}_{-80}	$4.34^{+0.12}_{-0.09}$	$23.7^{+0.3}_{-0.3}$	c
HIP 97135	409^{+12}_{-11}	5.815 ± 0.002	$0.354^{+0.143}_{-0.143}$	$-2.598^{+0.204}_{-0.205}$	3743^{+143}_{-137}	$82.1^{+6.4}_{-5.9}$	1191^{+42}_{-42}	c
HIP 97198	316^{+5}_{-4}	8.428 ± 0.001	$0.431^{+1.168}_{-0.266}$	$0.502^{+0.298}_{-1.200}$	4908^{+170}_{-134}	$8.32^{+0.48}_{-0.54}$	$36.2^{+0.7}_{-0.7}$	
HIP 97359	388^{+5}_{-5}	6.259 ± 0.001	$0.454^{+0.162}_{-0.162}$	$-2.138^{+0.189}_{-0.190}$	3820^{+133}_{-113}	$59.3^{+3.7}_{-3.9}$	676^{+13}_{-13}	c
HIP 97402	118^{+1}_{-1}	5.714 ± 0.001	$0.065^{+1.976}_{-0.049}$	$0.292^{+0.061}_{-1.988}$	4949^{+79}_{-83}	$10.6^{+0.4}_{-0.3}$	$60.2^{+0.5}_{-0.5}$	
HIP 98073	249^{+7}_{-7}	4.312 ± 0.003	$0.119^{+0.103}_{-0.103}$	$-2.792^{+0.164}_{-0.165}$	3940^{+198}_{-30}	$84.0^{+1.3}_{-7.9}$	1533^{+49}_{-49}	c
HIP 98443	493^{+9}_{-8}	6.360 ± 0.001	$0.208^{+0.084}_{-0.084}$	$-2.312^{+0.122}_{-0.123}$	4062^{+191}_{-122}	$59.0^{+3.7}_{-5.2}$	854^{+23}_{-23}	c
HIP 98610	409^{+4}_{-4}	6.171 ± 0.001	$0.108^{+0.016}_{-0.016}$	$-1.997^{+0.037}_{-0.037}$	3965^{+92}_{-128}	$57.7^{+3.9}_{-2.6}$	741^{+12}_{-12}	c
HIP 98762	592^{+11}_{-11}	7.391 ± 0.001	$0.595^{+0.342}_{-0.492}$	$-2.066^{+0.532}_{-0.582}$	3983^{+180}_{-148}	$47.1^{+3.7}_{-4.0}$	503^{+15}_{-15}	
HIP 99853	421^{+21}_{-19}	4.846 ± 0.002	$0.416^{+0.168}_{-0.168}$	$-3.693^{+0.270}_{-0.275}$	4954^{+105}_{-94}	$56.5^{+2.2}_{-2.3}$	1729^{+97}_{-97}	c
HIP 100172	175^{+1}_{-1}	7.282 ± 0.001	$0.538^{+1.049}_{-0.490}$	$0.524^{+0.502}_{-1.061}$	4814^{+37}_{-46}	$8.22^{+0.16}_{-0.13}$	$32.7^{+0.3}_{-0.3}$	
HIP 100180	613^{+10}_{-10}	7.113 ± 0.001	$0.239^{+0.096}_{-0.096}$	$-2.063^{+0.134}_{-0.134}$	3795^{+243}_{-293}	$65.1^{+11.3}_{-7.6}$	792^{+22}_{-22}	c
HIP 100390	308^{+4}_{-4}	5.959 ± 0.001	$0.513^{+0.762}_{-0.313}$	$-1.998^{+0.339}_{-0.788}$	4045^{+73}_{-70}	$44.8^{+1.6}_{-1.6}$	483^{+8}_{-8}	
HIP 100534	479^{+7}_{-7}	6.936 ± 0.001	$1.016^{+0.411}_{-0.411}$	$-2.483^{+0.442}_{-0.442}$	3754^{+104}_{-199}	$57.0^{+6.6}_{-3.0}$	581^{+13}_{-13}	c
HIP 100684	159^{+1}_{-1}	7.181 ± 0.001	$0.343^{+2.175}_{-0.243}$	$0.835^{+0.252}_{-2.184}$	4714^{+85}_{-94}	$8.24^{+0.34}_{-0.29}$	$30.2^{+0.2}_{-0.2}$	
HIP 101219	554^{+15}_{-14}	6.806 ± 0.001	$0.649^{+0.262}_{-0.262}$	$-2.562^{+0.319}_{-0.321}$	4058^{+281}_{-129}	$54.3^{+3.6}_{-6.8}$	720^{+27}_{-27}	c
HIP 101412	563^{+21}_{-19}	5.704 ± 0.002	$1.308^{+0.503}_{-0.430}$	$-4.358^{+0.509}_{-0.585}$	3708^{+224}_{-108}	123^{+8}_{-14}	2583^{+121}_{-121}	
HIP 101692	291^{+31}_{-26}	4.196 ± 0.003	$0.262^{+0.207}_{-0.207}$	$-3.388^{+0.410}_{-0.429}$	3920^{+162}_{-34}	104^{+2}_{-8}	2302^{+236}_{-236}	c
HIP 101841	835^{+26}_{-24}	6.771 ± 0.001	$0.847^{+0.242}_{-0.242}$	$-3.684^{+0.306}_{-0.308}$	3807^{+193}_{-57}	103^{+5}_{-10}	2021^{+93}_{-93}	c
HIP 101953	332^{+4}_{-4}	7.000 ± 0.001	$0.279^{+1.169}_{-0.251}$	$-0.887^{+0.278}_{-1.196}$	4579^{+85}_{-85}	$20.4^{+0.8}_{-0.7}$	165^{+3}_{-3}	
HIP 102377	500^{+7}_{-7}	6.065 ± 0.001	$0.163^{+1.412}_{-0.121}$	$-2.592^{+0.151}_{-1.443}$	4243^{+173}_{-127}	$59.6^{+3.8}_{-4.6}$	1038^{+24}_{-24}	
HIP 102440	262^{+17}_{-15}	4.517 ± 0.007	$0.177^{+0.143}_{-0.143}$	$-2.750^{+0.280}_{-0.289}$	3300^{+16}_{-16}	145^{+1}_{-1}	2244^{+155}_{-155}	c
HIP 102912	201^{+1}_{-1}	6.419 ± 0.001	$0.509^{+0.261}_{-0.188}$	$-0.606^{+0.204}_{-0.277}$	4084^{+131}_{-47}	$22.8^{+0.5}_{-1.4}$	131^{+1}_{-1}	
HIP 103035	272^{+2}_{-2}	7.146 ± 0.001	$0.424^{+0.294}_{-0.294}$	$-0.451^{+0.311}_{-0.311}$	5109^{+62}_{-71}	$11.7^{+0.3}_{-0.3}$	$83.8^{+1.0}_{-1.0}$	c
HIP 103242	930^{+59}_{-53}	5.845 ± 0.002	$0.362^{+0.011}_{-0.011}$	$-4.359^{+0.139}_{-0.147}$	3674^{+223}_{-154}	198^{+18}_{-22}	6443^{+503}_{-503}	c
HIP 103263	181^{+1}_{-1}	6.750 ± 0.001	$0.252^{+1.969}_{-0.217}$	$0.213^{+0.230}_{-1.983}$	4982^{+88}_{-78}	$9.90^{+0.31}_{-0.34}$	$54.4^{+0.5}_{-0.5}$	
HIP 103637	682^{+15}_{-15}	6.330 ± 0.001	$0.724^{+0.064}_{-0.064}$	$-3.563^{+0.112}_{-0.113}$	4994^{+394}_{-181}	$45.7^{+3.5}_{-6.5}$	1170^{+41}_{-41}	c
HIP 103868	507^{+12}_{-12}	6.016 ± 0.002	$1.156^{+0.723}_{-0.391}$	$-3.665^{+0.444}_{-0.777}$	3897^{+101}_{-107}	$81.5^{+4.7}_{-4.1}$	1379^{+46}_{-46}	
HIP 104172	132^{+1}_{-1}	5.838 ± 0.001	$0.104^{+0.030}_{-0.030}$	$0.123^{+0.041}_{-0.041}$	4858^{+12}_{-76}	$11.8^{+0.4}_{-0.4}$	$69.5^{+0.5}_{-0.5}$	c

Continued								
Target	d [pc]	G [mag]	A_G [mag]	M_G [mag]	T_{eff} [K]	R [R_{\odot}]	L [L_{\odot}]	rem.
HIP 105182	363 ⁺⁴ ₋₄	6.991 ± 0.001	0.334 ^{+0.248} _{-0.206}	-1.141 ^{+0.228} _{-0.270}	4274 ⁺²¹² ₋₁₂₁	27.5 ^{+1.6} _{-2.6}	228 ⁺⁴ ₋₄	
HIP 105205	267 ⁺³ ₋₃	6.332 ± 0.001	0.196 ^{+0.027} _{-0.027}	-0.997 ^{+0.053} _{-0.053}	4903 ⁺⁴⁶ ₋₇₀	18.5 ^{+0.5} _{-0.3}	178 ⁺³ ₋₃	c
HIP 105669	938 ⁺²⁸ ₋₂₇	6.893 ± 0.001	1.802 ^{+0.209} _{-0.209}	-4.769 ^{+0.272} _{-0.274}	4046 ⁺¹⁵⁰ ₋₁₅₉	90.1 ^{+7.5} _{-6.3}	1959 ⁺⁹³ ₋₉₃	c
HIP 105949	258 ⁺⁸ ₋₇	4.910 ± 0.004	0.589 ^{+0.270} _{-0.270}	-2.739 ^{+0.337} _{-0.339}	3500 ⁺¹⁹⁵ ₋₅₂	97.8 ^{+3.0} _{-10.1}	1293 ⁺⁴⁵ ₋₄₅	c
HIP 106306	148 ⁺¹ ₋₁	6.164 ± 0.001	0.077 ^{+0.031} _{-0.031}	0.237 ^{+0.047} _{-0.048}	4834 ⁺⁶⁶ ₋₅₄	11.5 ^{+0.3} _{-0.3}	64.6 ^{+0.6} _{-0.6}	c
HIP 106848	354 ⁺⁴ ₋₄	6.816 ± 0.001	0.381 ^{+0.018} _{-0.018}	-1.311 ^{+0.042} _{-0.042}	5328 ⁺²⁷² ₋₅₁	16.0 ^{+0.3} _{-1.5}	187 ⁺³ ₋₃	c
HIP 106973	414 ⁺⁵ ₋₅	6.322 ± 0.001	0.220 ^{+1.418} _{-0.157}	-1.985 ^{+0.185} _{-1.446}	4389 ⁺¹⁵⁴ ₋₇₅	39.5 ^{+1.4} _{-2.6}	521 ⁺¹⁰ ₋₁₀	
HIP 106974	493 ⁺¹⁰ ₋₁₀	6.789 ± 0.001	0.420 ^{+1.948} _{-0.396}	-2.093 ^{+0.440} _{-1.992}	4690 ⁺³⁰⁴ ₋₁₀₃	31.4 ^{+1.4} _{-3.7}	429 ⁺¹³ ₋₁₃	
HIP 107205	467 ⁺⁷ ₋₆	6.930 ± 0.001	0.378 ^{+0.153} _{-0.153}	-1.795 ^{+0.184} _{-0.184}	4091 ⁺¹⁸¹ ₋₁₃₁	42.0 ^{+2.8} _{-3.5}	445 ⁺¹⁰ ₋₁₀	c
HIP 107259	3071 ⁺³¹⁸² ₋₁₆₁₇	2.327 ± 0.005	1.540 ^{+0.207} _{-0.207}	-11.649 ^{+1.836} _{-1.756}	3707 ⁺¹⁸⁵ ₋₁₈₅	-	-	c d
HIP 107315	211 ⁺⁸ ₋₇	1.708 ± 0.022	0.231 ^{+0.231} _{-0.231}	-5.149 ^{+0.330} _{-0.333}	4457 ⁺²²³ ₋₂₂₃	-	-	a c d
HIP 107325	619 ⁺¹¹ ₋₁₁	7.680 ± 0.001	0.661 ^{+0.444} _{-0.191}	-1.941 ^{+0.229} _{-0.483}	4135 ⁺¹²⁵ ₋₆₈	38.3 ^{+1.3} _{-2.2}	385 ⁺¹¹ ₋₁₁	
HIP 107350	18.1 ^{+0.1} _{-0.1}	5.811 ± 0.001	0.060 ^{+0.120} _{-0.043}	4.460 ^{+0.047} _{-0.124}	5955 ⁺⁸⁷ ₋₈₉	1.01 ^{+0.03} _{-0.03}	1.15 ^{+0.01} _{-0.01}	
HIP 107723	274 ⁺⁶ ₋₆	5.339 ± 0.002	0.362 ^{+0.143} _{-0.143}	-2.213 ^{+0.189} _{-0.190}	3949 ⁺²⁶³ ₋₁₇₉	57.2 ^{+5.6} _{-6.9}	716 ⁺¹⁹ ₋₁₉	c
HIP 107923	389 ⁺⁶ ₋₅	6.228 ± 0.001	0.697 ^{+0.948} _{-0.395}	-2.419 ^{+0.426} _{-0.979}	4034 ⁺¹⁵⁷ ₋₁₀₄	50.5 ^{+2.7} _{-3.7}	608 ⁺¹³ ₋₁₃	
HIP 108030	404 ⁺⁶ ₋₆	7.133 ± 0.001	0.680 ^{+1.477} _{-0.485}	-1.578 ^{+0.517} _{-1.509}	4878 ⁺⁴⁹ ₋₅₅	19.7 ^{+0.4} _{-0.4}	198 ⁺⁴ ₋₄	
HIP 108202	735 ⁺¹⁸ ₋₁₇	7.165 ± 0.001	1.285 ^{+0.698} _{-0.483}	-3.452 ^{+0.534} _{-0.751}	3837 ⁺²³² ₋₁₀₈	73.8 ^{+4.3} _{-8.2}	1063 ⁺⁴⁰ ₋₄₀	
HIP 108233	357 ⁺⁴ ₋₄	6.298 ± 0.001	0.452 ^{+1.528} _{-0.393}	-1.919 ^{+0.417} _{-1.552}	4603 ⁺⁷⁴ ₋₆₉	29.9 ^{+0.9} _{-0.9}	363 ⁺⁶ ₋₆	
HIP 108296	312 ⁺¹¹ ₋₁₁	5.597 ± 0.003	0.166 ^{+0.064} _{-0.064}	-2.040 ^{+0.142} _{-0.144}	3954 ⁺²⁴⁶ ₋₂₀₆	57.6 ^{+6.5} _{-6.5}	730 ⁺³¹ ₋₃₁	c
HIP 108378	325 ⁺⁶ ₋₆	5.784 ± 0.001	1.210 ^{+0.715} _{-0.440}	-2.989 ^{+0.481} _{-0.756}	3965 ⁺²²³ ₋₁₈₇	54.7 ^{+5.5} _{-5.7}	665 ⁺¹⁶ ₋₁₆	
HIP 109247	459 ⁺⁷ ₋₇	6.744 ± 0.001	0.584 ^{+0.699} _{-0.365}	-2.150 ^{+0.398} _{-0.733}	4051 ⁺¹¹¹ ₋₉₁	46.4 ^{+2.2} _{-2.5}	523 ⁺¹² ₋₁₂	
HIP 109492	183 ⁺¹⁷ ₋₁₅	2.743 ± 0.001	0.547 ^{+0.210} _{-0.210}	-4.118 ^{+0.392} _{-0.408}	4656 ⁺²³³ ₋₂₃₃	-	-	c d
HIP 109602	561 ⁺³⁶ ₋₃₂	5.411 ± 0.002	0.629 ^{+0.940} _{-0.430}	-3.961 ^{+0.558} _{-1.075}	4187 ⁺⁴⁷³ ₋₄₈	94.0 ^{+2.2} _{-18.1}	2449 ⁺¹⁷⁴ ₋₁₇₄	
HIP 110504	3416 ⁺¹³⁶⁶ ₋₈₂₈	5.537 ± 0.006	0.293 ^{+0.209} _{-0.209}	-7.423 ^{+0.818} _{-0.946}	3588 ⁺⁴²⁵ ₋₁₀₈	-	-	c
HIP 110991	265 ⁺¹² ₋₁₁	3.87 ± 0.03	0.250 ^{+0.082} _{-0.082}	-3.501 ^{+0.202} _{-0.206}	5610 ⁺²⁸¹ ₋₂₈₁	-	-	a b c d
HIP 110992	280 ⁺⁷ ₋₇	5.396 ± 0.002	0.285 ^{+1.500} _{-0.246}	-2.128 ^{+0.301} _{-1.556}	4486 ⁺¹¹⁹ ₋₇₇	38.2 ^{+1.4} _{-2.0}	532 ⁺¹⁶ ₋₁₆	
HIP 111810	124 ⁺² ₋₂	5.577 ± 0.002	0.069 ^{+0.018} _{-0.018}	0.036 ^{+0.053} _{-0.054}	4981 ⁺³⁸ ₋₂₁	11.7 ^{+0.1} _{-0.2}	75.4 ^{+1.4} _{-1.4}	c
HIP 112098	378 ⁺¹¹ ₋₁₀	5.479 ± 0.002	0.703 ^{+1.041} _{-0.401}	-3.113 ^{+0.462} _{-1.103}	4099 ⁺⁷⁷² ₋₁₆₉	65.6 ^{+5.8} _{-19.2}	1096 ⁺³⁸ ₋₃₈	
HIP 112248	681 ⁺¹³ ₋₁₂	6.731 ± 0.001	0.979 ^{+1.003} _{-0.365}	-3.412 ^{+0.404} _{-1.043}	3867 ⁺¹³⁸ ₋₁₀₇	81.2 ^{+4.7} _{-5.5}	1328 ⁺⁴¹ ₋₄₁	
HIP 112987	540 ⁺¹¹ ₋₁₀	6.153 ± 0.001	0.185 ^{+0.075} _{-0.075}	-2.695 ^{+0.117} _{-0.118}	3932 ⁺¹¹² ₋₁₆₃	79.2 ^{+7.0} _{-4.3}	1352 ⁺⁴⁰ ₋₄₀	c
HIP 113561	3536 ⁺¹²⁷⁴ ₋₈₁₃	4.958 ± 0.002	1.030 ^{+0.332} _{-0.417}	-8.814 ^{+0.987} _{-1.003}	5052 ⁺⁴²⁷ ₋₃₁₈	-	-	
HIP 113881	60.1 ^{+0.5} _{-0.5}	1.25 ± 0.06	0.023 ^{+0.044} _{-0.023}	-2.672 ^{+0.102} _{-0.124}	3707 ⁺¹⁸⁵ ₋₁₈₅	-	-	a b c d
HIP 114155	164 ⁺¹² ₋₁₁	4.243 ± 0.004	0.337 ^{+1.402} _{-0.290}	-2.169 ^{+0.439} _{-1.561}	4302 ⁺¹⁴⁸ ₋₆₂	42.6 ^{+1.3} _{-2.8}	561 ⁺⁴² ₋₄₂	
HIP 115147	19.0 ^{+0.1} _{-0.1}	7.282 ± 0.001	0.093 ^{+0.127} _{-0.051}	5.801 ^{+0.053} _{-0.129}	5115 ⁺³⁰ ₋₈₈	0.76 ^{+0.02} _{-0.01}	0.353 ^{+0.001} _{-0.001}	
HIP 117299	492 ⁺²⁷ ₋₂₄	4.856 ± 0.002	0.460 ^{+1.062} _{-0.354}	-4.066 ^{+0.466} _{-1.179}	3940 ⁺¹⁴¹ ₋₃₁	130 ⁺² ₋₉	3652 ⁺²²³ ₋₂₂₃	
HIP 117956	528 ⁺¹⁶ ₋₁₅	5.669 ± 0.001	0.212 ^{+0.180} _{-0.180}	-3.156 ^{+0.244} _{-0.246}	4720 ⁺⁸⁰ ₋₇₂	55.4 ^{+1.7} _{-1.8}	1371 ⁺⁵⁵ ₋₅₅	c
HIP 118077	63.3 ^{+0.4} _{-0.4}	6.181 ± 0.002	0.108 ^{+0.034} _{-0.034}	2.066 ^{+0.047} _{-0.047}	6322 ⁺¹¹⁸ ₋₄₆₀	3.70 ^{+0.61} _{-0.13}	19.8 ^{+0.1} _{-0.1}	c f
HIP 120005	6.33 ^{+0.01} _{-0.01}	7.048 ± 0.001	0.056 ^{+0.785} _{-0.048}	7.984 ^{+0.050} _{-0.786}	3995 ⁺¹¹⁹ ₋₁₀₂	0.57 ^{+0.03} _{-0.03}	0.076 ^{+0.001} _{-0.001}	

a - Hipparcos parallax (van Leeuwen, 2007) was used for distance determination

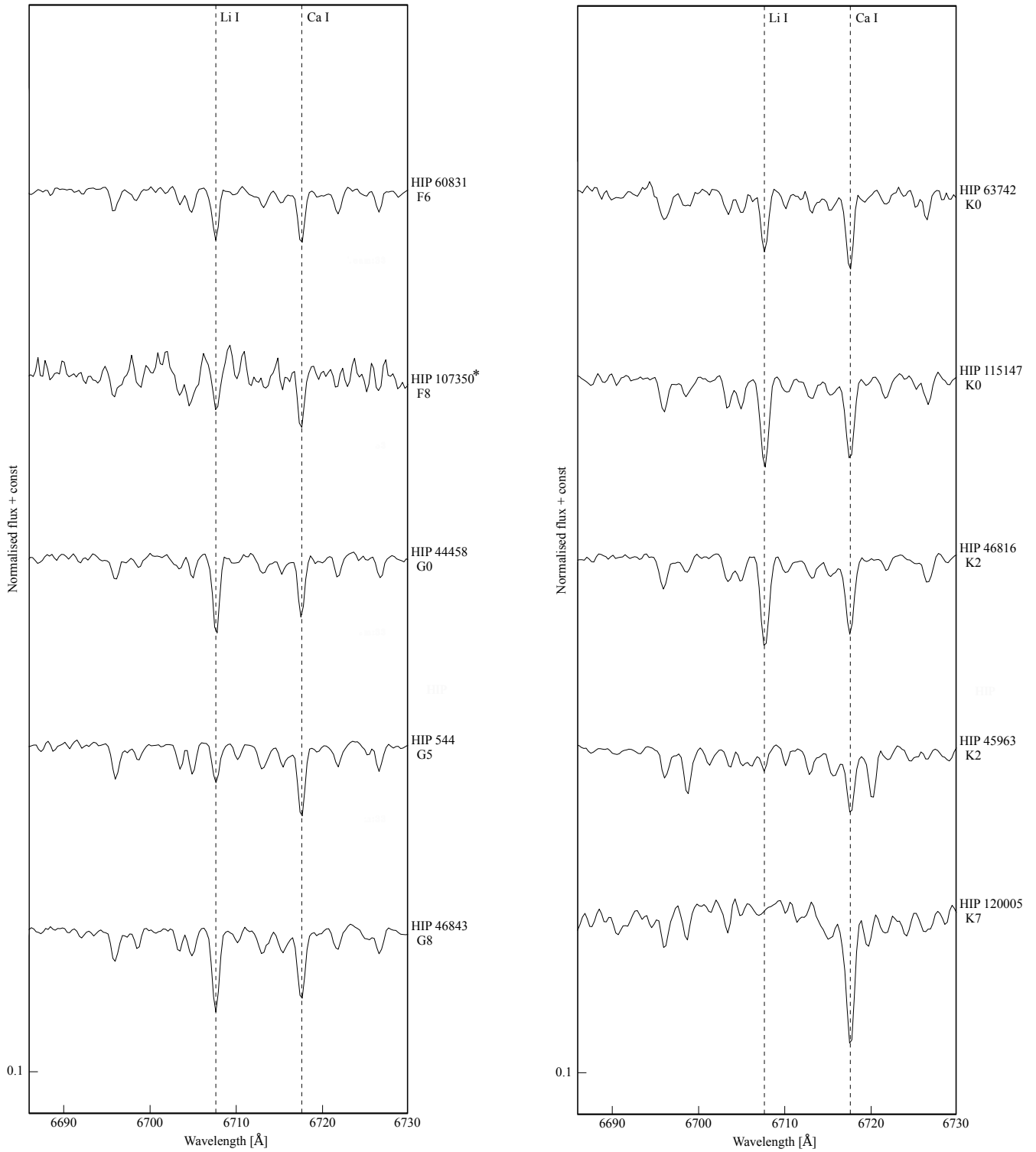
b - V -, and I -band magnitude from Hipparcos (Perryman et al., 1997) were transformed into G -band magnitude according to Jordi et al. (2010)

c - median A_V value taken from literature and converted to A_G

d - T_{eff} (Damiani et al., 2016) according to the Hipparcos spectral type

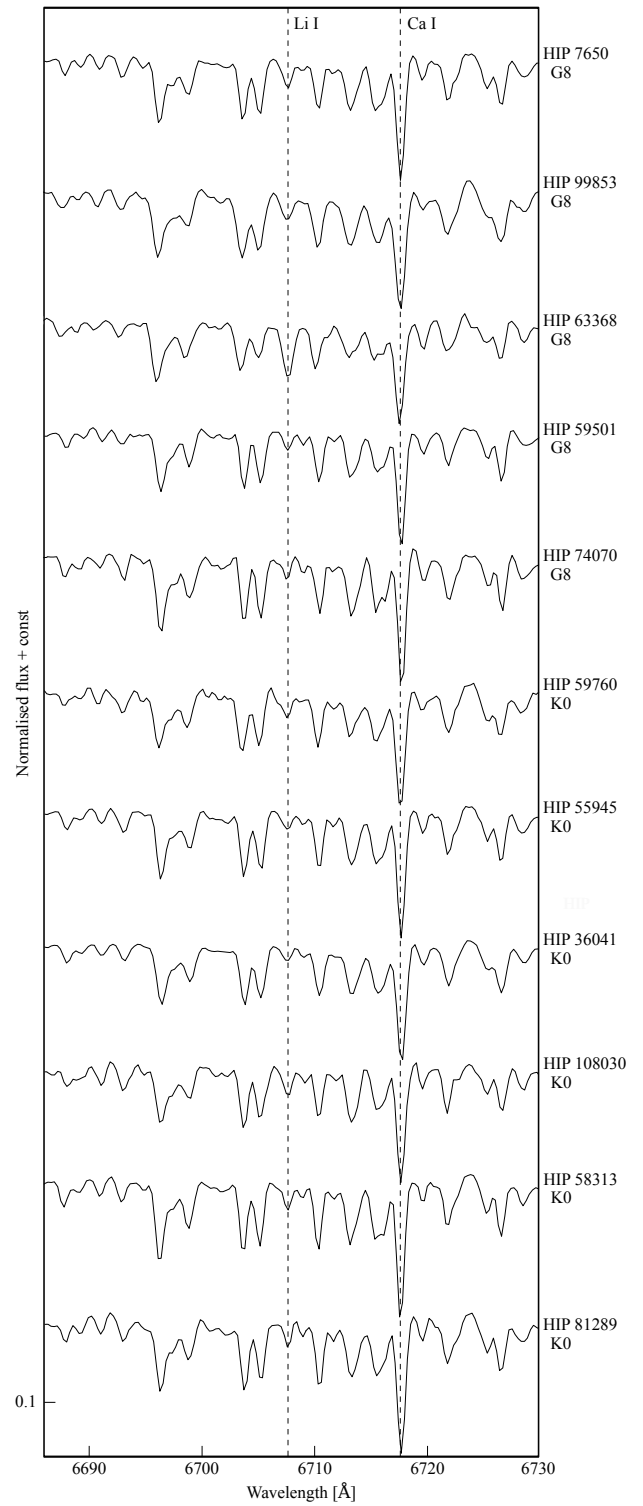
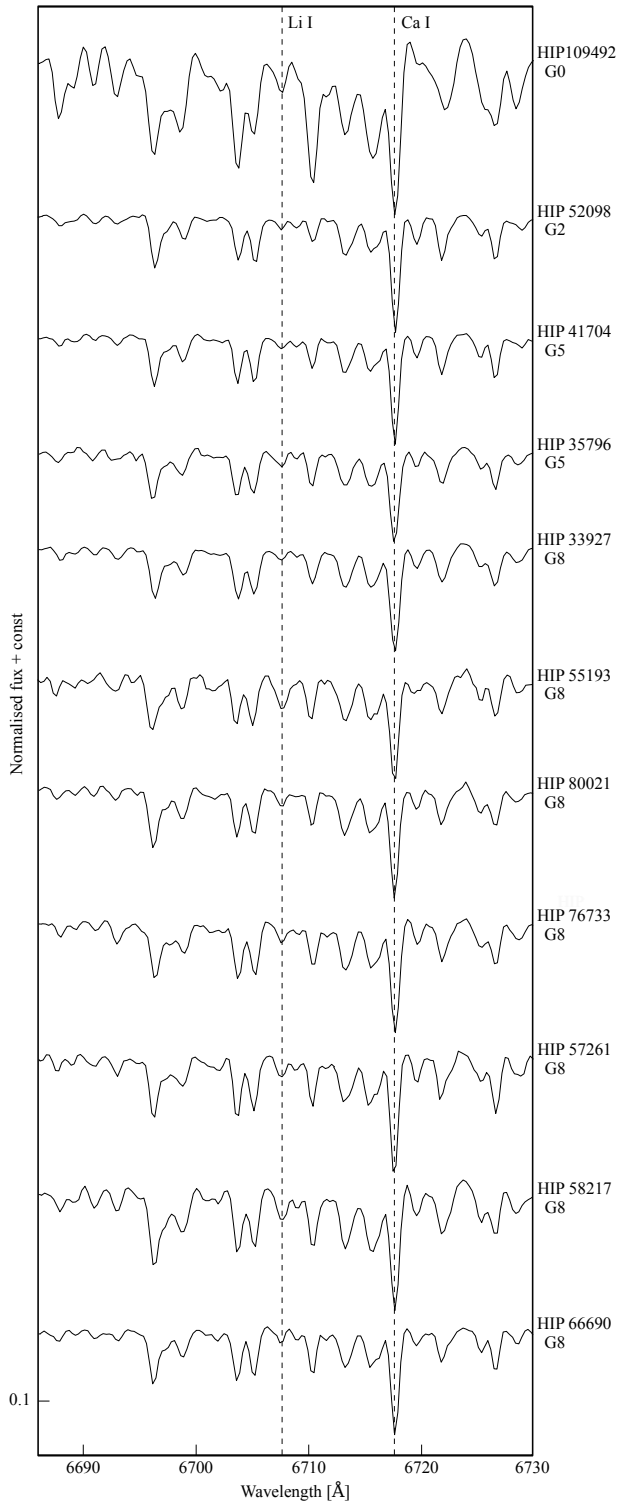
e - R and L from *Gaia* rejected because no gold/silver flag target

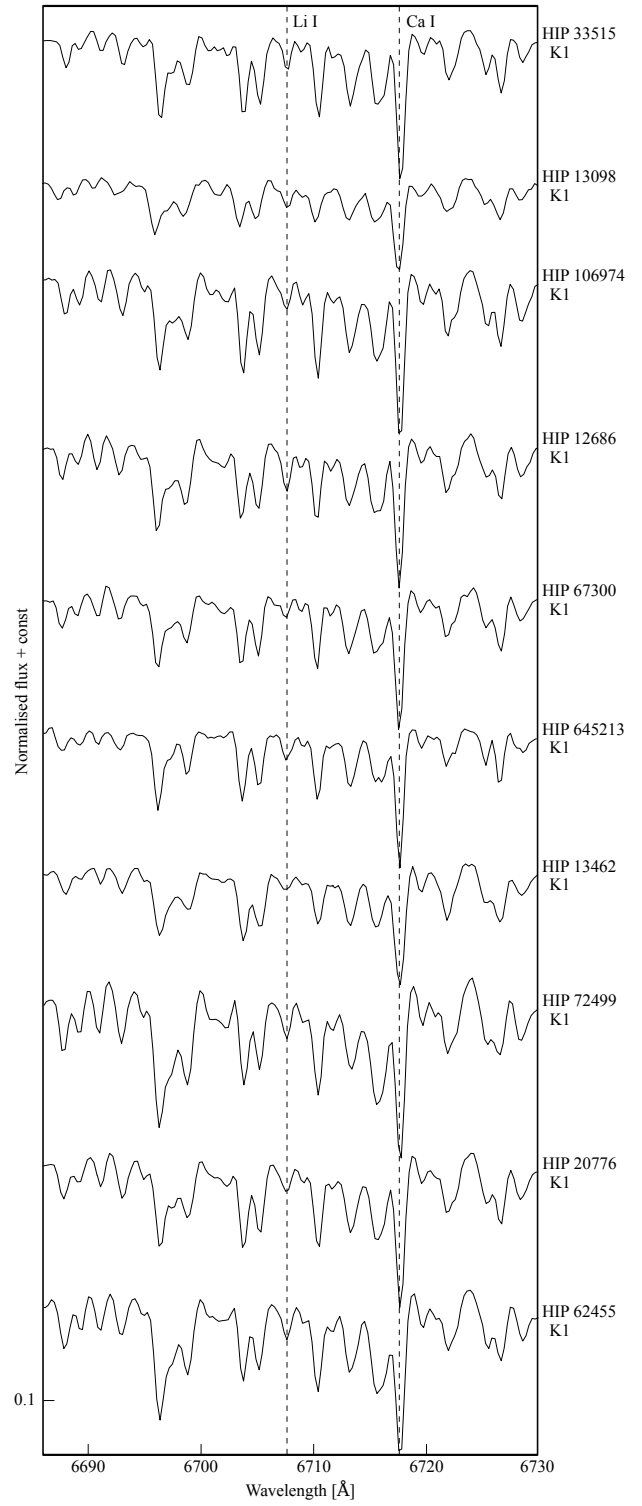
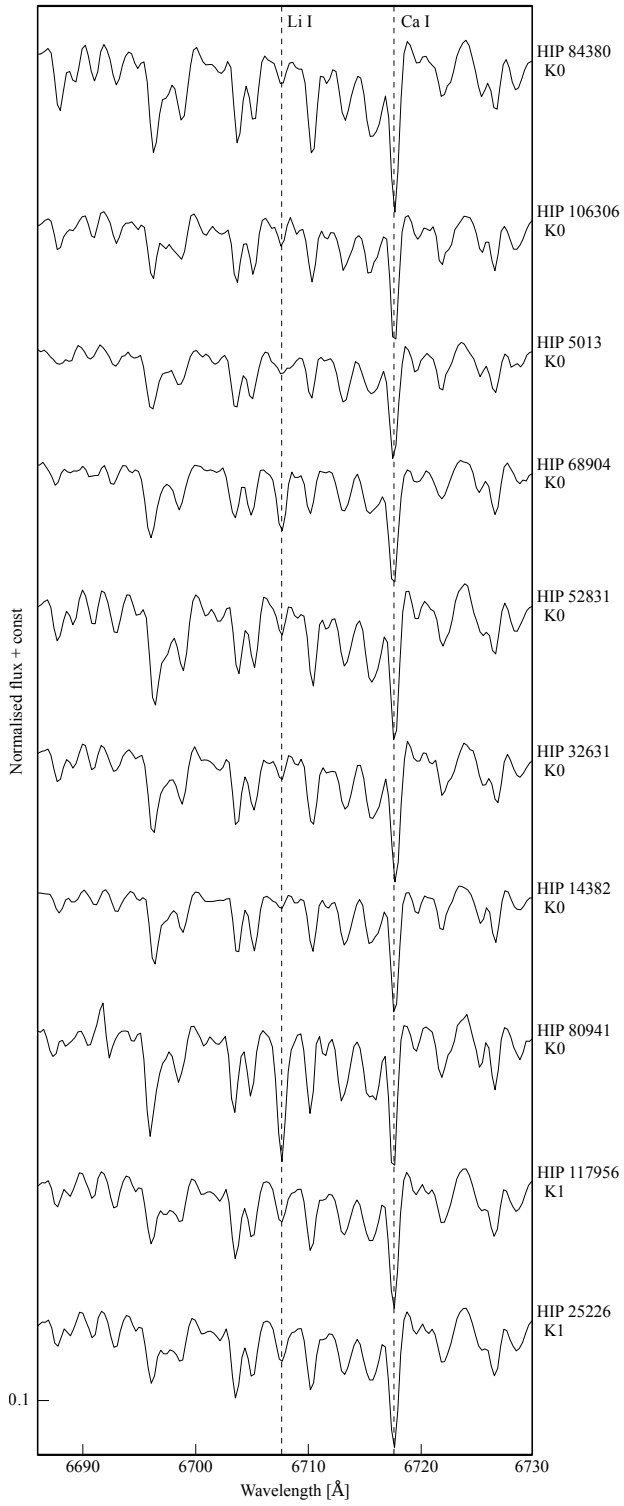
f - spectroscopic binary of two equal mass stars (therefore about 0.75 mag fainter compared to *Gaia* DR2 entry)

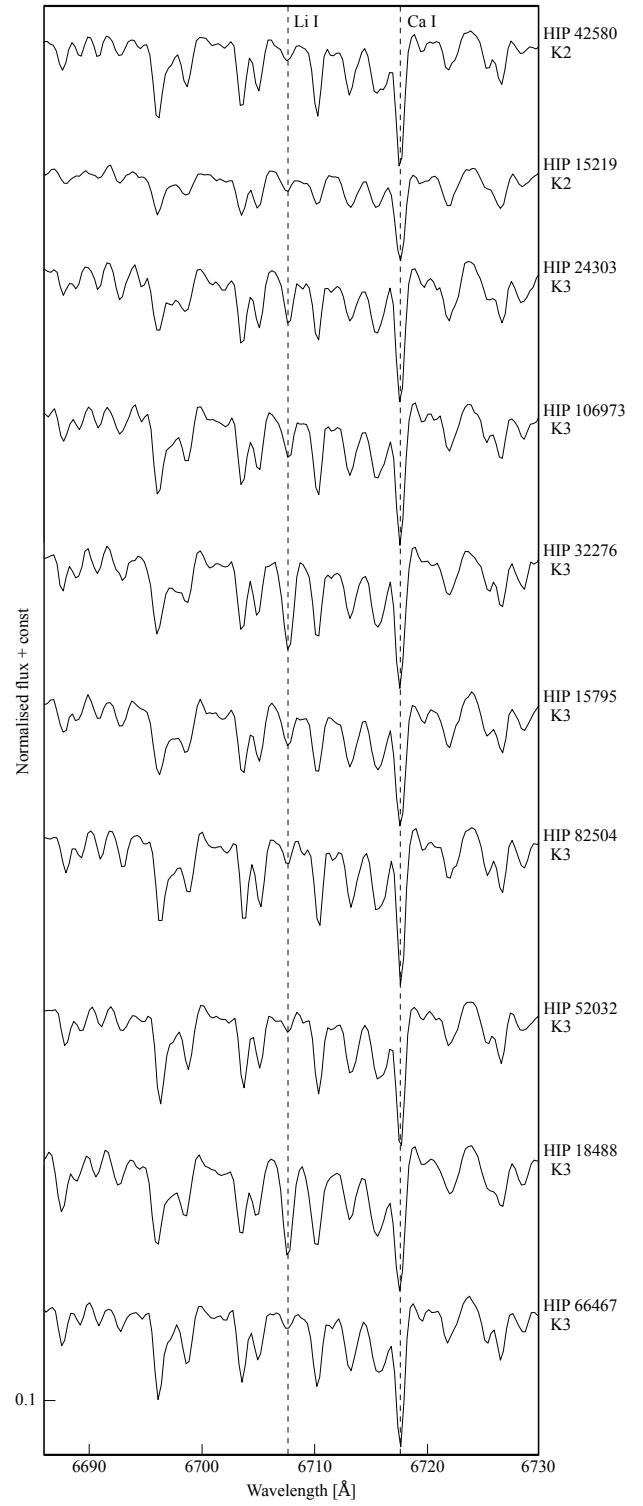
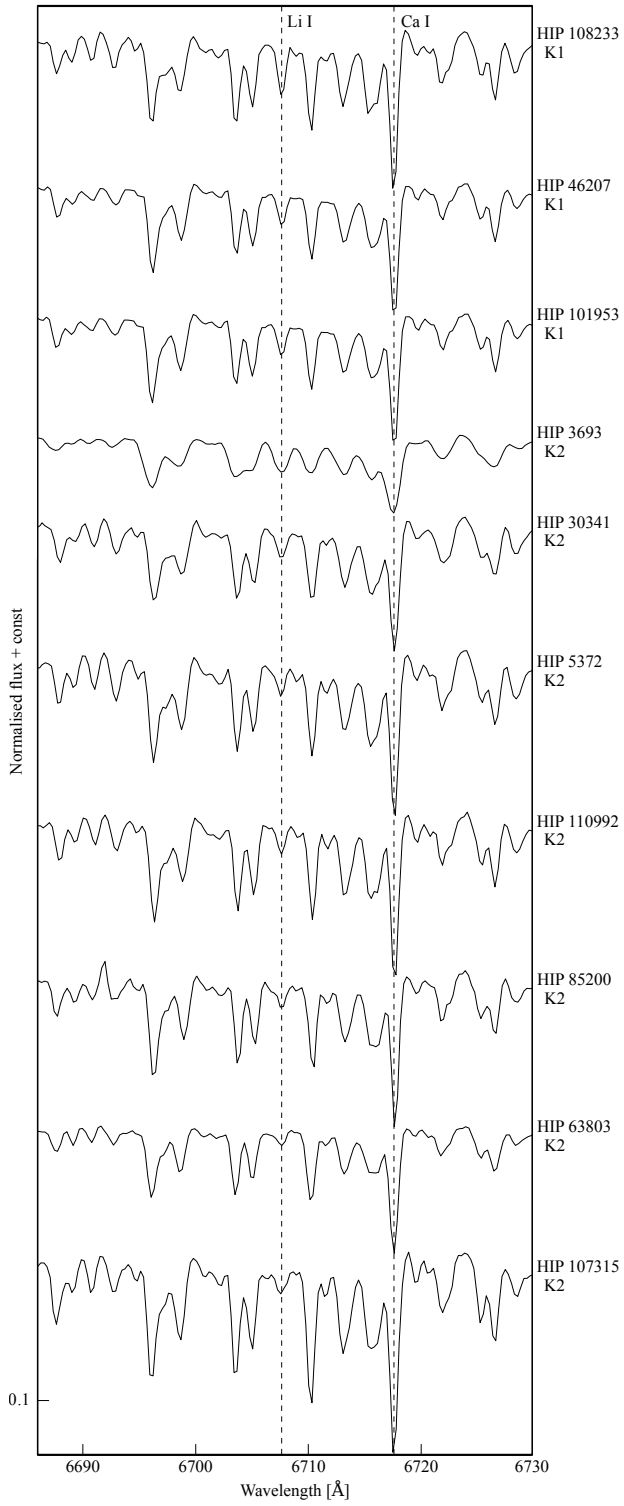
APPENDIX B: TARGET SPECTRA - DWARFS

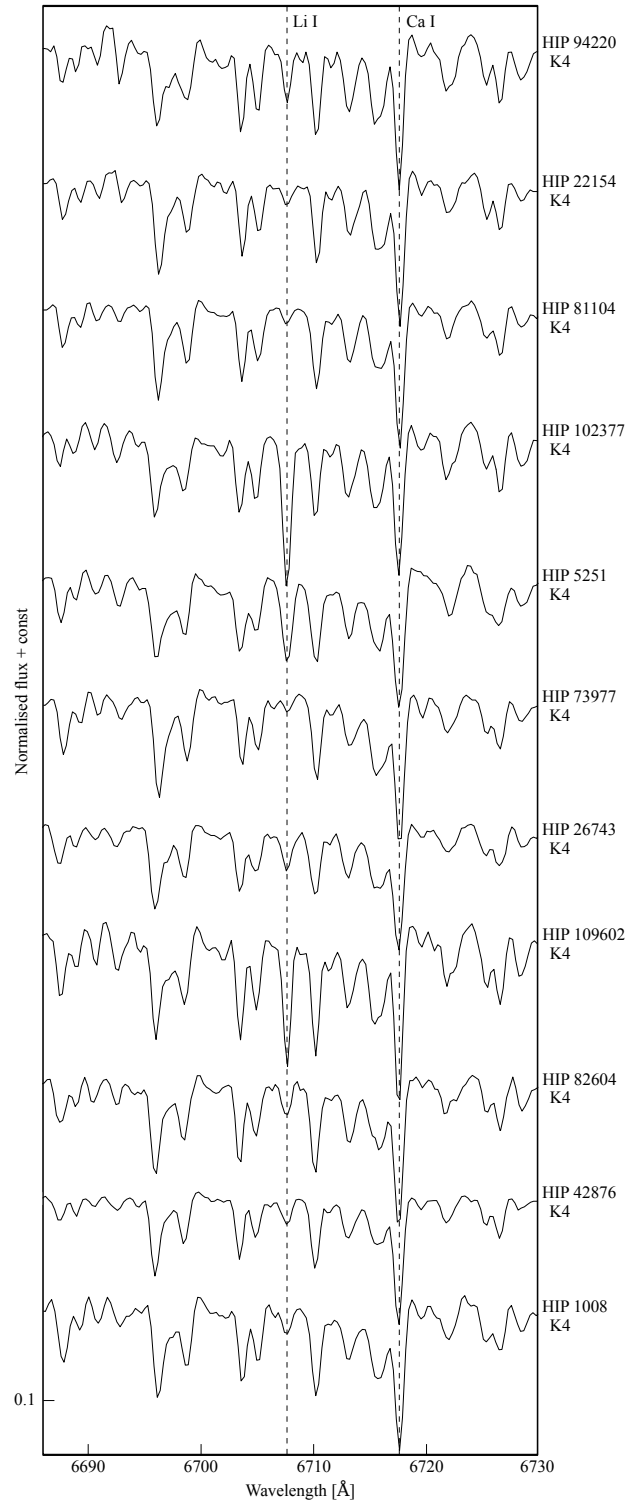
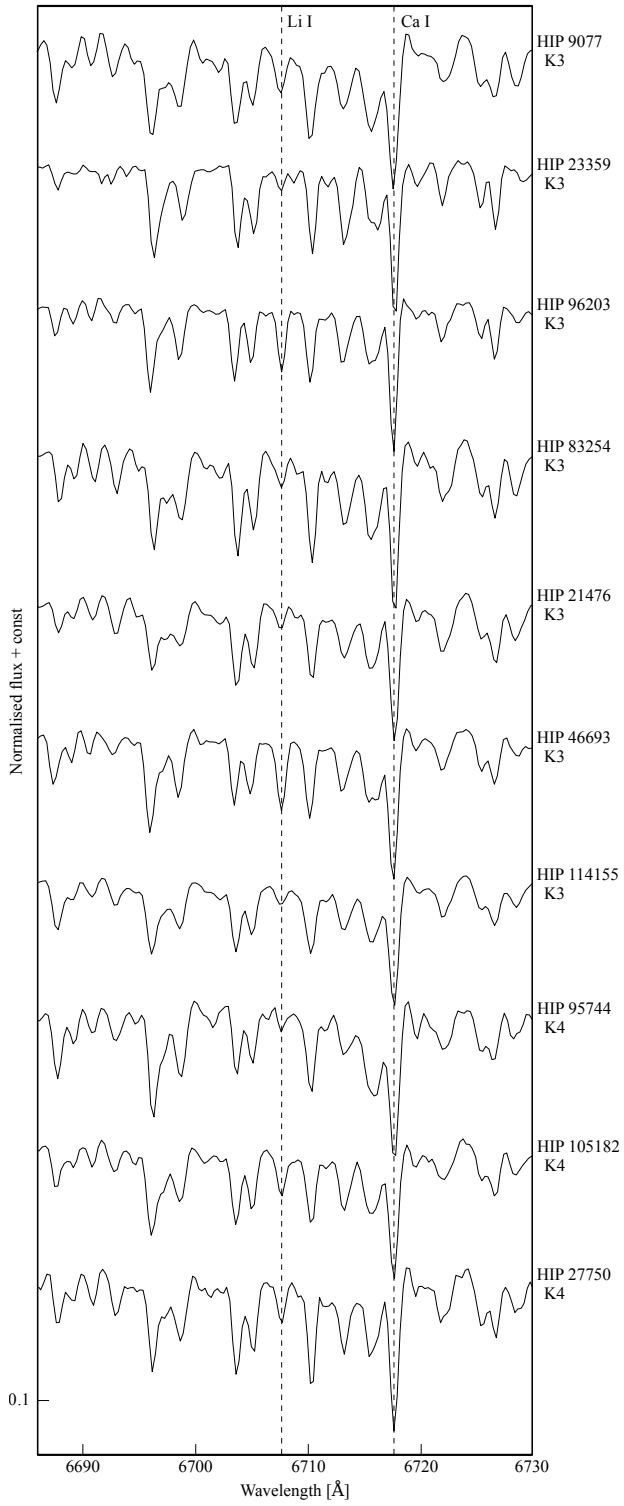
* This spectrum has only a signal-to-noise-ratio of 39.

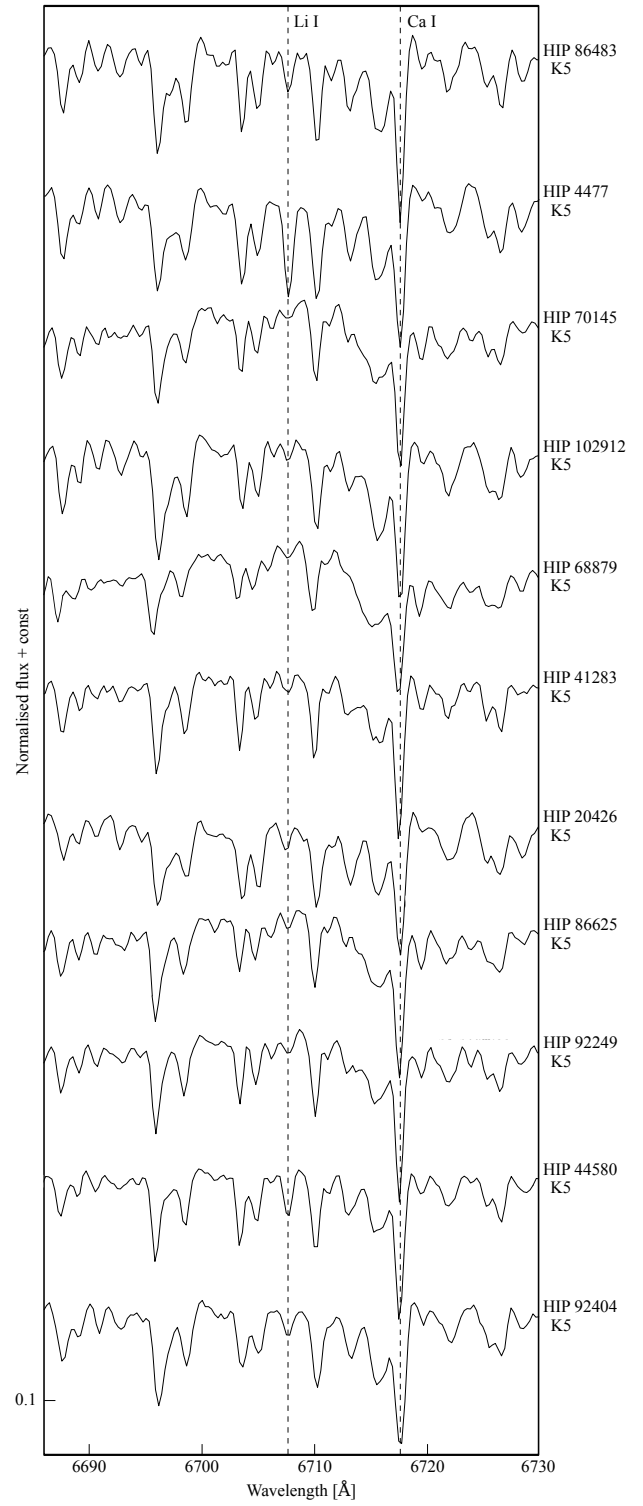
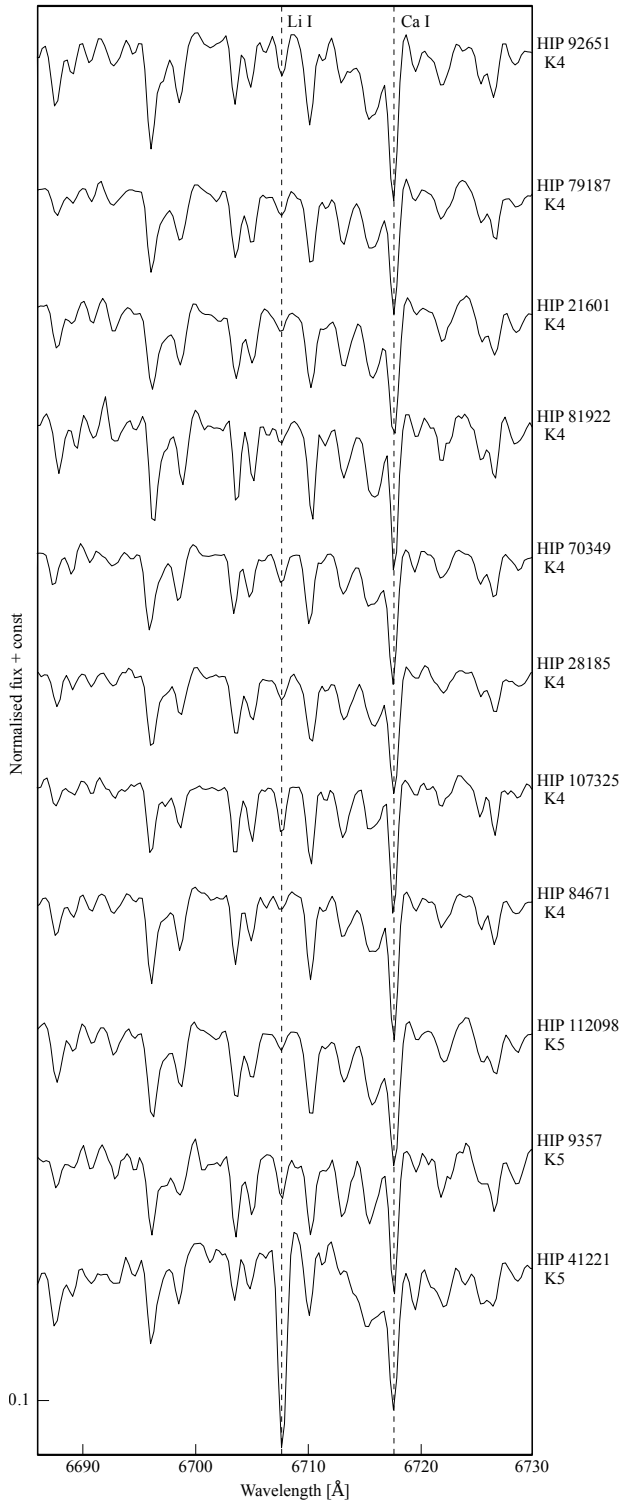
APPENDIX C: TARGET SPECTRA - GIANTS

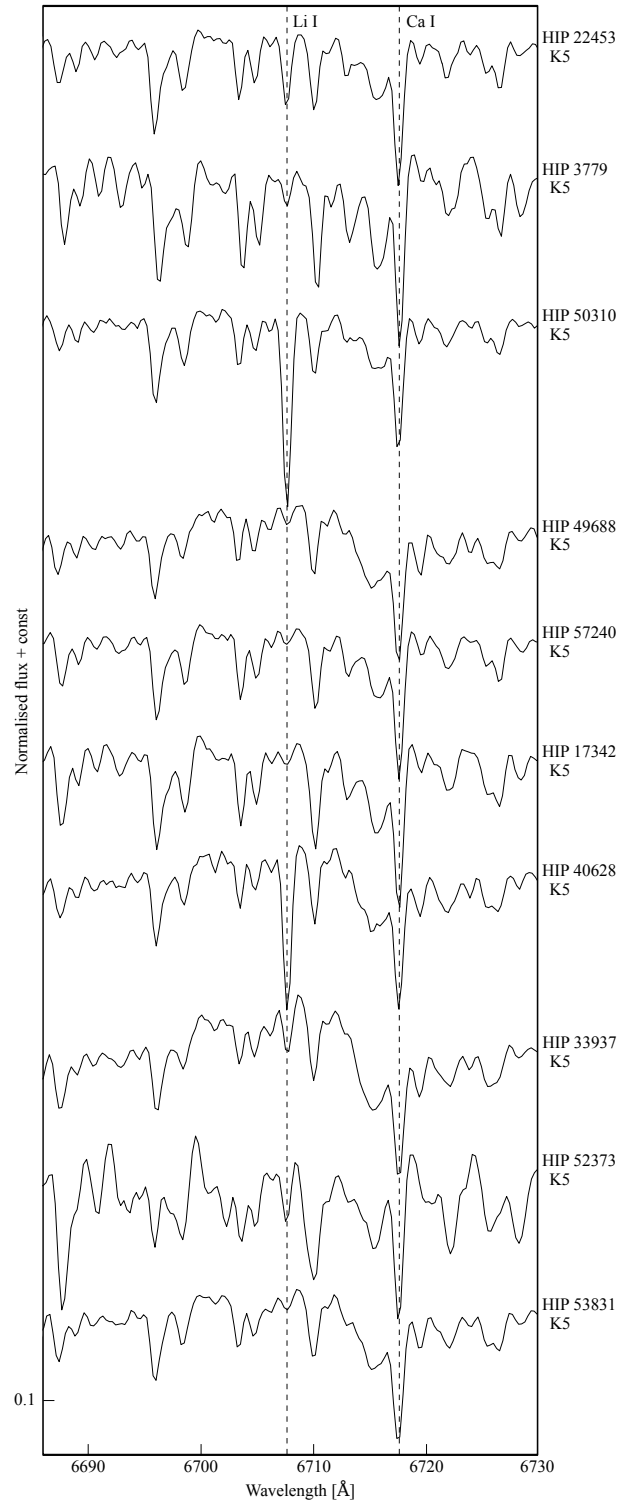
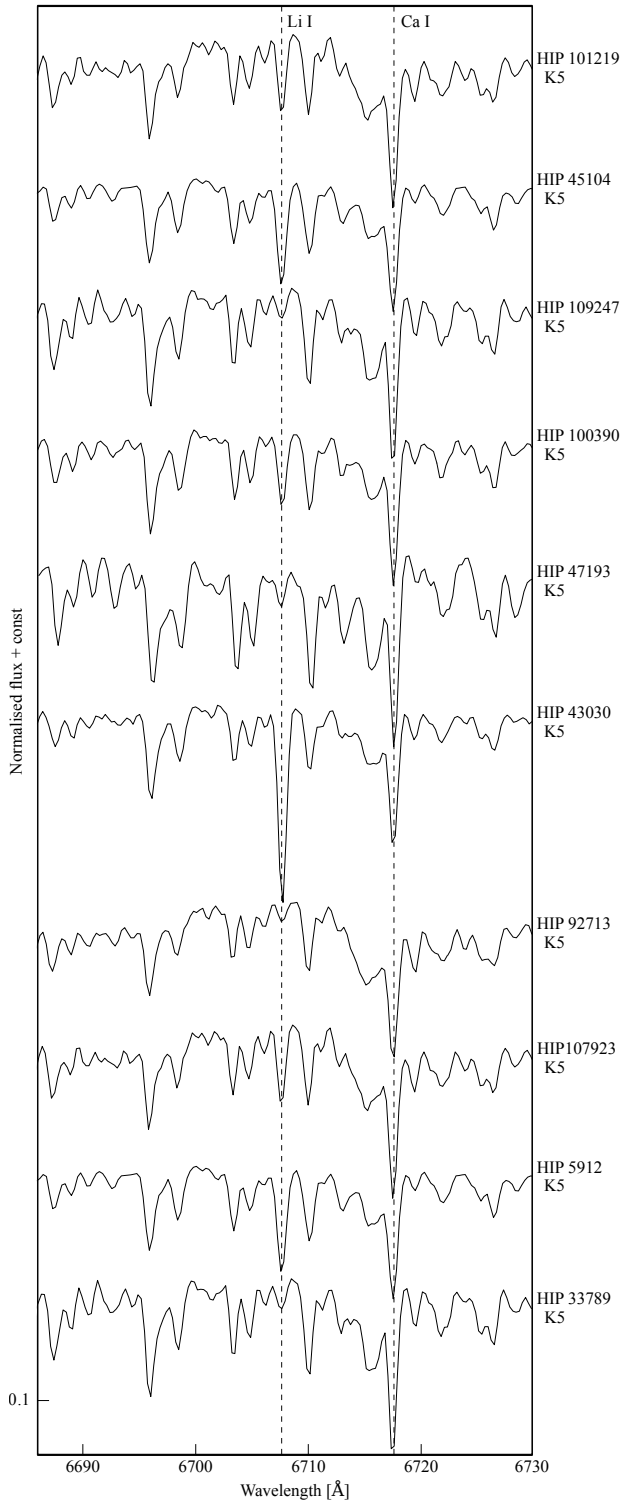


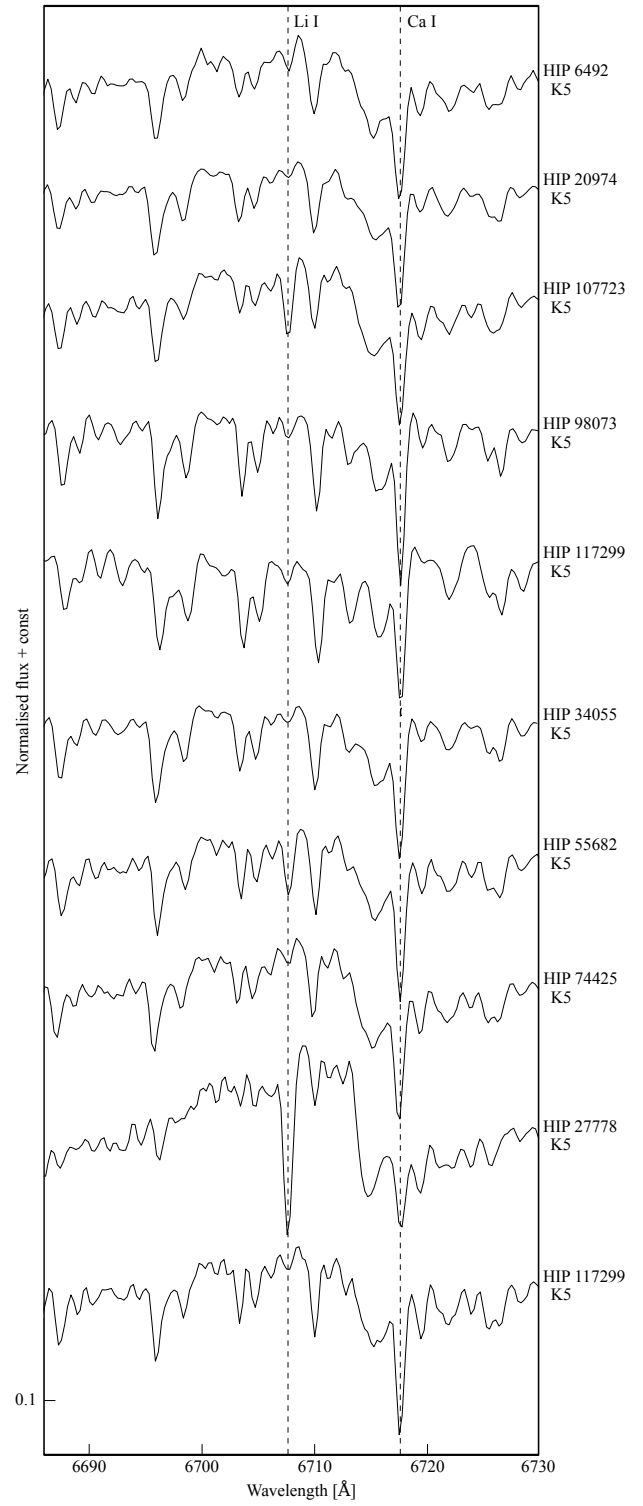
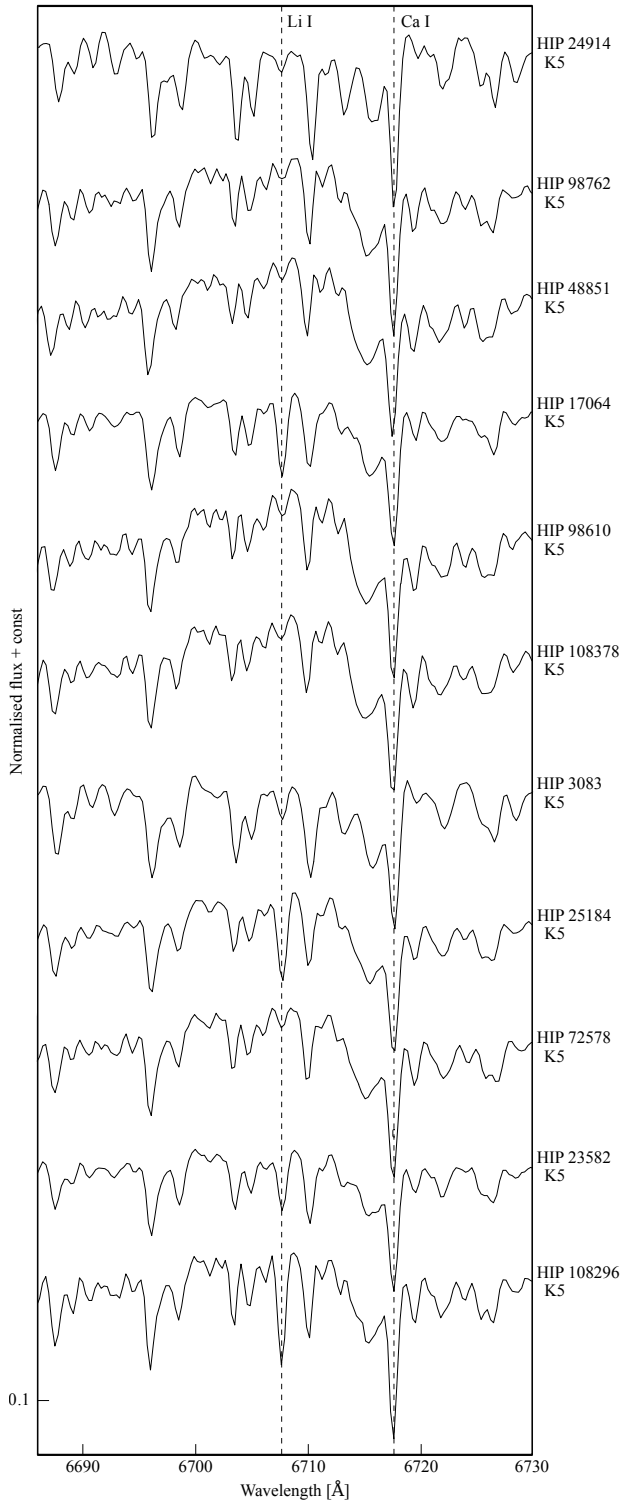


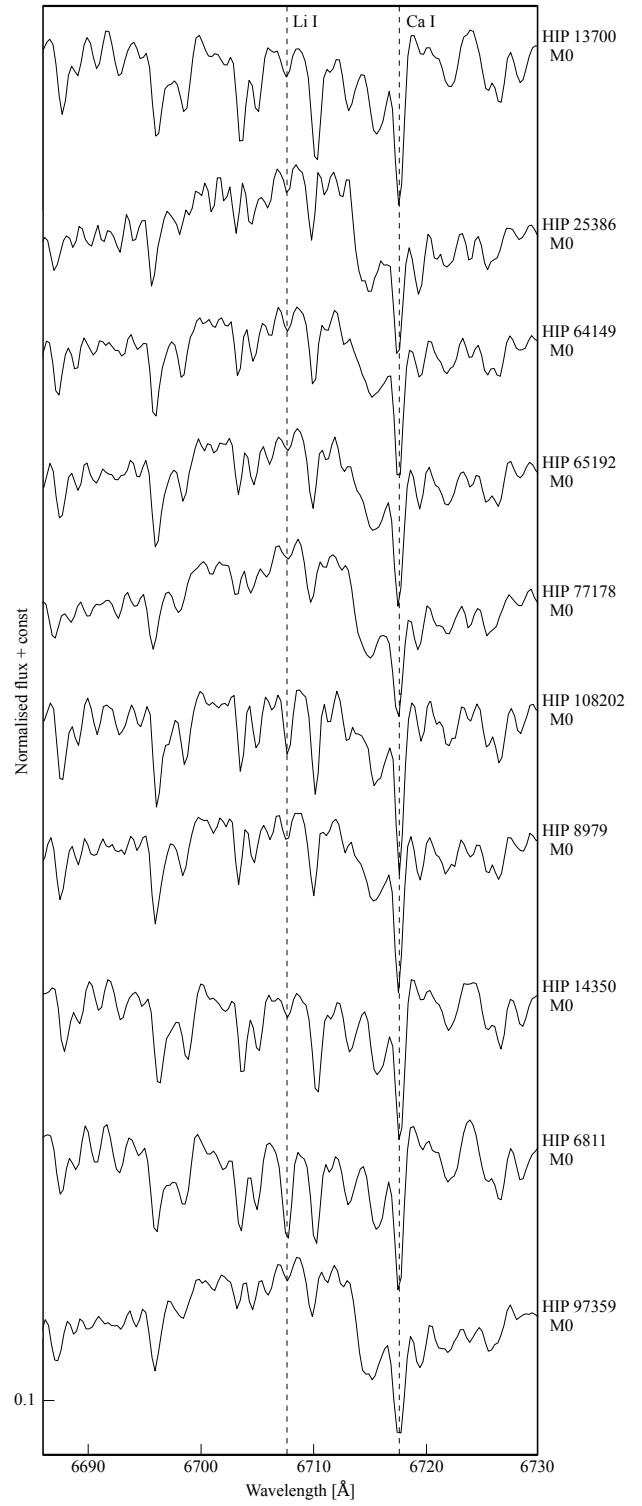
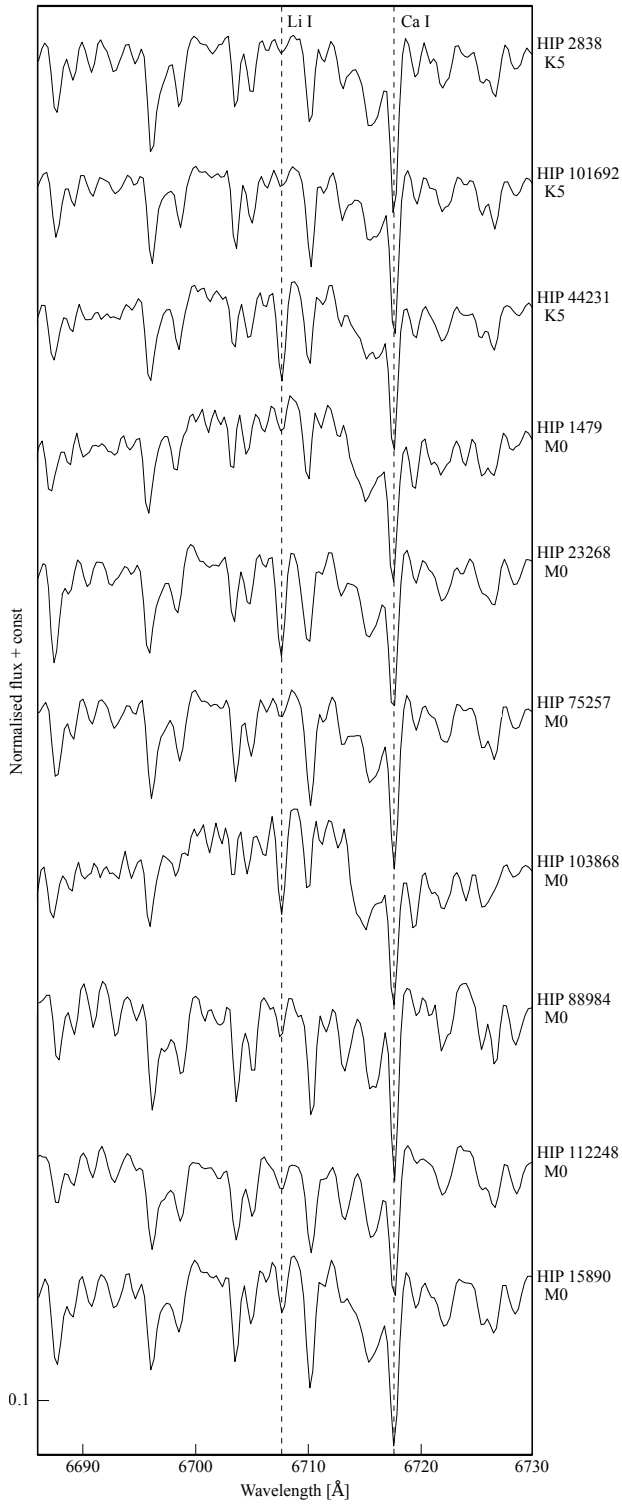


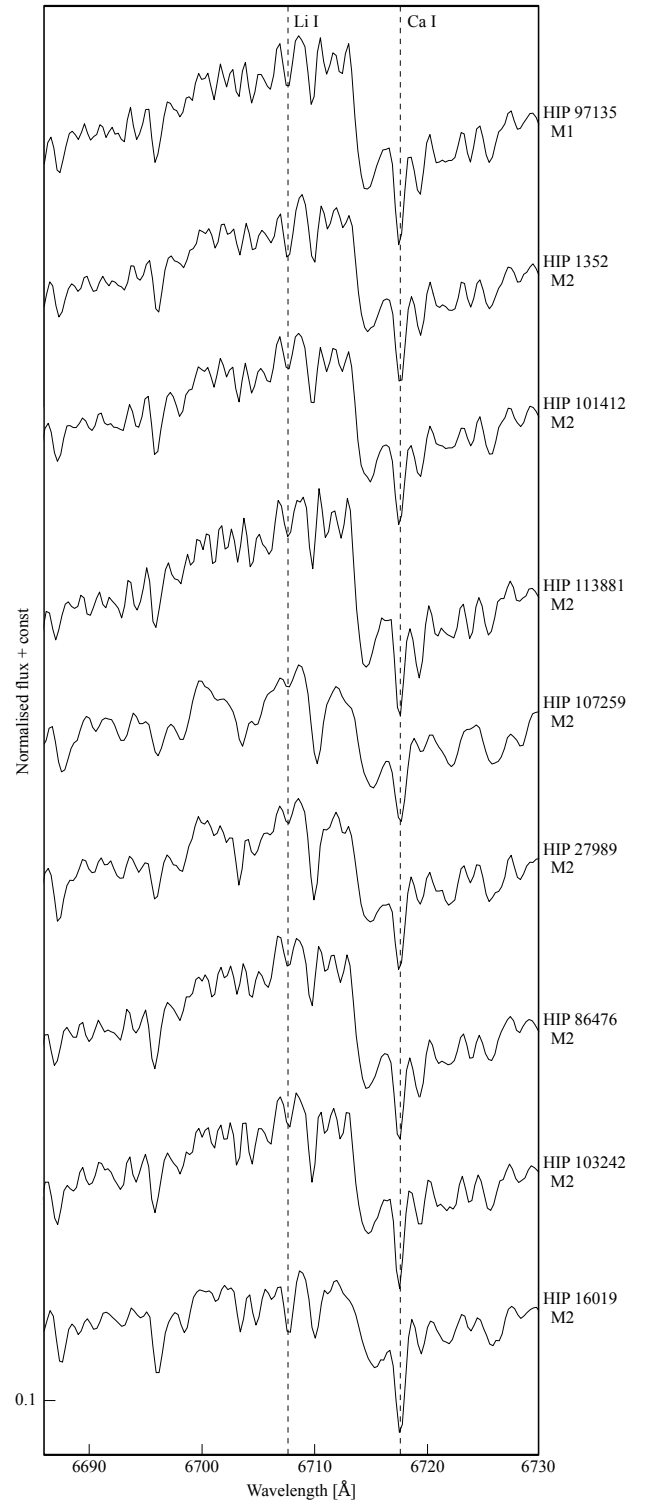
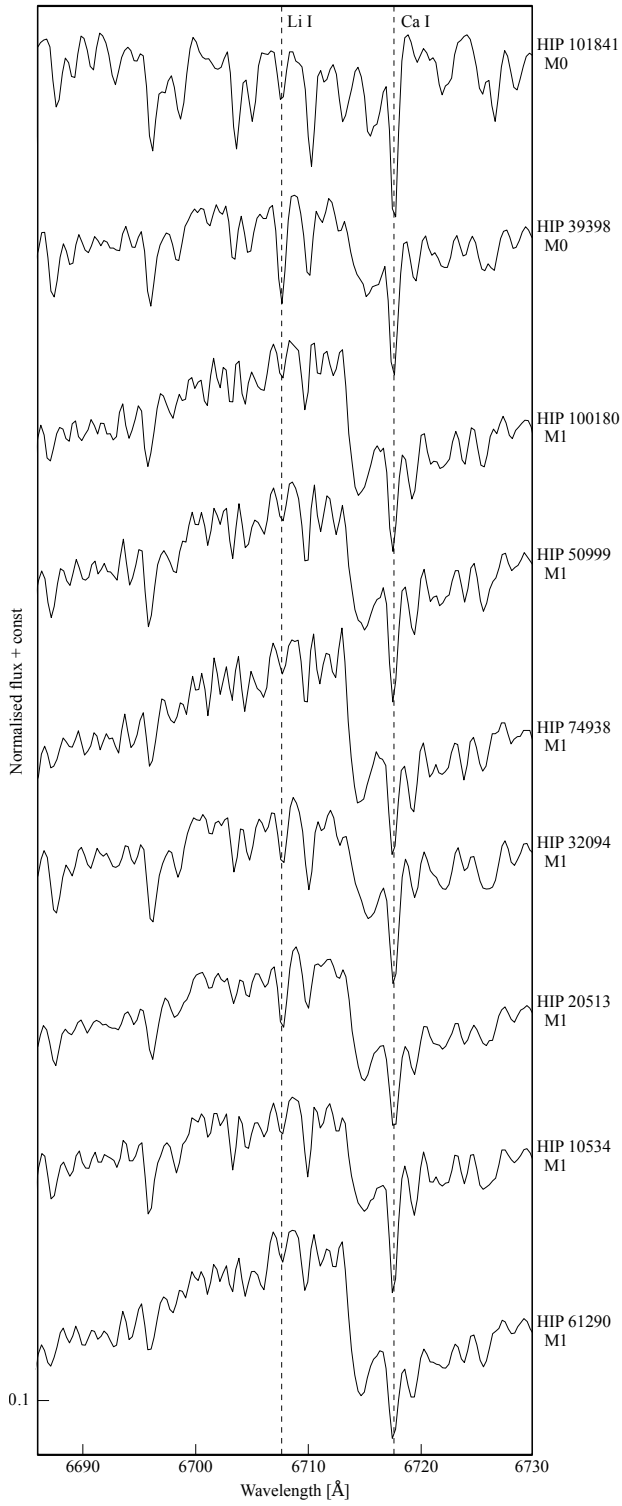


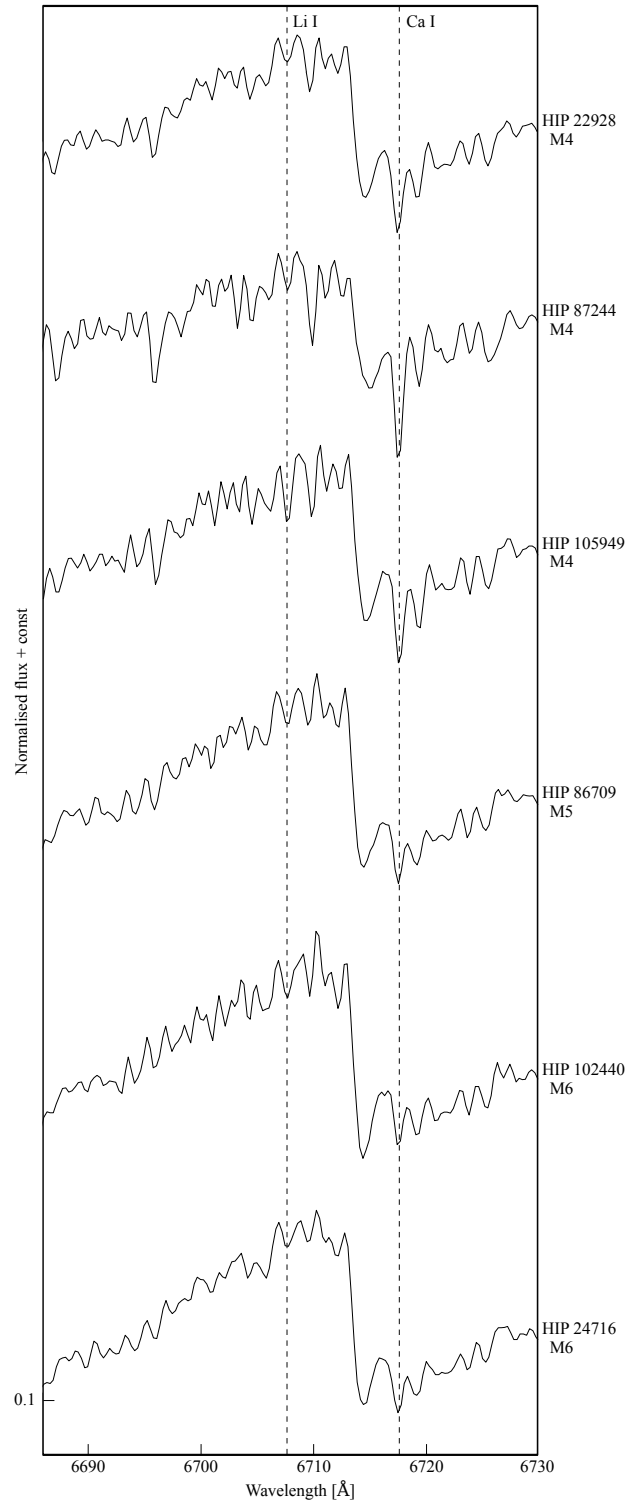
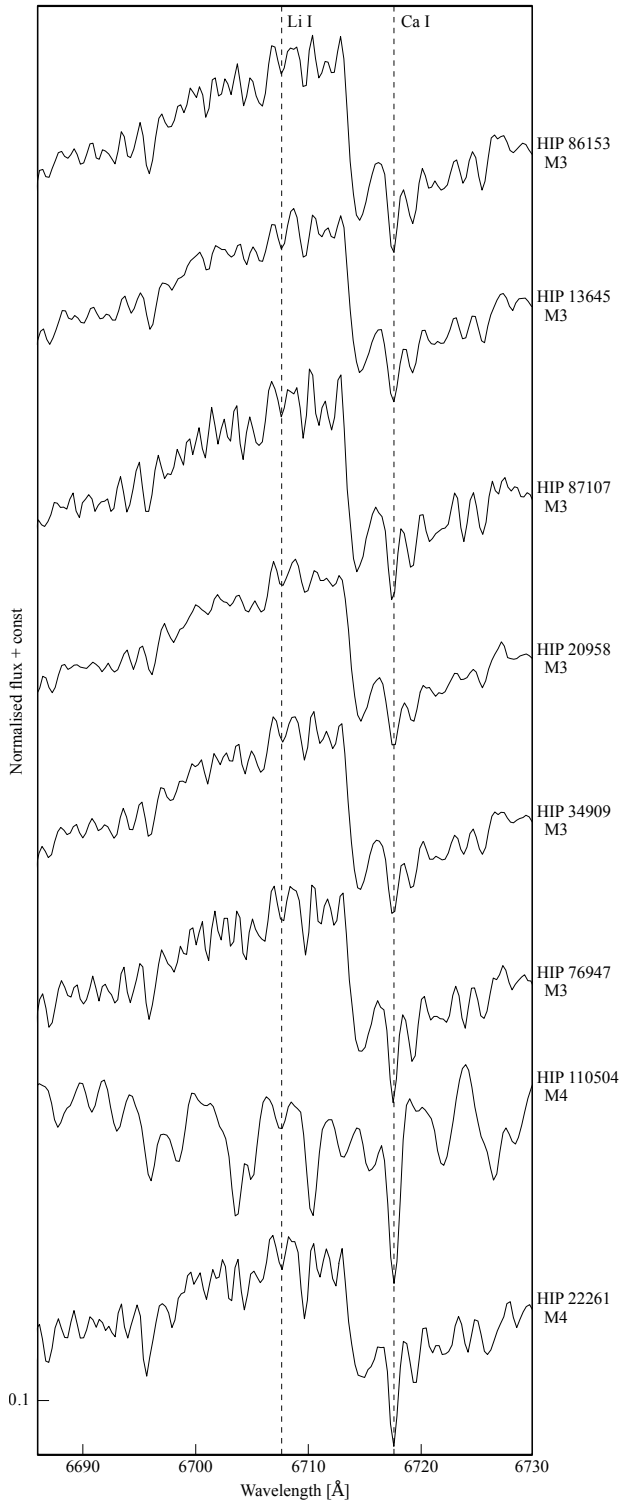












REFERENCES

- Anders, F., Khalatyan, A., Chiappini, C. et al. 2019, August, *A&A*, 628, A94.
- Andrae, R., Fouesneau, M., Creevey, O. et al. 2018, Aug, *A&A*, 616, A8.
- Bailer-Jones, C. A. L., Rybizki, J., Fouesneau, M., Mantelet, G., & Andrae, R. 2018, Aug, *AJ*, 156(2), 58.
- Bell, C. P. M., Mamajek, E. E., & Naylor, T. 2015, Nov, *MNRAS*, 454(1), 593-614.
- Binks, A. S., & Jeffries, R. D. 2014, Feb, *MNRAS*, 438(1), L11-L15.
- Bischoff, R., Mugrauer, M., Zehe, T. et al. 2017, Jul, *Astronomische Nachrichten*, 338(6), 671-679.
- Blaauw, A. 1961, May, *Bull. Astron. Inst. Netherlands*, 15, 265.
- Brandt, T. D., McElwain, M. W., Turner, E. L. et al. 2017, May, *VizieR Online Data Catalog*, J/ApJ/794/159.
- Bressan, A., Marigo, P., Girardi, L., Salasnich, B., Dal Cero, C., Rubele, S., & Nanni, A. 2012, November, *MNRAS*, 427(1), 127-145.
- Brewer, J. M., Fischer, D. A., Valenti, J. A., & Piskunov, N. 2016, August, *ApJS*, 225(2), 32.
- Casagrande, L., Schönrich, R., Asplund, M. et al. 2011, June, *A&A*, 530, A138.
- Coluzzi, R. 1993, Jul, *Bulletin d'Information du Centre de Donnees Stellaires*, 43, 7.
- Damiani, C., Meunier, J. C., Moutou, C., Deleuil, M., Ysard, N., Baudin, F., & Deeg, H. 2016, Nov, *A&A*, 595, A95.
- Fekel, F. C., Tomkin, J., & Williamson, M. H. 2010, Apr, *AJ*, 139(4), 1579-1591.
- Fűrész, G. 2008. (PhD dissertation). University of Szeged, Hungary.
- Franchini, M., Morossi, C., di Marcantonio, P., Malagnini, M. L., & Chavez, M. 2014, July, *MNRAS*, 442(1), 220-228.
- Gaia Collaboration, Brown, A. G. A., Vallenari, A. et al. 2018, Aug, *A&A*, 616, A1.
- Gazzano, J. C., de Laverny, P., Deleuil, M. et al. 2010, November, *A&A*, 523, A91.
- Gray, R. O., Corbally, C. J., Garrison, R. F. et al. 2006, July, *AJ*, 132(1), 161-170.
- Gray, R. O., Corbally, C. J., Garrison, R. F., McFadden, M. T., & Robinson, P. E. 2003, October, *AJ*, 126(4), 2048-2059.
- Gray, R. O., Graham, P. W., & Hoyt, S. R. 2001, April, *AJ*, 121(4), 2159-2172.
- Halbwachs, J. L., Mayor, M., & Udry, S. 2018, Nov, *A&A*, 619, A81.
- Heyne, T., Mugrauer, M., Bischoff, R. et al. 2020, January, *Astronomische Nachrichten*, 341(1), 99-117.
- Houdebine, E. R., Mullan, D. J., Bercu, B., Paletou, F., & Gebran, M. 2017, March, *ApJ*, 837(1), 96.
- Houdebine, E. R., Mullan, D. J., Paletou, F., & Gebran, M. 2016, May, *ApJ*, 822(2), 97.
- Imbert, M. 1977, September, *A&AS*, 29, 407-409.
- Irrgang, A., Desphande, A., Moehler, S., Mugrauer, M., & Janousch, D. 2016, Jun, *A&A*, 591, L6.
- Jordi, C., Gebran, M., Carrasco, J. M. et al. 2010, Nov, *A&A*, 523, A48.
- Karatas, Y., Bilir, S., & Schuster, W. J. 2005, July, *MNRAS*, 360(4), 1345-1354.
- Kunder, A., Kordopatis, G., Steinmetz, M. et al. 2017, February, *AJ*, 153(2), 75.
- Marsden, S. C., Petit, P., Jeffers, S. V. et al. 2014, November, *MNRAS*, 444(4), 3517-3536.
- Mugrauer, M. 2019, December, *MNRAS*, 490(4), 5088-5102.
- Mugrauer, M., Avila, G., & Guirao, C. 2014, Jan, *Astronomische Nachrichten*, 335(4), 417.
- Neuhäuser, R. 1997, Jan, *Science*, 276, 1363-1370.
- Ochsenbein, F., Bauer, P., & Marcout, J. 2000, Apr, *A&AS*, 143, 23-32.
- Passegger, V. M., Schweitzer, A., Shulyak, D. et al. 2019, Jul, *A&A*, 627, A161.
- Perryman, M. A. C., Lindegren, L., Kovalevsky, J. et al. 1997, Jul, *A&A*, 500, 501-504.
- Petigura, E. A., & Marcy, G. W. 2011, July, *ApJ*, 735(1), 41.
- Pfau, W. 1984, Jan, *Jenaer Rundschau*, 29(3), 121-122.
- Poveda, A., Ruiz, J., & Allen, C. 1967, Apr, *Boletin de los Observatorios Tonantzintla y Tacubaya*, 4, 86-90.
- Rajpurohit, A. S., Allard, F., Rajpurohit, S., Sharma, R., Teixeira, G. D. C., Mousis, O., & Rajpurohit, K. 2018, December, *A&A*, 620, A180.
- Ramírez, I., Fish, J. R., Lambert, D. L., & Allende Prieto, C. 2012, September, *ApJ*, 756(1), 46.
- Rojas-Ayala, B., Covey, K. R., Muirhead, P. S., & Lloyd, J. P. 2012, April, *ApJ*, 748(2), 93.
- Schweitzer, A., Passegger, V. M., Cifuentes, C. et al. 2019, May, *A&A*, 625, A68.
- Soderblom, D. R., Hillenbrand, L. A., Jeffries, R. D., Mamajek, E. E., & Naylor, T. 2014, January, Ages of Young Stars. H. Beuther, R. S. Klessen, C. P. Dullemond, et al. (Eds.), Protostars and Planets VI p. 219.
- Soderblom, D. R., Jones, B. F., Balachandran, S., Stauffer, J. R., Duncan, D. K., Fedele, S. B., & Hudon, J. D. 1993, September, *AJ*, 106, 1059.
- Stassun, K. G., Oelkers, R. J., Paegert, M. et al. 2019, October, *AJ*, 158(4), 138.
- Szentgyorgyi, A. H., & Fűrész, G. 2007, Jun, Precision Radial Velocities for the Kepler Era. S. Kurtz (Ed.), Revista Mexicana de Astronomia y Astrofisica Conference Series Vol. 28, p. 129-133.
- Tetzlaff, N., Neuhäuser, R., & Hohle, M. M. 2011, Jan, *MNRAS*, 410(1), 190-200.
- Torres, C. A. O., Quast, G. R., da Silva, L., de La Reza, R., Melo, C. H. F., & Sterzik, M. 2006, Dec, *A&A*, 460(3), 695-708.
- Torres, G., Andersen, J., & Giménez, A. 2010, February, *A&A Rev.*, 18(1-2), 67-126.
- Valenti, J. A., & Fischer, D. A. 2005, July, *ApJS*, 159(1), 141-166.
- van Leeuwen, F. 2007, Nov, *A&A*, 474(2), 653-664.
- Worley, C. C., de Laverny, P., Recio-Blanco, A., Hill, V., Bijaoui, A., & Ordenovic, C. 2012, June, *A&A*, 542, A48.
- Zuckerman, B., Song, I., Bessell, M. S., & Webb, R. A. 2001, Nov, *ApJ*, 562(1), L87-L90.

How cite this article: R. Bischoff, M. Mugrauer, G. Torres, et al. (2020), Identification of young nearby runaway stars based on Gaia data and the lithium test, *Astron. Nachr.*, 2020.

AUTHOR BIOGRAPHY

Richard Bischoff is a PhD student at the Astrophysical Institute and University Observatory Jena. His main field of research are photometry and spectroscopy of exoplanet candidate host stars.